Electronic Supplementary Information

for

Near-infrared fluorescent HaloTag ligands for efficient organelle labelling in living cells

Yoshiki Tanaka, Masayasu Taki* and Shigehiro Yamaguchi*

Table of Contents

1. Experimental details

General information

^{1}H, $^{13}C\{^{1}H\}$, and $^{31}P\{^{1}H\}$ NMR spectra were recorded with a JEOL ECZ 400 spectrometer (400 MHz for ^{1}H, 100 MHz for $^{13}C\{^{1}H\}$, and 162 MHz for $^{31}P\{^{1}H\}$) and JEOL ECA 500 II spectrometer (500 MHz for ^{1}H, 125 MHz for $^{13}C\{^{1}H\}$, and 202 MHz for $^{31}P\{^{1}H\}$) in CD_3OD, $CDCl_3$ and acetone-d_6. $^{13}C\{^{1}H\}$ NMR spectra were recorded with a JEOL ECA 600 II spectrometer equipped with an UltraCOOL probe (150 MHz) in CD_3OD and $CDCl_3$. The chemical shifts in ^{1}H NMR spectra are reported in δ ppm using the residual protons of the solvents as an internal standard ($CDCl_3$: δ 7.26, CD_3OD: δ 3.31 and Acetone-d_6: δ 2.05), and those in ^{13}C NMR spectra are reported using the solvent signals as an internal standard ($CDCl_3$: δ 77.16, CD_3OD: δ 49.00). The chemical shifts in ^{31}P NMR spectra are reported using H_3PO_4 (δ 0.00) as an external standard. The high-resolution mass spectra were measured with a Thermo Fisher Scientific Exactive with the ESI ionisation method. Thin layer chromatography (TLC) was performed on glass plates coated with 0.25 mm thickness of silica gel $60F_{254}$ (Merck). Column chromatography was performed using silica gel 60 (Kanto Chemicals). HPLC purification was performed on a preparative HPLC system (Shimadzu) using a C18 reverse phase column (YMC Triart C18, 20 × 250 mm). Unless otherwise noted, chemical reagents and solvents were purchased from commercial suppliers (Tokyo Chemical Industry (TCI), Sigma Aldrich, Kanto Chemicals, and FUJIFILM Wako Pure Chemical Corporation (Wako)) and used without further purification. Anhydrous THF, CH_3CN and DMF were purchased from Kanto Chemicals and further purified by Glass Contour Solvent Systems. *N*-ethyl-3-bromoaniline (**1**),[1] dimethyl 3-hydroxythiophene-2,5-dicarboxylate (**6**),[2] 3,7-bis(diethylamino)-5-phenyl-10*H*-acridophosphin-10-one 5-oxide (**10**),[3] 3,7-diamino-5-phenyl-10*H*-acridophosphin-10-one 5-oxide (**12**),[4] 2-(2-((6-chlorohexyl)oxy)ethoxy)ethan-1-amine・TFA[5] were synthesised according to the literature methods.

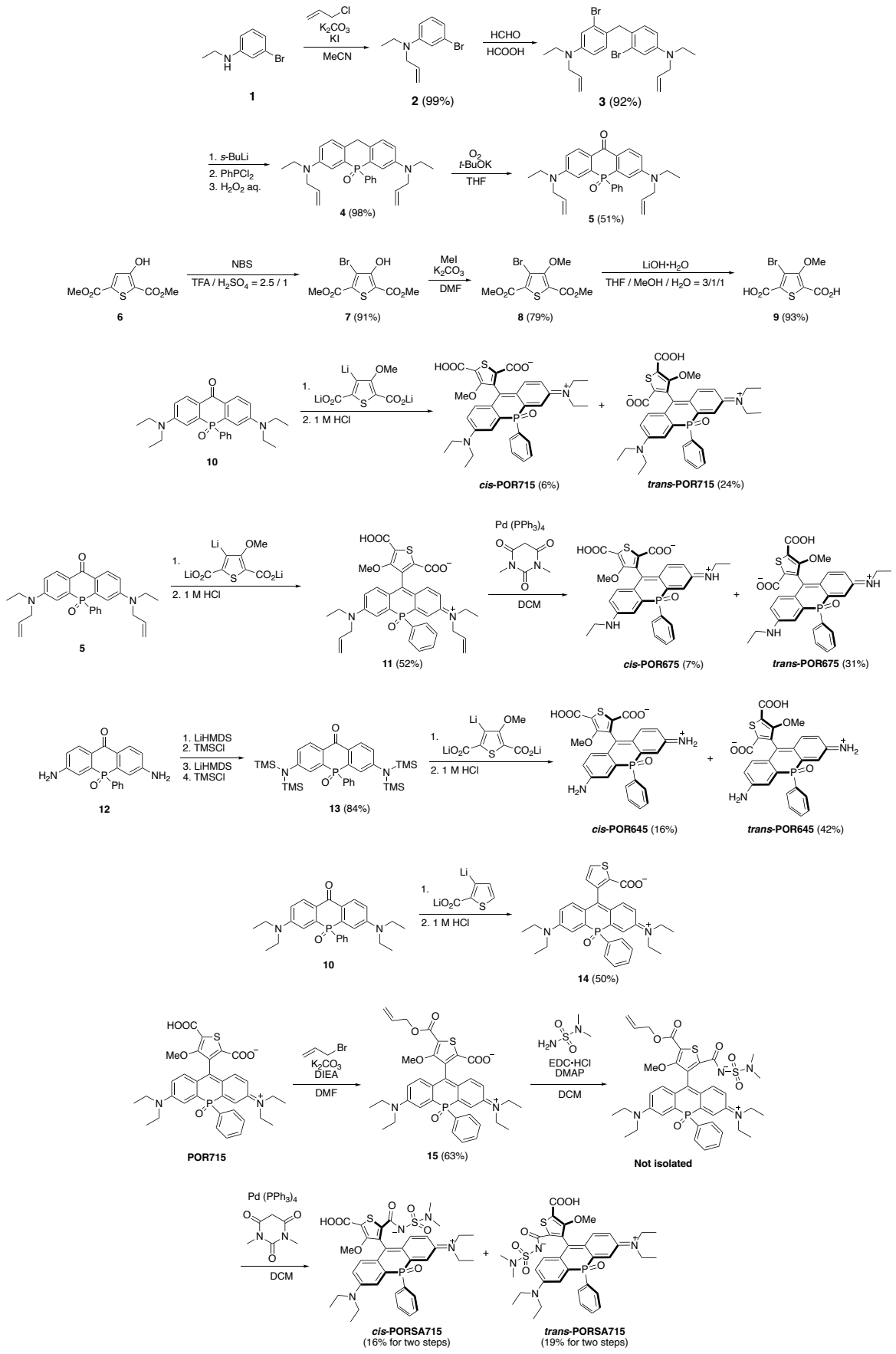

Scheme S1. Synthesis of *P*–rhodamines**.**

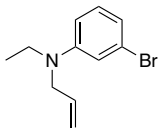

2

Compound 2. To a suspension of *N*-ethyl-3-bromoaniline (1.32 g, 6.60 mmol), K_2CO_3 (1.82 g, 13.2 mmol), and KI (108 mg, 0.648 mmol) in anhydrous CH_3CN (10 mL) was added allyl chloride (1.62 mL, 19.9 mmol) at room temperature. The resulting solution was stirred for 19 h at 95 ºC. After cooling to room temperature, the reaction mixture was diluted with water and extracted with EtOAc three times. The combined organic layers were washed with water, and brine, dried over anhydrous Na_2SO_4, filtered, and concentrated under reduced pressure. The chemical structure of the resulting brawn oil of **2** (1.56 g, 6.50 mmol, 99%) was confirmed based on reported data[6] and used without further purification.

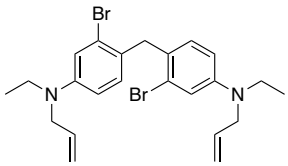

3

Compound 3. To a solution of **2** (41.6 g, 173 mmol) in HCOOH (240 mL) was added HCHO solution (37%, 85.3 g, 1.05 mol) at room temperature. The resulting solution was stirred for 13 h at 60 ºC. After cooing to 0 ºC, the solution was neutralized with 10 M NaOH aq. and sat. $NaHCO_3$ aq. The aqueous layer was extracted with EtOAc three times. The combined organic layers were washed with sat. $NaHCO_3$ aq., water, and brine, dried over anhydrous Na_2SO_4, filtered, and concentrated under reduced pressure. The crude mixture was purified by silica-gel column chromatography, eluting with hexane/CH_2Cl_2 (5/1, v/v, R_f = 0.25), to afford 39.2 g (80.0 mmol, 92%) of **3** as orange oil. ^{1}H NMR ($CDCl_3$, 400 MHz) δ 6.89 (d, J = 2.4 Hz, 2H), 6.82 (d, J = 9.2 Hz, 2H), 6.53 (dd, J = 9.2, 2.4 Hz, 2H), 5.87-5.78 (m, 2H), 5.19-5.13 (m, 4H), 3.97 (s, 2H), 3.86-3.84 (m, 4H), 3.34 (q, J = 7.0 Hz, 4H), 1.15 (t, J = 7.0 Hz, 6H). ^{13}C NMR ($CDCl_3$, 100 MHz) δ 147.8 (C), 134.1 (CH), 131.0 (CH), 126.6 (C), 125.8 (C), 116.2 (CH_2), 115.8 (CH), 111.6 (CH), 52.7 (CH_2), 44.9 (CH_2), 39.9 (CH_2), 12.4 (CH_3). HRMS (ESI) m/z calcd. for $C_{23}H_{29}{}^{79}Br^{81}BrN_2$ $[M+H]^+$: 493.0672; found: 493.0667.

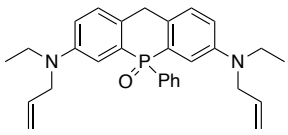

4

Compound 4. To a solution of **3** (5.51 g, 11.2 mmol) in anhydrous THF (90 mL) was added *sec*-BuLi (1.22 M in cyclohexane and *n*-hexane, 18.5 mL, 22.6 mmol) at –78 °C. The mixture was stirred for 1.5 h at the same temperature, followed by dropwise addition of *P,P*-dichlorophenylphosphine (1.60 mL, 11.8 mmol). The resulting solution was stirred for 14 h at –78 °C. After warming to 0 ºC, 34% H_2O_2 aq. (5 mL) was added, and the mixture was stirred for 2 h at 0 °C and then quenched with the sat. Na_2SO_3 aq. After removal of THF *in vacuo*, the aqueous layer was extracted with CH_2Cl_2 three times. The combined organic layers were washed

with brine, dried over anhydrous Na_2SO_4, filtered, and concentrated under reduced pressure. The resulting crude was purified by silica-gel column chromatography, eluting with CH_2Cl_2/acetone (19/1, v/v, 1% TEA, R_f = 0.68), to afford 5.03 g (11.0 mmol, 98%) of **4** as a pale yellow solid. ^{1}H NMR ($CDCl_3$, 500 MHz) δ 7.49-7.43 (m, 4H), 7.39-7.36 (m, 1H), 7.31 (td, J = 7.1, 2.3 Hz, 2H), 7.17 (dd, J = 8.4, 6.1 Hz, 2H), 6.76 (dd, J = 8.4, 3.1 Hz, 2H), 5.87-5.80 (m, 2H), 5.17-5.12 (m, 4H), 3.99-3.89 (m, 4H), 3.81 (d, J = 18.0 Hz, 1H), 3.65 (dd, J = 18.0, 3.4 Hz, 1H), 3.50-3.37 (m, 4H), 1.16 (t, J = 7.3 Hz, 6H). ^{13}C NMR ($CDCl_3$, 100 MHz) δ 147.1 (d, J = 12.5 Hz, C), 134.7 (d, J = 105.0 Hz, C), 134.1 (s, CH), 131.1 (d, J = 2.9 Hz, CH), 130.8 (d, J = 9.6 Hz, CH), 129.7 (d, J = 100.2 Hz, C), 129.1 (d, J = 11.6 Hz, CH), 128.8 (d, J = 8.7 Hz, C), 128.4 (d, J = 12.5 Hz, CH), 116.2 (s, CH_2), 115.4 (s, CH), 113.7 (d, J = 7.7 Hz, CH), 52.7 (s, CH_2), 44.9 (s, CH_2), 35.3 (d, J = 9.6 Hz, CH_2), 12.3 (s, CH_3). ^{31}P NMR ($CDCl_3$, 202 MHz) δ 14.4. HRMS (ESI) m/z calcd. for $C_{29}H_{34}N_2OP$ $[M+H]^+$: 457.2404; found: 457.2409.

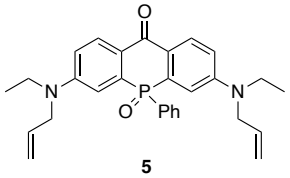

5

Compound 5. To a solution of **4** (4.52 g, 9.90 mmol) in anhydrous THF (90 mL) was added dropwise a solution of *t*-BuOK (1.02 g, 9.05 mmol) in anhydrous THF (30 mL) in triplicate every 1 h at room temperature under oxygen atmosphere. The reaction mixture was stirred further for 1.5 h at room temperature. After removal of the solvent, a mixture of CH_2Cl_2/acetone (9/1, v/v) was added, and the mixture was filtered through a pad of silica-gel. The filtrate was concentrated under reduced pressure and the crude product was purified by silica-gel column chromatography, eluting with CH_2Cl_2/acetone (100/0–9/1), to afford 2.37 g (5.04 mmol, 51%) of **5** as a yellow solid. R_f = 0.53 (10% acetone in CH_2Cl_2, v/v). ^{1}H NMR ($CDCl_3$, 400 MHz) δ 8.27 (dd, J = 9.2, 6.1 Hz, 2H), 7.61-7.56 (m, 2H), 7.41-7.36 (m, 1H), 7.34-7.30 (m, 2H), 7.13 (dd, J = 15.0, 3.0 Hz, 2H), 6.85 (dd, J = 9.2, 3.0 Hz, 2H), 5.83-5.74 (m, 2H), 5.14-5.08 (m, 4H), 4.05-3.92 (m, 4H), 3.55-3.38 (m, 4H), 1.17 (t, J = 7.0 Hz, 6H). ^{13}C NMR ($CDCl_3$, 125 MHz) δ 180.2 (d, J = 8.5 Hz, C), 150.9 (d, J = 12.1 Hz, C), 135.1 (d, J = 106.2 Hz, C), 134.7 (d, J = 97.8 Hz, C), 132.5 (s, CH), 131.4 (d, J = 9.7 Hz, CH), 130.6 (d, J = 10.9 Hz, CH), 128.6 (d, J = 12.1 Hz, CH), 124.4 (d, J = 7.2 Hz, C), 116.9 (s, CH_2), 114.7 (s, CH), 112.0 (d, J = 8.4 Hz, CH), 52.5 (s, CH_2), 45.1 (s, CH_2), 12.4 (s, CH_3). One CH peak was overlapped. ^{31}P NMR ($CDCl_3$, 162 MHz) δ 6.8. HRMS (ESI) m/z calcd. for $C_{29}H_{31}N_2O_2PNa$ $[M+Na]^+$: 493.2016; found: 493.2007.

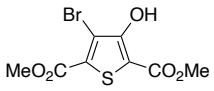

7

Compound 7. To a solution of dimethyl 3-hydroxythiophene-2,5-dicarboxylate (4.40 g, 20.4 mmol, **6**) in a mixture of TFA (11 mL) and H_2SO_4 (4 mL) was added NBS (3.80 g, 21.4 mmol) portionwise at room temperature. The resulting mixture was stirred for 17 h at room temperature, poured on ice, and extracted with CH_2Cl_2 four times. The combined organic layers were washed with brine, dried over anhydrous Na_2SO_4, filtered, and concentrated under reduced pressure. The ^{1}H NMR analysis confirmed that the obtained white solid of **7**

was pure enough to be used for the next step without further purification. Yield: 5.48 g (18.6 mmol, 91%). ^{1}H NMR ($CDCl_3$, 400 MHz) δ 9.60 (s, 1H), 3.91 (s, 3H), 3.88 (s, 3H). ^{13}C NMR ($CDCl_3$, 100 MHz) δ 165.5 (C), 160.5 (C), 160.1 (C), 130.6 (C), 108.1 (C), 107.4 (C), 52.8 (CH_3). One CH_3 peak was overlapped. HRMS (ESI) *m*/*z* calcd. for $C_8H_6{}^{79}BrO_5S$ [M–H$^-$]: 292.9124; found: 292.9124.

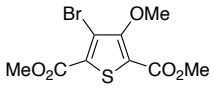

8

Compound 8. To a suspension of **7** (7.02 g, 23.8 mmol) and K_2CO_3 (6.56 g, 47.5 mmol) in a mixture of anhydrous DMF (13 mL) and CH_3CN (13 mL) was added iodomethane (7.40 mL, 119 mmol) at room temperature. The resulting mixture was stirred for 46 h at 90 ºC. After cooling to room temperature, 100 mL water was added. The insoluble material was collected by filtration, washed with 0.5 M HCl aq. and water, dried, and recrystallized from EtOAc. The desired compound **8** was obtained as a colourless solid (5.81 g, 18.8 mmol, 79%). ^{1}H NMR ($CDCl_3$, 400 MHz) δ 4.01 (s, 3H), 3.92 (s, 3H), 3.91 (s, 3H) ^{13}C NMR ($CDCl_3$, 100 MHz) δ 160.6 (C), 160.5 (C), 158.8 (C), 129.7 (C), 121.5 (C), 114.8 (C), 62.8 (CH_3), 52.8 (CH_3), 52.7 (CH_3) HRMS (ESI) *m*/*z* calcd. for $C_9H_9{}^{81}BrO_5SNa$ [M+Na]$^+$: 332.9226; found: 332.9225.

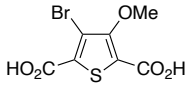

9

Compound 9. To a solution of **8** (5.39 g, 17.4 mmol) in a mixture of CH_3OH (38 mL) and THF (110 mL) was added $LiOH{\cdot}H_2O$ (3.66 g, 87.2 mmol) in H_2O (38 mL), and the resulting mixture was stirred for 37 h at room temperature. After neutralization with sat. NH_4Cl aq., the organic solvent was removed by rotary evaporation, followed by filtration through a pad of Celite. The filtrate was then acidified with 1 M HCl aq. The resulting solid was collected by filtration and washed twice with water and three times with hexane/Et_2O = 1/1. After drying *in vacuo*, compound **9** was obtained as a white solid (4.57 g, 16.3 mmol, 93%). ^{1}H NMR (CD_3OD, 400 MHz) δ 3.96 (s, 3H) ^{13}C NMR (CD_3OD, 100 MHz) δ 164.3 (C), 163.9 (C), 158.8 (C), 134.6 (C), 124.2 (C), 112.9 (C), 62.8 (CH_3) HRMS (ESI) *m*/*z* calcd. for $C_7H_3{}^{81}BrO_5SNa$ [M–2H+Na]$^-$: 302.8767; found: 302.8768.

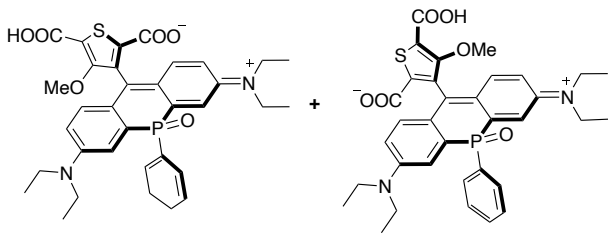

***cis*-POR715** ***trans*-POR715**

POR715. To a solution of **9** (169 mg, 0.600 mmol) in anhydrous THF (8 mL) was slowly dropwise added *n*-BuLi (1.62 M in *n*-hexane, 1.10 mL, 1.78 mmol) at −78 °C, and the resulting mixture was stirred for 20 min at the same temperature. After warming to room temperature, the solution was stirred for another 40 min, to which

was added a solution of *P*-xanthone **10** (90.8 mg, 0.203 mmol) in THF (3 mL). The reaction mixture was stirred for 1 h at 60 ºC. After cooling to room temperate, 1 M HCl aq. (7 mL) was added, and the mixture was further stirred for 1 h at 50 ºC. The solvent was then removed by rotary evaporation, and the resulting mixture was diluted with water and washed with Et_2O twice, followed by extraction of the aqueous layer with CH_2Cl_2 six times. The combined organic layers were washed with brine, dried over anhydrous Na_2SO_4, filtered, and concentrated under reduced pressure. The resulting crude was purified by silica-gel column chromatography, eluting with CH_2Cl_2/CH_3OH (9/1, v/v, 0–0.1% TFA). R_f = 0.15 (10% CH_3OH in CH_2Cl_2 containing 0.1% TFA). The obtained compound was further purified by reversed phase HPLC (ODS, 5 mM $HCOONH_4$ aq./CH_3CN, 80/20 to 70/30) to afford ***cis*-POR715** (7.5 mg, 12 μmol, 6%) and ***trans*-POR715** (30.9 mg, 49.0 μmol, 24%) as a dark green solid. ***cis*-POR715:** ^{1}H NMR (CD_3OD, 400 MHz) δ 7.76 (dd, J = 12.8, 7.6 Hz, 2H), 7.65-7.60 (m, 3H), 7.54 (td, J = 7.6, 3.5 Hz, 2H), 7.31 (dd, J = 9.8, 6.1 Hz, 2H), 7.00 (dd, J = 9.8, 2.8 Hz, 2H), 3.79 (s, 3H), 3.75 (q, J = 7.0 Hz, 8H), 1.29 (t, J = 7.0 Hz, 12H). ^{13}C NMR (CD_3OD, 150 MHz) δ 162.9 (s, C), 162.8 (s, C), 160.0 (s, C), 158.6 (d, J = 5.8 Hz, C), 155.1 (d, J = 13.0 Hz, C), 140.7 (d, J = 8.7 Hz, CH), 139.2 (d, J = 95.4 Hz, C), 137.1 (s, C), 136.1 (s, C), 134.4 (s, CH), 133.9 (d, J = 109.8 Hz, C), 130.8 (d, J = 11.6 Hz, CH), 130.6 (d, J = 13.0 Hz, CH), 124.7 (d, J = 7.2 Hz, C), 124.4 (s, C), 120.6 (d, J = 7.2 Hz, CH), 117.1 (s, CH), 63.7 (s, CH_3), 47.6 (s, CH_2), 13.1 (s, CH_3). ^{31}P NMR (CD_3OD, 202 MHz) δ 9.6. HRMS (ESI) *m*/*z* calcd. for $C_{34}H_{36}N_2O_6PS$ $[M+H]^+$: 631.2027; found: 631.2041. ***trans*-POR715**: ^{1}H NMR (CD_3OD, 400 MHz) δ 7.91 (dd, J = 13.4, 7.3 Hz, 2H), 7.62-7.50 (m, 5H), 7.30 (dd, J = 9.8, 6.1 Hz, 2H), 7.00 (dd, J = 9.8, 2.4 Hz, 2H), 3.84 (s, 3H), 3.72 (q, J = 7.0 Hz, 8H), 1.26 (t, J = 7.0 Hz, 12H). ^{13}C NMR (CD_3OD, 125 MHz) δ 163.1 (s, C), 162.9 (s, C), 160.4 (s, C), 158.8 (d, J = 7.2 Hz, C), 155.1 (d, J = 13.3 Hz, C), 140.7 (d, J = 8.5 Hz, CH), 139.6 (d, J = 94.2 Hz, C), 137.3 (s, C), 135.7 (s, C), 134.3 (s, CH), 133.5 (d, J = 109.8 Hz, C), 131.3 (d, J = 10.9 Hz, CH), 130.5 (d, J = 13.3 Hz, CH), 124.6 (d, J = 6.0 Hz, C), 123.9 (s, C), 120.9 (d, J = 7.2 Hz, CH), 117.1 (s, CH), 63.5 (s, CH_3), 47.6 (s, CH_2), 13.1 (s, CH_3). ^{31}P NMR (CD_3OD, 162 MHz) δ 9.3. HRMS (ESI) *m*/*z* calcd. for $C_{34}H_{36}N_2O_6PS$ $[M+H]^+$: 631.2027; found: 631.2037.

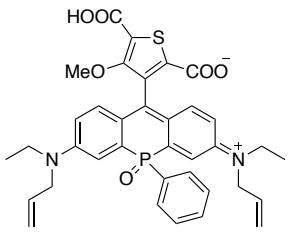

11

Compound 11. The title compound was synthesized according to a similar procedure for **POR715** using *P*-xanthone **5** (282 mg, 0.600 mmol) instead of *P*-xanthone **10**. The product was purified by silica-gel column chromatography, eluting with $CHCl_3$/CH_3OH (9/1, v/v, 0.1% TFA), followed by precipitation by addition of Et_2O to a solution of the product in CH_2Cl_2/EtOH (9/1) with frequent sonication. The compound was obtained as a mixture of *cis*- and *trans*-isomers and used for the next reaction without separation. R_f = 0.23 (10% CH_3OH in CH_2Cl_2 containing 0.1% TFA, v/v). Yield: 223 mg (0.340 mmol, 57%). ^{1}H NMR (CD_3OD, 400 MHz) δ 7.86 (dd, J = 12.8, 7.9 Hz, *trans*), 7.72 (dd, J = 12.8, 7.9 Hz, *cis*), 7.64-7.48 (m, 5H), 7.35-7.31 (m, 2H), 7.02 (brd, J

= 9.8 Hz, 2H), 5.95-5.82 (m, 2H), 5.25-5.06 (m, 4H), 4.34-4.28 (m, 4H), 3.84-3.69 (m, 7H), 1.31-1.25 (m, 6H). ^{31}P NMR (CD_3OD, 162 MHz) δ 9.4, 9.1. HRMS (ESI) *m*/*z* calcd. for $C_{36}H_{36}N_2O_6PS$ $[M+H]^+$: 655.2027; found: 655.2030.

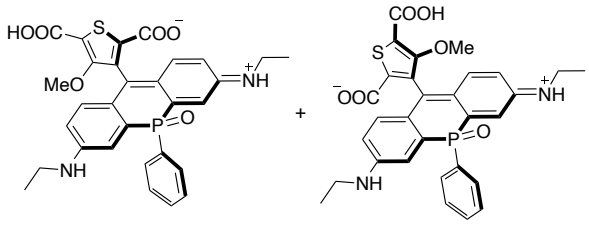

***cis*-POR675** ***trans*-POR675**

POR675. A solution of **11** (174 mg, 0.266 mmol), dimethylbarbituric acid (209 mg, 1.34 mmol), and $Pd(PPh_3)_4$ (60.6 mg, 52.4 μmol) in a mixture of anhydrous CH_2Cl_2 (5 mL) and anhydrous CH_3OH (5 mL) was stirred for 16 h at room temperature, and then concentrated under reduced pressure. The resulting mixture was purified by silica-gel column chromatography eluting with CH_2Cl_2/CH_3OH (17/3, v/v, 0.1% TFA). R_f = 0.28 (15% CH_3OH in CH_2Cl_2 containing 0.1% TFA, v/v). The obtained compound was further purified by reversed phase HPLC (ODS, water/CH_3CN containing 0.1% TFA, 70/30 to 65/35) to afford ***cis*-POR675** (10.5 mg, 18.3 μmol, 7%) and ***trans*-POR675** (46.7 mg, 81.3 μmol, 31%) as a turquoise blue solid. ***cis*-POR675:** ^{1}H NMR (CD_3OD, 400 MHz) δ 7.74 (dd, *J* = 12.8, 7.3 Hz, 2H), 7.62 (t, *J* = 7.3 Hz, 1H), 7.54 (td, *J* = 7.3, 3.6 Hz, 2H), 7.45 (d, *J* = 17.1 Hz, 2H), 7.31 (brs, 2H), 6.84 (d, *J* = 9.8 Hz, 2H), 3.79 (s, 3H), 3.48 (q, *J* = 7.3 Hz, 4H), 1.29 (t, *J* = 7.3 Hz, 6H). ^{13}C NMR (CD_3OD, 150 MHz) δ 162.8 (s, C), 162.6 (s, C), 160.1 (s, C), 159.0 (d, *J* = 5.8 Hz, C), 157.4 (d, *J* = 13.0 Hz, C), 142.5 (s, CH), 137.4 (s, C), 135.4 (s, C), 134.4 (s, CH), 133.7 (d, *J* = 109.8 Hz, C), 130.9 (d, *J* = 10.1 Hz, CH), 130.6 (d, *J* = 13.0 Hz, CH), 124.7 (s, C), 124.3 (s, C), 114.4 (s, CH), 63.7 (s, CH_3), 39.6 (s, CH_2), 14.0 (s, CH_3). One C peak and one CH peak were overlapped. ^{31}P NMR (CD_3OD, 162 MHz) δ 8.2. HRMS (ESI) *m*/*z* calcd. for $C_{30}H_{28}N_2O_6PS$ $[M+H]^+$: 575.1401; found: 575.1402. ***trans*-POR675:** ^{1}H-NMR (CD_3OD, 400 MHz) δ 7.88 (dd, *J* = 12.8, 7.3 Hz, 2H), 7.60 (td, *J* = 7.3, 2.0 Hz, 1H), 7.51 (td, *J* = 7.3, 3.3 Hz, 2H), 7.39 (dd, *J* = 15.9, 2.4 Hz, 2H), 7.29 (brs, 2H), 6.84 (dd, *J* = 9.5, 2.4 Hz, 2H), 3.84 (s, 3H), 3.45 (q, *J* = 7.3 Hz, 4H), 1.27 (t, *J* = 7.3 Hz, 7H). ^{13}C NMR (CD_3OD, 150 MHz) δ 162.9 (s, C), 162.6 (s, C), 160.5 (s, C), 159.0 (s, C), 157.4 (d, *J* = 13.0 Hz, C), 142.2 (brs, CH), 137.7 (s, C), 134.7 (s, C), 134.2 (s, CH), 133.4 (d, *J* = 109.8 Hz, C), 131.4 (d, *J* = 10.1 Hz, CH), 130.4 (d, *J* = 13.0 Hz, CH), 124.9 (brs, CH), 124.6 (s, C), 123.8 (s, C), 114.4 (brs, CH), 63.6 (s, CH_3), 39.6 (s, CH_2), 14.0 (s, CH_3). One C peak was overlapped. ^{31}P NMR (CD_3OD, 162 MHz) δ 8.1. HRMS (ESI) *m*/*z* calcd. for $C_{30}H_{28}N_2O_6PS$ $[M+H]^+$: 575.1401; found: 575.1395.

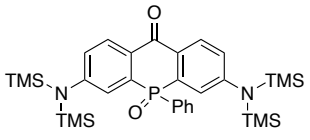

13

Compound 13. To a suspension of *P*-xanthone **12** (80.4 mg, 0.240 mmol) in anhydrous THF (12 mL) was slowly dropwise added LiHMDS (0.572 M prepared in anhydrous THF, 1.60 mL, 0.916 mmol) at −78 °C and

the resulting mixture was stirred for 5 min at the same temperature. TMSCl (0.130 mL, 1.03 mmol) was added at −78 °C and the reaction solution was allowed to warm up to room temperature, and stirring was continued for 10 min. The mixture was again cooled to −78 °C and LiHMDS (0.900 mL, 0.515 mmol) was added. After stirring for 2 min, TMSCl (0.0700 mL, 0.554 mmol) was added, and the solution was stirred for 20 h at room temperate. All volatiles were removed under reduced pressure, the resulting mixture was redissolved in CH_2Cl_2 and filtered. The filtrate was evaporated, the crude was dissolved in hexane and filtered again. The filtrate was concentrated under reduced pressure and dried *in vacuo* to afford **13** (126 mg, 0.201 mmol, 84%) as a yellow solid. ^{1}H NMR (CD_3OD, 500 MHz) δ 8.36 (dd, J = 9.0, 5.0 Hz, 2H), 7.58-7.53 (m, 3H), 7.47 (td, J = 7.3, 3.0 Hz, 2H), 7.38-7.34 (m, 4H), 0.06 (s, 36H). ^{13}C NMR (CD_3OD, 100 MHz) δ 182.0 (d, J = 9.6 Hz, C), 156.8 (d, J = 12.5 Hz, C), 135.6 (s, CH), 134.0 (d, J = 97.3 Hz, C), 133.7 (s, CH), 133.6 (d, J = 110.8 Hz, C), 132.5 (d, J = 6.7 Hz, C), 132.4 (d, J = 5.8 Hz, CH), 131.7 (d, J = 10.6 Hz, CH), 131.6 (d, J = 11.6 Hz, CH), 130.2 (d, J = 12.5 Hz, CH), 2.2 (s, CH_3). ^{31}P NMR (CD_3OD, 202 MHz) δ 5.8. HRMS (ESI) m/z calcd. for $C_{31}H_{47}N_2O_2PSi_4Na$ $[M+Na]^+$: 645.2345; found: 645.2343.

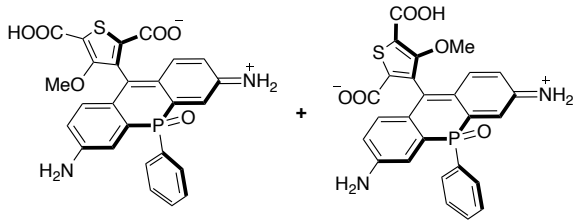

***cis*-POR645** ***trans*-POR645**

POR645. To a solution of **9** (100 mg, 0.356 mmol) in anhydrous THF (5 mL) was slowly dropwise added *n*-BuLi (1.59 M in *n*-hexane, 0.68 mL, 1.08 mmol) at −78 °C, and the resulting mixture was stirred for 20 min at the same temperature. After warming to room temperature, the solution was stirred for another 20 min, to which was added a solution of *P*-xanthone **13** (74.8 mg, 0.120 mmol) in THF (2 mL). The reaction mixture was stirred for 1 h at 60 ºC. After cooling to room temperate, 1 M HCl aq. (5 mL) was added, and the mixture was further stirred for 1 h at 50 ºC, followed by neutralization with sat $NaHCO_3$ aq. The solvent was then removed by rotary evaporation, and the resulting mixture was dissolved in CH_3OH and filtered. The filtrate was concentrated, and the resulting mixture was purified by silica-gel column chromatography, eluting with CH_2Cl_2/CH_3OH (8/2, v/v, 0.1% TFA). R_f = 0.25 (20% CH_3OH in CH_2Cl_2 containing 0.1% TFA). The obtained compound was further purified by reversed phase HPLC (ODS, water/CH_3CN containing 0.1% TFA, 80/20 to 60/40) to afford ***cis*-POR715** (9.8 mg, 19 μmol, 16%) and ***trans*-POR715** (26.0 mg, 50.1 μmol, 42%) as a dark blue solid. ***cis*-POR645:** ^{1}H NMR (CD_3OD, 400 MHz) δ 7.74 (dd, J = 12.8, 7.1 Hz, 2H), 7.63 (t, J = 7.1 Hz, 1H), 7.55 (td, J = 7.1, 3.5 Hz, 2H), 7.45 (dd, J = 15.3, 2.4 Hz, 2H), 7.27 (dd, J = 9.3, 5.8 Hz, 2H), 6.79 (dd, J = 9.3, 2.4 Hz, 2H), 3.80 (s, 3H). ^{13}C NMR (CD_3OD, 150 MHz) δ 162.7 (s, C), 162.5 (s, C), 160.3 (d, J = 7.2 Hz, C), 159.9 (d, J = 13.0 Hz, C), 142.0 (d, J = 8.7 Hz, CH), 140.4 (d, J = 95.4 Hz, C), 137.4 (s, C), 135.3 (s, C), 134.4 (s, CH), 133.4 (d, J = 109.8 Hz, C), 130.9 (d, J = 11.6 Hz, CH), 130.6 (d, J = 13.0 Hz, CH), 124.7 (d, J = 5.8 Hz, C), 124.3 (s, C), 123.1 (d, J = 7.2 Hz, CH), 118.7 (s, CH), 63.7 (s, CH_3). One C peak was overlapped. ^{31}P NMR (CD_3OD, 162 MHz) δ 7.9. HRMS (ESI) m/z calcd. for $C_{26}H_{20}N_2O_6PS$ $[M+H]^+$: 519.0775; found: 519.0776. ***trans*-**

POR645: ^{1}H NMR (CD_3OD, 400 MHz) δ 7.88 (dd, J = 13.1, 7.3 Hz, 2H), 7.61 (t, J = 7.3 Hz, 1H), 7.52 (td, J = 7.3, 3.3 Hz, 2H), 7.38 (dd, J = 15.9, 2.4 Hz, 2H), 7.26 (dd, J = 9.2, 6.1 Hz, 2H), 6.79 (dd, J = 9.2, 2.4 Hz, 2H), 3.85 (s, 3H). ^{13}C NMR (CD_3OD, 125 MHz) δ 162.9 (s, C), 162.6 (s, C), 160.5 (s, C), 160.4 (d, J = 7.2 Hz, C), 160.0 (d, J = 13.3 Hz, C), 142.0 (d, J = 8.5 Hz, CH), 140.8 (d, J = 94.2 Hz, C), 137.7 (s, C), 134.6 (s, C), 134.3 (s, CH), 133.1 (d, J = 111.1 Hz, C), 131.4 (d, J = 12.1 Hz, CH), 130.5 (d, J = 13.3 Hz, CH), 124.6 (d, J = 6.0 Hz, C), 123.8 (s, C), 123.5 (d, J = 7.2 Hz, CH), 118.7 (s, CH), 63.6 (s, CH_3). ^{31}P NMR (CD_3OD, 162 MHz) δ 7.6. HRMS (ESI) m/z calcd. for $C_{26}H_{20}N_2O_6PS$ $[M+H]^+$: 519.0775; found: 519.0777.

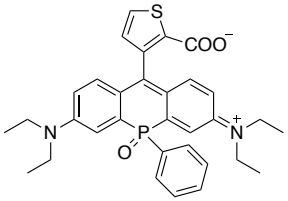

14

Compound 14. To a solution of 3-bromothiophene-2-carboxylic acid (112 mg, 0.539 mmol) in anhydrous THF (4.0 mL) was dropwise added *sec*-BuLi (1.22 M in cyclohexane and *n*-hexane, 0.890 mL, 1.09 mmol) at –78 °C. After stirring for 1.5 h at the same temperature, a solution of *P*-xanthone **10** (80.4 mg, 0.180 mmol) in anhydrous THF (3.0 mL) was added to the mixture at the same temperature. The reaction mixture was allowed to warm up to room temperature and further stirred at 50 °C for 1 h. Then 5 mL of l M HCl aq. was added at room temperature and stirring was continued for 30 min at 50 °C. After removal of the solvent under reduced pressure, the resulting mixture was diluted with water and washed with Et_2O three times. The aqueous layer was extracted with CH_2Cl_2 seven times, and the combined organic layers were washed with brine, dried over Na_2SO_4, filtered, and concentrated. The mixture was purified by silica gel column chromatography, eluting with CH_2Cl_2 /CH_3OH (49/1 to 9/1, v/v, containing 0.1% TFA). R_f = 0.52 (10% CH_3OH in CH_2Cl_2 containing 0.1% TFA). The obtained compound was further purified by reversed phase HPLC (ODS, water/CH_3CN containing 0.1% TFA, 60/40 to 0/100) to afford **14** (50.0 mg, 89.8 μmol, 50%) as a green solid. ^{1}H NMR (CD_3OD, 500 MHz) δ 8.03 (d, J = 4.6 Hz, 1H), 7.93 (dd, J = 13.0, 7.7 Hz, *trans*), 7.73 (dd, J = 13.0, 7.7 Hz, *cis*), 7.63-7.49 (m, 5H), 7.22-7.18 (m, 3H), 6.98-6.95 (m, 2H), 3.77-3.67 (m, 8H), 1.29-1.20 (m, 12H). ^{31}P NMR (CD_3OD, 202 MHz) δ 9.5, 9.2. HRMS (ESI) m/z calcd. for $C_{32}H_{34}N_2O_3PS$ $[M+H]^+$: 557.2022; found: 557.2018.

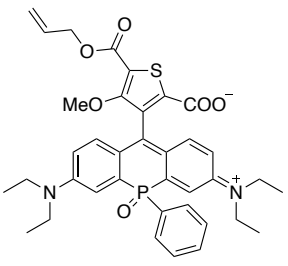

15

Compound 15. To a solution of **POR715** (115 mg, 0.182 mmol) in anhydrous DMF (3.0 mL) was added K_2CO_3 (51.9 mg, 0.376 mmol) and DIEA (63.6 μL, 0.365 mmol). Allyl bromide (23.0 μL, 0.272 mmol) was added to

the suspension at 0 ºC, and the mixture was stirred for 3 h at room temperature. The reaction mixture was diluted with 1 M HCl aq. and extracted with $CHCl_3$ three times. The organic layer was washed with 0.1 M HCl aq. and brine, dried over Na_2SO_4, filtered, and concentrated under reduced pressure. The resulting crude was purified by silica-gel column chromatography, eluting with CH_2Cl_2/CH_3OH (19/1 to 9/1, v/v, containing 0.1% TFA), to afford **14** (69.8 mg, 0.104 mmol, 57%) as a dark green solid. R_f = 0.48 (10% CH_3OH in CH_2Cl_2 containing 0.1% TFA). ^{1}H NMR (CD_3OD, 500 MHz) δ 7.91 (dd, J = 13.0, 7.3 Hz, 2H), 7.62-7.58 (m, 1H), 7.55 (dd, J = 16.1, 2.9 Hz, 2H), 7.51 (td, J = 7.3, 3.3 Hz, 2H), 7.30 (dd, J = 9.8, 6.1 Hz, 2H), 7.00 (dd, J = 9.8, 2.9 Hz, 2H), 6.13-6.05 (m, 1H), 5.50-5.46 (m, 1H), 5.36-5.33 (m, 1H), 4.88-4.87 (m, 2H), 3.84 (s, 3H), 3.72 (q, J = 6.9 Hz, 8H), 1.26 (t, J = 6.9 Hz, 12H). ^{13}C NMR (CD_3OD, 150 MHz) δ 162.4 (s, C), 161.0 (s, C), 160.9 (s, C), 157.9 (d, J = 5.8 Hz, C), 155.1 (d, J = 13.0 Hz, C), 140.5 (d, J = 8.7 Hz, CH), 139.5 (d, J = 93.9 Hz, C), 137.5 (s, C), 135.4 (s, C), 134.3 (s, CH), 133.5 (d, J = 109.8 Hz, C), 133.0 (s, CH), 131.2 (d, J = 10.1 Hz, CH), 130.5 (d, J = 13.0 Hz, CH), 124.4 (d, J = 5.8 Hz, C), 122.3 (s, C), 121.0 (d, J = 7.2 Hz, CH), 119.3 (s, CH_2), 117.1 (s, CH), 67.3 (s, CH_2), 63.7 (s, CH_3), 47.6 (s, CH_2), 13.1 (s, CH_3). ^{31}P NMR (CD_3OD, 202 MHz) δ 9.2. HRMS (ESI) m/z calcd. for $C_{37}H_{40}N_2O_6PS$ $[M+H]^+$: 671.2340; found: 671.2340.

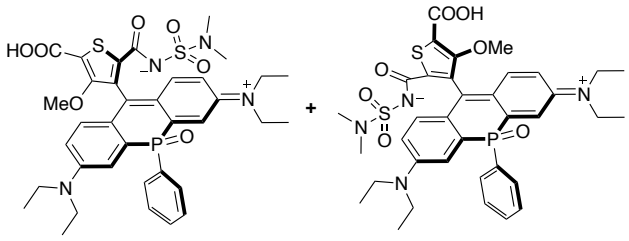

***cis*-PORSA715** ***trans*-PORSA715**

PORSA715. A solution of **15** (16.5 mg, 24.6 μmol), EDC·HCl (7.2 mg, 38 μmol), DMAP (4.6 mg, 38 μmol), and *N,N*-dimethylsulfamide (21.8 mg, 0.176 mmol) in anhydrous CH_2Cl_2 (2 mL) was stirred for 17 h at room temperature. EDC·HCl (6.1 mg, 32 μmol) and *N,N*-dimethylsulfamide (18.1 mg, 0.146 mmol) were added again, and the reaction solution was further stirred for 5 h at the same temperature. The mixture was diluted with water, acidified with 0.1 M HCl aq., and extracted with CH_2Cl_2 for seven times. The organic layers were washed with brine, dried over Na_2SO_4, filtrated, and concentrated under reduced pressure. The amide compound obtained was dissolved in anhydrous CH_2Cl_2 (2 mL), to which was added dimethylbarbituric acid (15.4 mg, 98.6 μmol) and $Pd(PPh_3)_4$ (12.6 mg, 10.9 μmol). After the mixture was stirred for 16 h at room temperature, the resulting suspension was filtered and washed the precipitate with CH_3OH. The filtrate was then evaporated, and the crude product was dissolved in a mixture of water and CH_3CN (1/1, v/v) containing 0.1% TFA, followed by filtration through Presep® (Wako, ODS). The compound was purified by reversed phase HPLC, eluting with H_2O/CH_3CN (60/40 to 30/70, v/v, containing 0.1% TFA), to afford ***cis*-PORSA715** (2.9 mg, 3.9 μmol, 16% for two steps) and ***trans*-PORSA715** (3.4 mg, 4.6 μmol, 19% for two steps) as a green solid. ***cis*-PORSA715:** ^{1}H NMR (CD_3OD, 400 MHz) δ 7.78 (dd, J = 12.5, 6.9 Hz, 2H), 7.57 (t, J = 6.9 Hz, 1H), 7.52 (td, J = 6.9, 3.2 Hz, 2H), 7.10-7.02 (m, 4H), 6.97 (dd, J = 9.2, 2.4 Hz, 2H), 3.48-3.35 (m, 8H), 3.22 (s, 3H), 2.69 (s, 6H), 1.07 (t, J = 7.0 Hz, 12H). ^{13}C NMR (CD_3OD, 150 MHz) δ 164.1 (s, C), 163.1 (s, C), 156.9 (s, C), 155.4 (s, C), 148.8 (d, J = 11.6 Hz, C), 136.2 (d, J = 111.3 Hz, C), 133.0 (s, CH), 132.5 (d, J = 10.1 Hz, CH), 132.1 (s, C), 131.6 (s,

C), 130.8 (d, J = 10.1 Hz, CH), 130.7 (d, J = 105.5 Hz, C), 129.6 (d, J = 13.0 Hz, CH), 124.8 (d, J = 7.2 Hz, C), 117.3 (s, CH), 114.0 (d, J = 8.7 Hz, CH), 62.6 (s, CH_3), 45.3 (s, CH_2), 38.2 (s, CH_3), 12.5 (s, CH_3). One C peak was overlapped. ^{31}P NMR (CD_3OD, 162 MHz) δ 9.8. HRMS (ESI) m/z calcd. for $C_{36}H_{42}N_4O_7PS_2$ $[M+H]^+$: 737.2228; found: 737.2224. ***trans*-PORSA715:** ^{1}H NMR ($CDCl_3$, 400 MHz) δ 7.97 (dd, J = 12.5, 7.0 Hz, 2H), 7.46-7.41 (m, 3H), 7.07 (t, J = 8.4 Hz, 2H), 6.82 (d, J = 14.7 Hz, 2H), 6.71 (d, J = 8.4 Hz, 2H), 3.31-3.10 (m, 11H), 2.90 (s, 6H), 0.95 (t, J = 7.0 Hz, 12H). ^{13}C NMR ($CDCl_3$, 150 MHz) δ 164.0 (s, C), 162.5 (s, C), 157.3 (s, C), 153.3 (s, C), 147.3 (d, J = 13.0 Hz, C), 133.5 (d, J = 112.7 Hz, C), 133.3 (s, C), 132.4 (d, J = 11.6 Hz, CH), 131.7 (s, CH), 129.4 (d, coupling partner was overlapped with 128.8., C), 128.8 (d, J = 10.1 Hz, CH), 128.3 (d, J = 13.0 Hz, CH), 128.0 (s, C), 123.8 (d, J = 5.8 Hz, C), 115.9 (s, CH), 113.5 (d, J = 8.7 Hz, CH), 62.8 (s, CH_3), 44.2 (s, CH_2), 38.4 (s, CH_3), 12.3 (s, CH_3). One C peak was overlapped. ^{31}P NMR ($CDCl_3$, 162 MHz) δ 11.2. HRMS (ESI) m/z calcd. for $C_{36}H_{42}N_4O_7PS_2$ $[M+H]^+$: 737.2228; found: 737.2219.

General procedure for the synthesis of fluorescent HaloTag ligands

A solution of each POR dye, 2-(2-((6-chlorohexyl)oxy)ethoxy)ethan-1-amine･TFA (1.2 eq.), HBTU (1.2 eq.), and DIEA (5.0 eq.) in DMSO was stirred for 3 h at room temperature. The reaction mixture was diluted with a mixture of water and CH_3CN (1/1, v/v) containing 0.1% TFA, followed by filtration through Presep® (Wako, ODS). The filtrate was purified by reversed phase HPLC, eluting with H_2O/CH_3CN containing 0.1% TFA, to yield the target compounds.

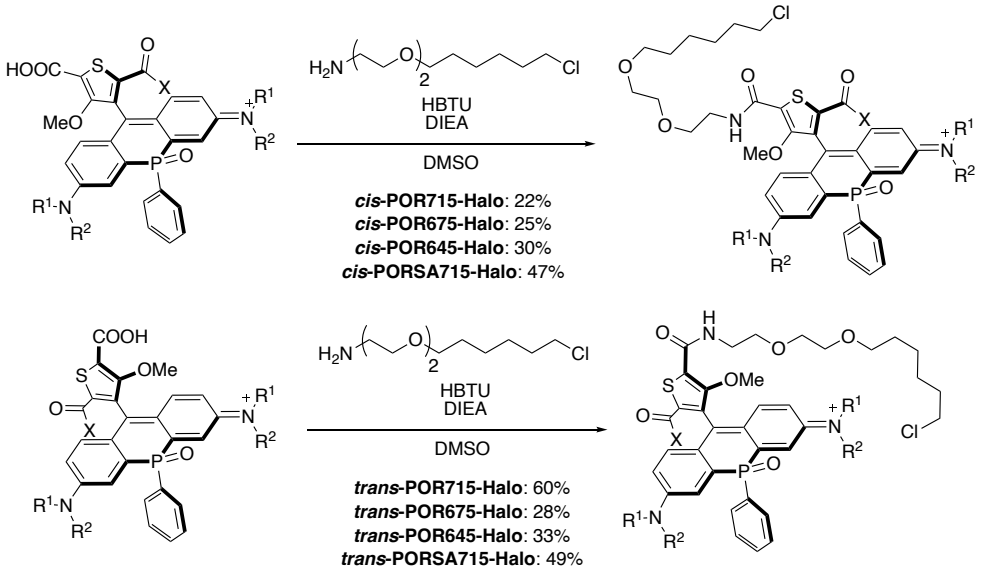

Scheme S2. Synthesis of fluorescent HaloTag ligands.

***cis*-POR715-Halo.** 1.0 mg yield (1.2 μmol, 22%) as a dark green solid. ^{1}H NMR (CD_3OD, 400 MHz) δ 8.50 (brs, 1H), 7.73-7.60 (m, 5H), 7.51 (td, J = 7.6, 2.8 Hz, 2H), 7.42 (dd, J = 9.7, 6.4 Hz, 2H), 7.00 (dd, J = 9.7, 2.4 Hz, 2H), 3.75 (q, J = 7.7 Hz, 8H), 3.67-3.52 (m, 11H), 3.46-3.40 (m, 4H), 1.66-1.59 (m, 2H), 1.50-1.43 (m, 2H), 1.31-1.21 (m, 16H). ^{31}P NMR (162 MHz, CD_3OD): δ 9.7. HRMS (ESI) m/z calcd. for $C_{44}H_{56}ClN_3O_7PS$ $[M+H]^+$: 836.3260; found: 836.3257. A satisfactory ^{13}C NMR spectrum was not obtained due to a small amount of product and the splitting of carbon signals.

***trans*-POR715-Halo.** 1.2 mg yield (1.4 μmol, 60%) as a dark green solid. ^{1}H NMR (CD_3OD, 500 MHz) δ 8.21 (t, J = 5.4 Hz, 1H), 7.92 (dd, J = 13.0, 6.5 Hz, 2H), 7.60 (td, J = 6.5, 1.5 Hz, 1H), 7.58-7.50 (m, 4H), 7.38 (dd, J = 9.8, 6.1 Hz, 2H), 7.02 (dd, J = 9.8, 2.7 Hz, 2H), 3.77-3.63 (m, 17H), 3.58-3.56 (m, 2H), 3.52 (t, J = 6.5 Hz, 2H), 3.44 (t, J = 6.5 Hz, 2H), 1.74-1.68 (m, 2H), 1.54-1.48 (m, 2H), 1.42-1.29 (m, 4H), 1.26 (t, J = 7.3 Hz, 12H). ^{31}P NMR (162 MHz, CD_3OD): δ 9.2. HRMS (ESI) *m*/*z* calcd. for $C_{44}H_{56}ClN_3O_7PS$ $[M+H]^+$: 836.3260; found: 836.3251. A satisfactory ^{13}C NMR spectrum was not obtained due to a small amount of product and the splitting of carbon signals.

***cis*-POR675-Halo.** 1.0 mg yield (1.3 μmol, 25%) as a turquoise blue solid. ^{1}H NMR (CD_3OD, 400 MHz) δ 8.19 (t, J = 5.2 Hz, 1H), 7.73-7.63 (m, 3H), 7.58-7.48 (m, 4H), 7.36 (brs, 2H), 6.86 (d, J = 9.2 Hz, 2H), 3.67-3.40 (m, 19H), 1.66-1.59 (m, 2H), 1.50-1.42 (m, 3H), 1.33-1.22 (m, 10H). ^{31}P NMR (202 MHz, CD_3OD): δ 8.5. HRMS (ESI) *m*/*z* calcd. for $C_{40}H_{48}ClN_3O_7PS$ $[M]^+$: 780.2634; found: 780.2641. A satisfactory ^{13}C NMR spectrum was not obtained due to a small amount of product and the splitting of carbon signals.

***trans*-POR675-Halo.** 1.6 mg yield (2.1 μmol, 28%) as a turquoise blue solid. ^{1}H NMR (CD_3OD, 400 MHz) δ 8.19 (t, J = 5.5 Hz, 1H), 7.89 (dd, J = 13.4, 7.4 Hz, 2H), 7.61 (t, J = 7.4 Hz, 1H), 7.53 (td, J = 7.4, 2.8 Hz, 2H), 7.41-7.35 (m, 4H), 6.85 (dd, J = 9.8, 2.4 Hz, 2H), 3.74 (s, 3H), 3.68-3.64 (m, 6H), 3.58-3.56 (m, 2H), 3.52 (t, J = 6.7 Hz, 2H), 3.49-3.42 (m, 6H), 1.75-1.68 (m, 2H), 1.55-1.48 (m, 2H), 1.44-1.26 (m, 10H). ^{31}P NMR (202 MHz, CD_3OD): δ 8.1. HRMS (ESI) *m*/*z* calcd. for $C_{40}H_{48}ClN_3O_7PS$ $[M+H]^+$: 780.2634; found: 780.2631. A satisfactory ^{13}C NMR spectrum was not obtained due to a small amount of product and the splitting of carbon signals.

***cis*-POR645-Halo.** 1.0 mg yield (1.4 μmol, 30%) as a dark blue solid. ^{1}H NMR (CD_3OD, 400 MHz) δ 8.19 (t, J = 6.0 Hz, 1H), 7.73-7.64 (m, 3H), 7.58 (td, J = 7.8, 3.2 Hz, 2H), 7.48 (dd, J = 15.6, 2.2 Hz, 2H), 7.32 (dd, J = 9.2, 6.1 Hz, 2H), 6.81 (dd, J = 9.2, 2.2 Hz, 2H), 3.67-3.55 (m, 11H), 3.47-3.40 (m, 4H), 1.65-1.60 (m, 2H), 1.50-1.43 (m, 2H), 1.33-1.25 (m, 4H). ^{31}P NMR (162 MHz, CD_3OD): δ 7.9. HRMS (ESI) *m*/*z* calcd. for $C_{36}H_{40}ClN_3O_7PS$ $[M+H]^+$: 724.2008; found: 724.2008. A satisfactory ^{13}C NMR spectrum was not obtained due to a small amount of product.

***trans*-POR645-Halo.** 1.1 mg yield (1.5 μmol, 33%) as a dark blue solid. ^{1}H NMR (CD_3OD, 500 MHz) δ 8.22 (t, J = 5.4 Hz, 1H), 7.89 (dd, J = 13.0, 7.3 Hz, 2H), 7.62 (t, J = 7.3 Hz, 1H), 7.53 (td, J = 7.3, 3.1 Hz, 2H), 7.38 (dd, J = 15.3, 2.3 Hz, 2H), 7.34 (dd, J = 9.4, 5.7 Hz, 2H), 6.80 (dd, J = 9.4, 2.3 Hz, 2H), 3.74 (s, 3H), 3.69-3.63 (m, 4H), 3.58-3.56 (m, 2H), 3.53 (t, J = 6.5 Hz, 2H), 3.44 (t, J = 6.5 Hz, 2H), 1.74-1.69 (m, 2H), 1.55-1.49 (m, 2H), 1.43-1.30 (m, 4H). ^{31}P NMR (202 MHz, CD_3OD): δ 7.6. HRMS (ESI) *m*/*z* calcd. for $C_{36}H_{40}ClN_3O_7PS$ $[M+H]^+$: 724.2008; found: 724.2011. A satisfactory ^{13}C NMR spectrum was not obtained due to a small amount of product and the splitting of carbon signals.

***cis*-PORSA715-Halo.** 1.7 mg yield (1.8 μmol, 47%) as a green solid. ^{1}H NMR (CD_3OD, 500 MHz) δ 8.06 (t, J = 5.0 Hz, 1H), 7.78 (dd, J = 12.6, 7.1 Hz, 2H), 7.59 (t, J = 7.1 Hz, 1H), 7.55 (td, J = 7.1, 3.0 Hz, 2H), 7.18-7.02 (m, 4H), 6.97 (dd, J = 9.2, 3.1 Hz, 2H), 3.64-3.34 (m, 20H), 3.07 (s, 3H), 2.69 (s, 6H), 1.70-1.64 (m, 2H), 1.45-1.23 (m, 6H), 1.09 (t, J = 6.9 Hz, 12H). ^{31}P NMR (202 MHz, CD_3OD): δ 9.6. HRMS (ESI) m/z calcd. for $C_{46}H_{62}ClN_5O_8PS_2$ $[M+H]^+$: 942.3461; found: 942.3464. A satisfactory ^{13}C NMR spectrum was not obtained due to a small amount of product and the splitting of carbon signals.

***trans*-PORSA715-Halo.** 1.2 mg yield (1.3 μmol, 49%) as a green solid. ^{1}H NMR (Acetone-d_6, 400 MHz) δ 8.01 (dd, J = 12.2, 7.1 Hz, 2H), 7.58-7.51 (m, 2H), 7.47 (td, J = 7.1, 2.8 Hz, 2H), 7.18 (dd, J = 9.0, 6.1 Hz, 2H), 6.93 (dd, J = 9.0, 2.8 Hz, 2H), 6.83 (dd, J = 14.4, 2.8 Hz, 2H), 3.61-3.26 (m, 23H), 2.86 (s, 6H), 1.77-1.70 (m, 2H), 1.50-1.38 (m, 4H), 1.35-1.29 (m, 2H), 1.03 (t, J = 7.0 Hz, 12H). ^{31}P NMR (162 MHz, Acetone-d_6): δ 4.7. HRMS (ESI) m/z calcd. for $C_{46}H_{62}ClN_5O_8PS_2$ $[M+H]^+$: 942.3461; found: 942.3471. A satisfactory ^{13}C NMR spectrum was not obtained due to a small amount of product and the splitting of carbon signals.

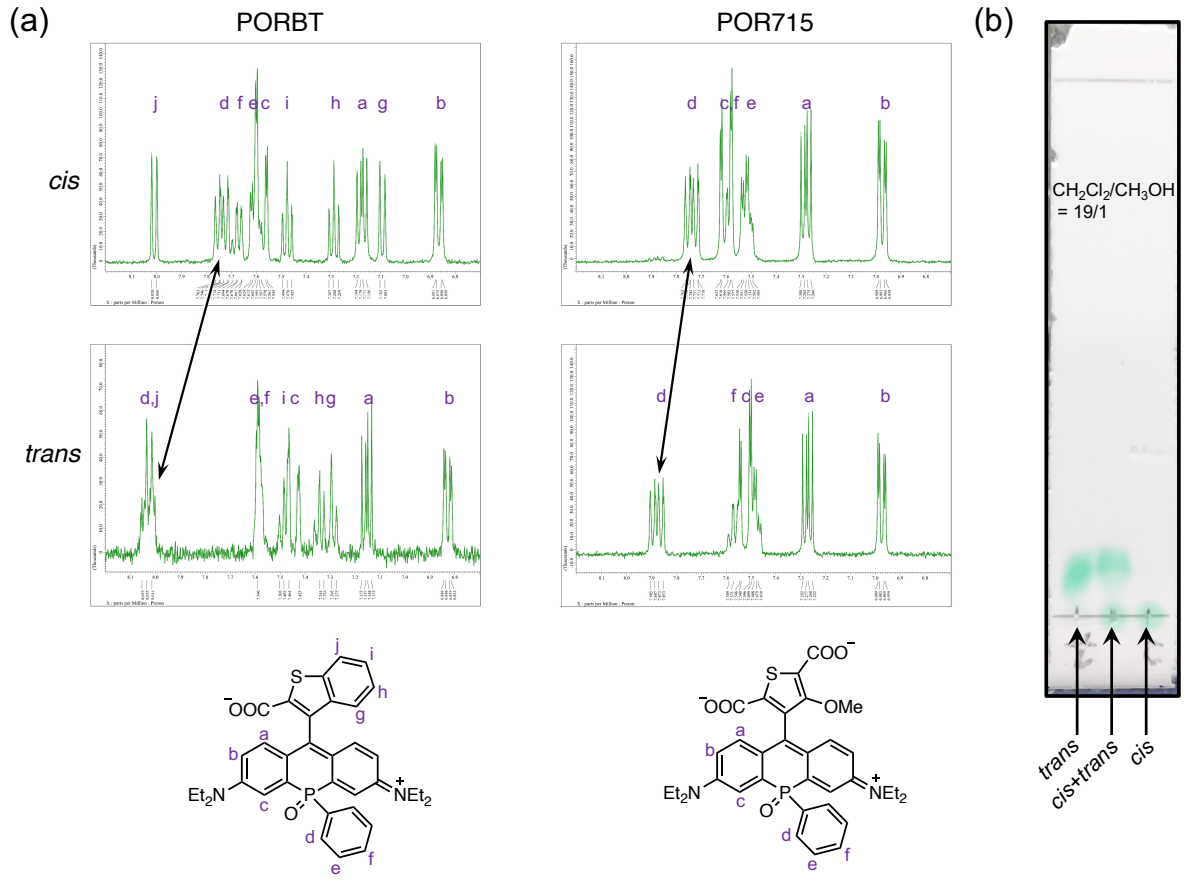

Fig. S1 (a) ^{1}H NMR spectra of *cis*-PORBT (top, left), *trans*-PORBT (bottom, left), *cis*-POR715 (top, right), and *trans*-POR715 (bottom, right) in CD_3OD with the corresponding peak assignments. (b) TLC of *cis*- and *trans*-POR715-Halo eluted with CH_2Cl_2/CH_3OH = 19/1.

2. Theoretical calculations

The geometry optimizations for ***trans*-POR715**, ***trans*-POR675**, and ***trans*-POR645** were carried out using density functional theory (DFT) at the level of M06-2X[7]/6-31+G[8] in aqueous phase using the SMD solvation model,[9] implemented in the Gaussian 16 Revision B.01 software package.[10] All stationary points were optimized without any symmetry assumptions and characterized by frequency analysis at the same level of theory (the number of imaginary frequencies, NIMAG, was 0). The cartesian coordinates of the optimized geometries are given in Tables S1~S3. The excitation energies for the optimized structures were calculated based on TD-DFT at the M06-2X/6-31+G(d) level of theory, using the SMD solvent model in water. The calculation results are shown in Fig. S2.

Table S1. Cartesian coordinate of *trans*-POR715 in the S_0 optimized at the M06-2X/6-31+G level of theory with water using the SMD.

atom	X	Y	Z	atom	X	Y	Z
H	2.21520982	2.23710156	0.15764788	H	5.53924133	-4.3158983	-0.686398
C	2.34370191	1.21308485	-0.1757923	C	6.25722754	-0.0660316	-1.2137151
C	2.72110204	-1.4172818	-1.0222627	H	5.97389212	0.92125681	-1.5863769
C	1.20196986	0.36001129	-0.2688192	H	7.00816096	-0.458494	-1.9012783
C	3.61005513	0.79481853	-0.4977625	C	6.83306489	0.02674345	0.19921785
C	3.85622626	-0.5399499	-0.9516855	H	7.6537599	0.75008763	0.21336382
C	1.46765656	-0.9755322	-0.6914357	H	7.22293691	-0.9413157	0.5244203
H	4.42651902	1.49535792	-0.392043	H	6.07393308	0.35365903	0.91654491
H	2.84810945	-2.4480191	-1.3319146	C	-6.3089478	-1.0913638	-0.6262354
C	-0.0990643	0.85062658	0.02867884	H	-6.190038	-0.0693342	-0.9912473
P	0.11954409	-2.2161482	-0.7438836	H	-6.9975931	-1.5941965	-1.3098967
C	-1.4057408	-1.2226193	-0.515121	C	-6.8624293	-1.1129764	0.79668987
C	-2.5965869	-1.8652287	-0.7138847	H	-7.8288385	-0.6018408	0.82633597
H	-2.591989	-2.9009172	-1.0332968	H	-6.1826722	-0.6095761	1.49084051
C	-3.8462863	-1.1816515	-0.5153331	H	-7.0061021	-2.1431764	1.13670886
C	-3.7767274	0.17970781	-0.0736334	C	-5.1127683	-3.2301673	-1.0850543
H	-4.6834119	0.73161652	0.13260599	H	-6.0834731	-3.5765342	-0.7213784
C	-2.5704447	0.79999672	0.11776419	H	-4.3535897	-3.79355	-0.5385073
H	-2.5748707	1.82911346	0.45919194	C	-4.9995113	-3.4568535	-2.5907514
C	-1.3192781	0.14559799	-0.1128126	H	-4.0303114	-3.1186724	-2.96979
O	0.10997701	-3.1408067	-2.0818024	H	-5.7882194	-2.9140537	-3.1206637
C	0.30866406	-3.2469789	0.77022514	H	-5.1049048	-4.5224547	-2.8132477

C	0.58722078	-4.8024485	3.05368664	C	-0.1964416	2.28019806	0.43867746
C	0.40582071	-2.6208933	2.01753885	C	-0.10312	2.75267427	1.7172347
C	0.34812298	-4.6357191	0.64866772	C	-0.4033479	3.32470594	-0.5247504
C	0.48916726	-5.4156193	1.80180534	C	-0.4568914	4.58241253	0.02409691
C	0.54535216	-3.4070512	3.16256851	S	-0.2547133	4.52534682	1.79739626
H	0.37216534	-1.5363398	2.09970728	O	-0.5849756	3.02870212	-1.8610503
H	0.2715813	-5.1023007	-0.3278546	C	0.60077375	3.17287428	-2.7305348
H	0.52212157	-6.4960312	1.71894989	H	1.28433486	2.34181366	-2.5474166
H	0.62158266	-2.9327533	4.13458291	H	0.21777927	3.13780252	-3.7478257
H	0.69636619	-5.4096564	3.94551887	H	1.08858259	4.12921992	-2.535467
N	-5.0188112	-1.8001743	-0.729445	C	0.09889894	1.97838205	2.97804817
N	5.08759451	-0.9630167	-1.3009955	C	-0.6725944	5.87419952	-0.600983
C	5.35176357	-2.381694	-1.6203377	O	0.20156381	0.70707764	2.87108467
H	6.31934644	-2.415763	-2.1227308	O	-0.8523157	5.82346222	-1.9438195
H	4.60896947	-2.7321063	-2.3424871	H	-1.0026867	6.71004435	-2.3392825
C	5.37483501	-3.2781214	-0.3815896	O	0.15287603	2.6435358	4.07273103
H	4.43026739	-3.2303135	0.16930109	O	-0.7004314	6.94597851	0.03007463
H	6.18239701	-2.9854769	0.29419766				

Table S2. Cartesian coordinate of *trans*-POR675 in the S_0 optimized at the M06-2X/6-31+G level of theory with water using the SMD.

atom	X	Y	Z	atom	X	Y	Z
H	1.72097403	-2.3534945	0.24300351	C	-0.8594913	-6.3127399	-1.2502806
C	0.72029246	-2.4321763	-0.1671158	H	0.17822547	-6.2026032	-1.578297
C	-1.8485776	-2.6604049	-1.2328402	H	-1.341821	-7.0156209	-1.9309261
C	-0.0472669	-1.2428256	-0.3630468	C	-0.9241633	-6.8350994	0.18408752
C	0.25033322	-3.6809165	-0.4924907	H	-0.3868055	-7.7850943	0.2557272
C	-1.0504663	-3.8369496	-1.0522862	H	-1.9622609	-7.0009847	0.48556143
C	-1.3628453	-1.4293325	-0.8920882	H	-0.4681377	-6.1288142	0.88451052
H	0.87828871	-4.5456146	-0.3215665	C	-0.9920762	6.34412003	-1.2325539
H	-2.8528848	-2.7711777	-1.6345842	H	0.05219202	6.25050106	-1.5444009
C	0.51161812	0.03116451	-0.0764456	H	-1.4767694	7.03414769	-1.9246037
P	-2.4981894	-0.001408	-1.0746671	C	-1.0876708	6.87344418	0.19745016
C	-1.3966905	1.45148811	-0.8838831	H	-0.5684557	7.83329583	0.27134011
C	-1.9078678	2.67242098	-1.2221995	H	-0.6296643	6.17947463	0.90878329

H	-2.911378	2.76252481	-1.6309209	H	-2.1329555	7.02251267	0.48242175
C	-1.1365396	3.86563313	-1.0315999	C	1.90453567	0.04625077	0.45311954
C	0.15952279	3.73731958	-0.4532835	C	2.26544929	-0.040383	1.76778971
H	0.76266996	4.61606489	-0.2653644	C	3.03485138	0.15062464	-0.4266383
C	0.65526833	2.4981647	-0.130573	C	4.24508482	0.13719176	0.22156133
H	1.64830041	2.44192462	0.3012864	S	4.03255979	-0.01176	1.98789209
C	-0.0802828	1.29229378	-0.3474007	O	2.85692094	0.30666916	-1.7864376
O	-3.3586491	-0.0072898	-2.4541314	C	3.008352	-0.9117178	-2.6077553
C	-3.5990278	-0.0164879	0.4007762	H	2.12809246	-1.5440935	-2.4773389
C	-5.2547093	-0.0330194	2.628574	H	3.08069819	-0.5607391	-3.6345412
C	-3.0273685	-0.0309201	1.67748596	H	3.91615461	-1.4429465	-2.317196
C	-4.9818725	-0.0104644	0.22125004	C	1.38593955	-0.1470833	2.97001298
C	-5.8124925	-0.0189499	1.34718213	C	5.59298775	0.26381611	-0.3016921
C	-3.8643291	-0.0390587	2.79481249	O	0.12124214	-0.1245444	2.77178322
H	-1.9458107	-0.0362991	1.80296277	O	5.65572885	0.44004867	-1.6443271
H	-5.4045739	0.00055332	-0.7779694	H	6.5763764	0.54717184	-1.9689273
H	-6.889133	-0.0145743	1.22047517	O	1.96462363	-0.2473643	4.10895112
H	-3.4333192	-0.0502115	3.78974124	O	6.61209724	0.2294602	0.41036389
H	-5.9017764	-0.039312	3.49881312	H	-2.4896427	-5.0529344	-1.7921541
N	-1.6546899	5.04631722	-1.3990665	H	-2.5919927	5.0518605	-1.787521
N	-1.5483676	-5.0283878	-1.4143296				

Table S3. Cartesian coordinate of *trans*-POR645 in the S_0 optimized at the M06-2X/6-31+G level of theory with water using the SMD.

atom	X	Y	Z	atom	X	Y	Z
H	1.59735093	-2.365893	0.19695661	H	-5.5038005	0.03898013	-0.9205755
C	0.59463653	-2.4364336	-0.2091734	H	-7.0304423	0.03823956	1.04660579
C	-1.9845252	-2.6430571	-1.2692912	H	-3.6295792	0.00794926	3.68820303
C	-0.1611607	-1.240134	-0.4186956	H	-6.0911233	0.02341179	3.3452464
C	0.10193275	-3.6787088	-0.5193039	N	-1.7050886	5.08297947	-1.3675513
C	-1.2021536	-3.8206309	-1.0668565	N	-1.6977756	-5.0257826	-1.3834279
C	-1.4770352	-1.4132616	-0.9464672	C	1.80009425	0.03044341	0.40308675
H	0.70158053	-4.5664259	-0.3529649	C	2.14813101	-0.0575016	1.72090782
H	-2.990243	-2.7455079	-1.6683184	C	2.93787368	0.12047118	-0.4677412
C	0.41058925	0.02978517	-0.1343286	C	4.14218622	0.09573191	0.19122993

P	-2.5925588	0.02745907	-1.1551014	S	3.91288068	-0.0475055	1.95603349
C	-1.4813365	1.47029412	-0.9391923	O	2.77177849	0.27361704	-1.8291995
C	-1.9892923	2.69968444	-1.261252	C	2.92163966	-0.9489809	-2.6449212
H	-2.9918508	2.80134026	-1.6683563	H	2.03672181	-1.5754184	-2.5177413
C	-1.2112125	3.8783498	-1.0474157	H	3.00284987	-0.6023811	-3.6725053
C	0.08536227	3.73819374	-0.4813959	H	3.82420969	-1.4844178	-2.3460507
H	0.67798709	4.62748864	-0.2992601	C	1.25275363	-0.1520403	2.91233801
C	0.57886009	2.49617612	-0.1723858	C	5.49577667	0.20777017	-0.3208541
H	1.57254782	2.42840995	0.25588586	O	-0.0086655	-0.1059147	2.69701564
C	-0.1684272	1.29855413	-0.4029555	O	5.57083776	0.38135885	-1.6631478
O	-3.4196113	0.02960175	-2.5547283	H	6.49499799	0.47847581	-1.9808472
C	-3.7240568	0.02423336	0.29664051	O	1.81521042	-0.2653475	4.05780179
C	-5.4259548	0.023477	2.48873623	O	6.50846719	0.16441214	0.39966475
C	-3.1791454	0.01515437	1.58507604	H	-2.6275818	-5.1223822	-1.7707827
C	-5.1026694	0.03228174	0.08758217	H	-2.6299999	5.17859681	-1.7667987
C	-5.9567253	0.03194222	1.19590721	H	-1.1525388	-5.866106	-1.2400272
C	-4.0394302	0.01489802	2.68439345	H	-1.1628478	5.9239869	-1.216805
H	-2.1002998	0.0075031	1.73371633				

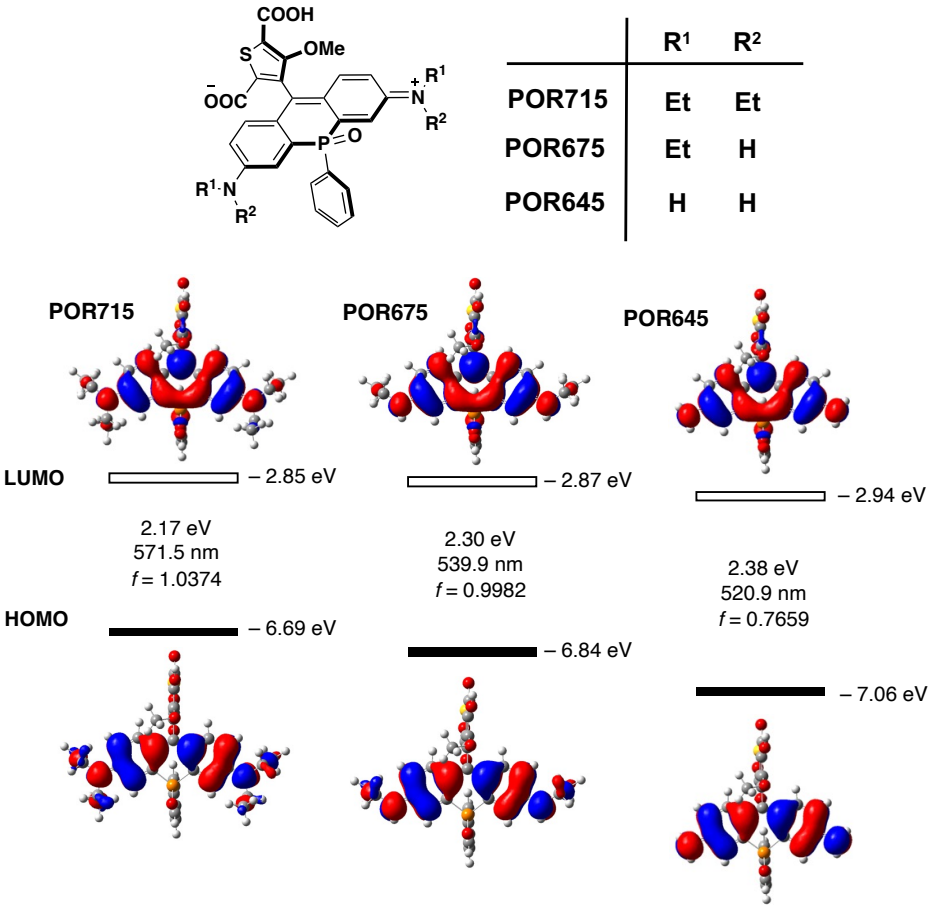

Fig. S2 Energy diagram, Kohn-Sham HOMOs and LUMOs, and the TD-DFT vertical excitation wavelengths, and oscillator strengths (*f*) for the *trans*-form of **POR715**, **POR675**, and **POR645** (from left to right) calculated at the M06-2X/6-31+G(d) level of theory with the SMD solvent model.

3. Photophysical properties

Photophysical measurements. UV-vis absorption and emission spectra were measured with HORIBA Duetta fluorescence and absorbance spectrometer using a 1 cm square quartz cuvette. Absolute fluorescence quantum yields (Φ_F) were determined using a HAMAMATSU Quantaurus-QY (C11347-11 or C13534) spectrometer equipped with a calibrated integrating sphere system.

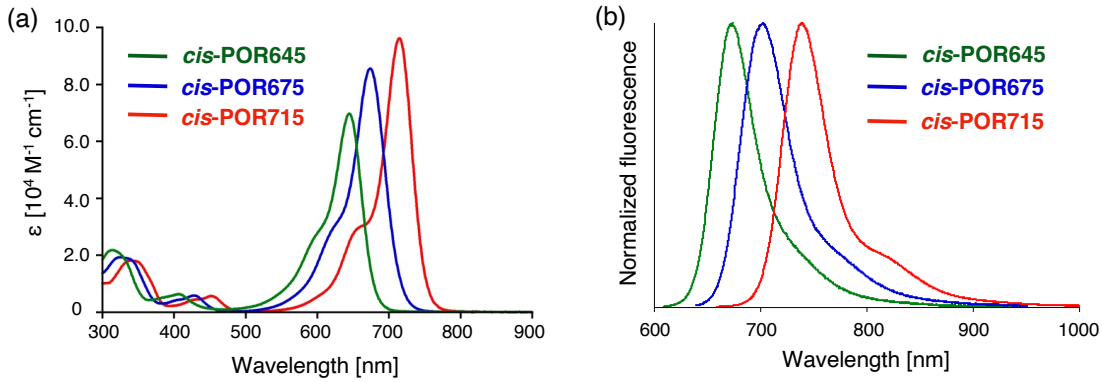

Fig. S3 a) Absorption and b) normalized emission spectra of the *cis*-form of **POR645** (green), **POR675** (blue), and **POR715** (red) in 50 mM HEPES buffer (pH = 7.4).

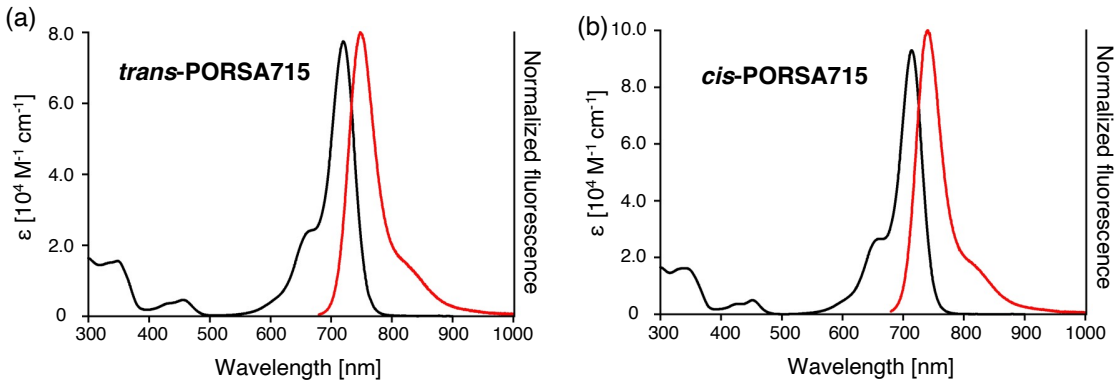

Fig. S4 Absorption and emission spectra of a) ***trans*-PORSA715** and b) ***cis*-PORSA715** in 50 mM HEPES buffer (pH = 7.4).

Determination of $D_{0.5}$ values. Absorption spectra of each POR dye in water-dioxane mixtures containing 5%, 10%, 20%, 30%, 40%, 50%, 60%, 70%, 80%, 90%, and 100% of water (v/v) were measured using SpectraMax i3 (Molecular Devices). Except *trans*-PORSA715, each absorbance at the maximum wavelength was normalized to the values observed in 100% water solution. A_{water} represents the absorbance in 100% water at the chosen wavelength. For *trans*-PORSA715, A_{water} is assumed to be identical to that of *trans*-POR715. Normalized absorbance (A/A_{water}) was plotted against dielectric constant of water-dioxane mixture[11] and the $D_{0.5}$ values were determined by sigmoidal fitting to Eq. 1:

$$A/A_{\text{water}} = \frac{1}{1 + 10^{a(D_{0.5} - D)}} \qquad \text{(Eq. 1)}$$

where D is the dielectric constant of the corresponding dioxane-water mixture and a is Hill slope coefficient determining the steepness of a dose-responsive curve.[12]

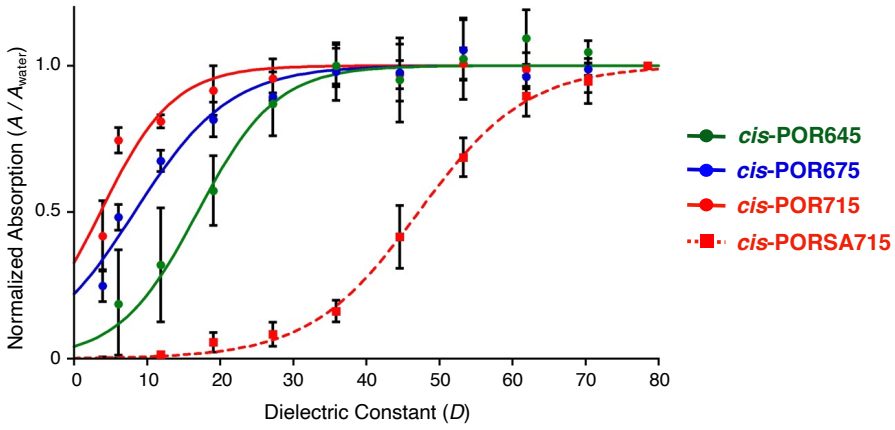

Fig. S5 Normalized absorbance (A/A_{water}) plotted as a function of dielectric constant with fitting curves for determination of $D_{0.5}$. *cis*-POR645 (green circle, solid line), *cis*-POR675 (blue circle, solid line), *cis*-POR715 (red circle, solid line), *cis*-PORSA715 (red square, dashed line). Error bars show the standard deviation (n = 3–5).

Chemical stability against pH. Solutions of each dye (5 μM) in three different aqueous pH buffers (pH = 4.2: citric acid/citric acid 3Na, pH = 7.1: HEPES, pH = 10.2: H_3BO_3/NaOH) was prepared. After that, they were left for 3 h at room temperature in the darkness. The absorption and fluorescence spectra were recorded with HORIBA Duetta fluorescence and absorbance spectrometer.

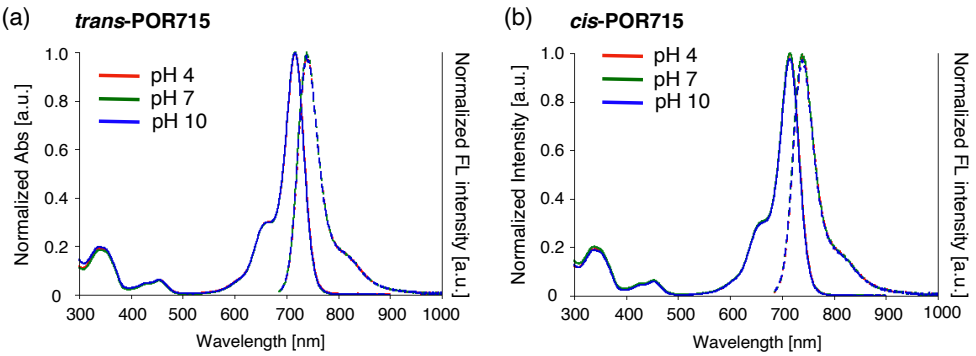

Fig. S6 Absorption (solid line) and fluorescence (dashed line) spectra of a) *trans*-POR715 and b) *cis*-POR715 in various pH buffer. pH 4: red, pH 7: green, pH 10: blue.

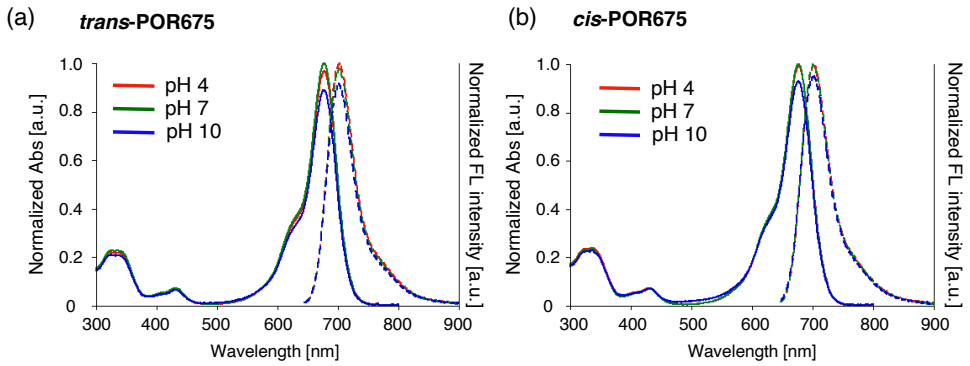

Fig. S7 Absorption (solid line) and fluorescence (dashed line) spectra of a) *trans*-POR675 and b) *cis*-POR675 in various pH buffer. pH 4: red, pH 7: green, pH 10: blue.

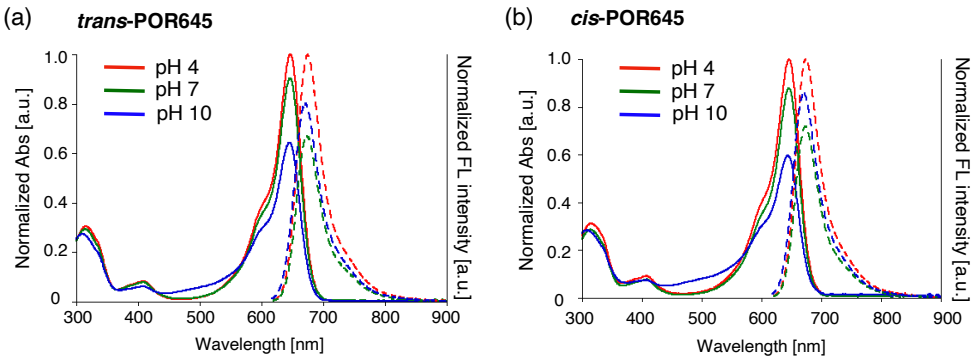

Fig. S8 Absorption (solid line) and fluorescence (dashed line) spectra of a) *trans*-POR645 and b) *cis*-POR645 in various pH buffer. pH 4: red, pH 7: green, pH 10: blue.

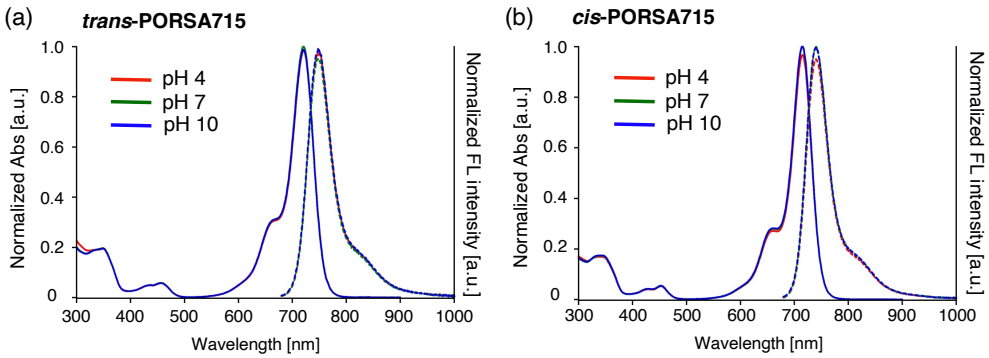

Fig. S9 Absorption (solid line) and fluorescence (dashed line) spectra of a) *trans*-PORSA715 and b) *cis*-PORSA715 in various pH buffer. pH 4: red, pH 7: green, pH 10: blue.

Chemical stability against glutathione (GSH). Solutions of each dye (5 μM) in 50 mM or 200 mM HEPES buffer with 10 mM GSH was prepared. After that, they were left for 5 h at room temperature in the darkness. The absorption and fluorescence spectra were recorded with HORIBA Duetta fluorescence and absorbance spectrometer.

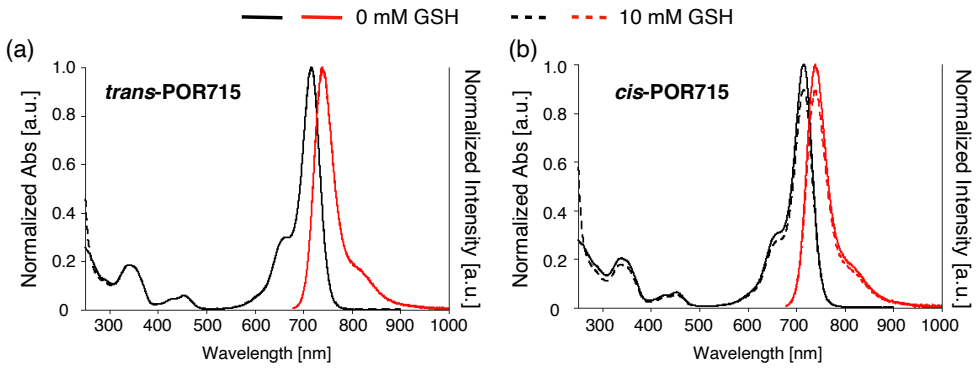

Fig. S10 Absorbance (black) and fluorescence (red) spectra of a) *trans*-POR715 and b) *cis*-POR715 in 50 mM HEPES buffer without (solid line) and with (dashed line) 10 mM GSH. Spectra were normalized to those for 0 mM GSH.

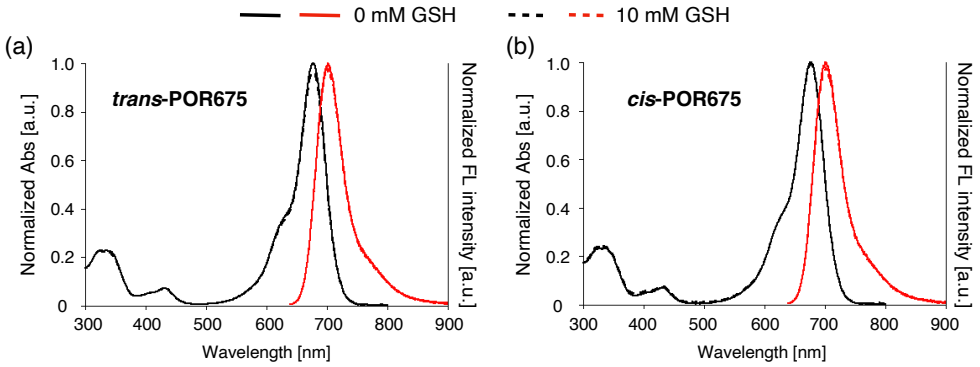

Fig. S11 Absorbance (black) and fluorescence (red) spectra of a) *trans*-POR675 and b) *cis*-POR675 in 50 mM HEPES buffer without (solid line) and with (dashed line) 10 mM GSH. Spectra were normalized to those for 0 mM GSH.

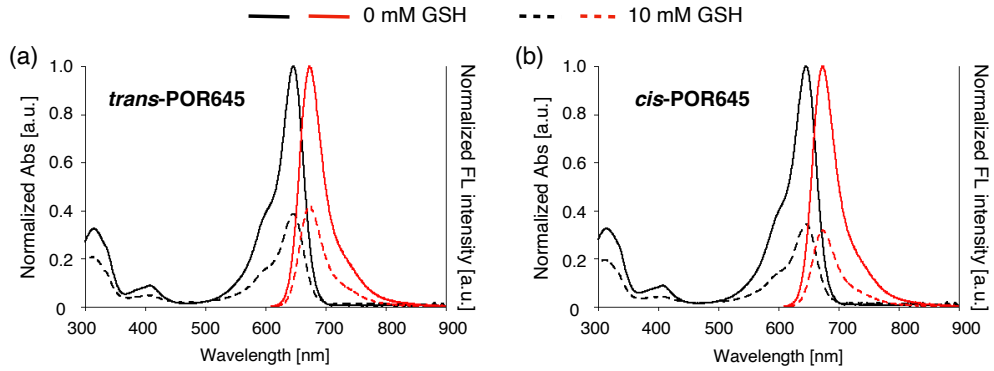

Fig. S12 Absorbance (black) and fluorescence (red) spectra of a) *trans*-POR645 and b) *cis*-POR645 in 50 mM HEPES buffer without (solid line) and with (dashed line) 10 mM GSH. Spectra were normalized to those for 0 mM GSH.

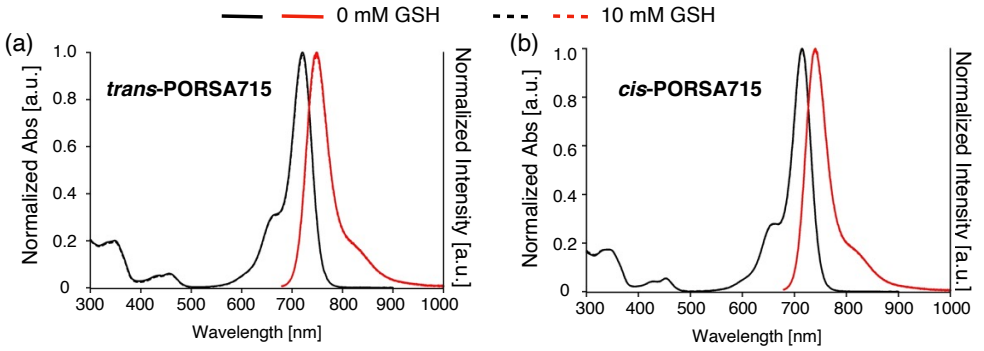

Fig. S13 Absorbance (black) and fluorescence (red) spectra of a) *trans*-PORSA715 and b) *cis*-PORSA715 in 50 mM HEPES buffer without (solid line) and with (dashed line) 10 mM GSH. Spectra were normalized to those for 0 mM GSH.

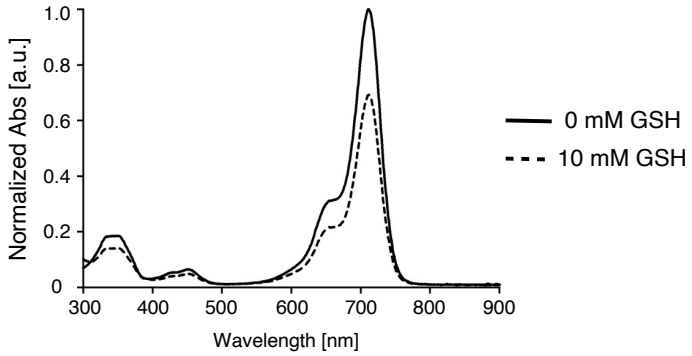

Fig. S14 Absorbance spectra of POR **14** in 200 mM HEPES buffer without (solid line) and with (dashed line) 10 mM GSH. Spectra were normalized to those for 0 mM GSH.

Spectral properties of the protein-bound form. As an isolated HaloTag protein, K381-HaloTag (truncated conventional kinesin) was used in this study. The absorption and fluorescence spectra of *trans*-POR675-Halo, *trans*-PORSA715-Halo, and *cis*-PORSA715-Halo were measured before and after labelling with the HaloTag protein. A solution of 3.3 µM HaloTag protein in PBS was prepared, to which a dye solution (200 µM in DMSO/PBS, 1:1) was added at a 1:100 dilution. The resulting mixture was incubated in the dark at room temperature for 3 h. The absorption spectra of *trans*-PORSA715-Halo was also assessed in the presence and absence of 1% BSA in 50 mM HEPES buffer. Absorbance spectra were recorded using the Duetta fluorometer (HORIBA) and emission measurements were performed in a 384-well plate format using a SpectraMax i3 (Molecular Devices).

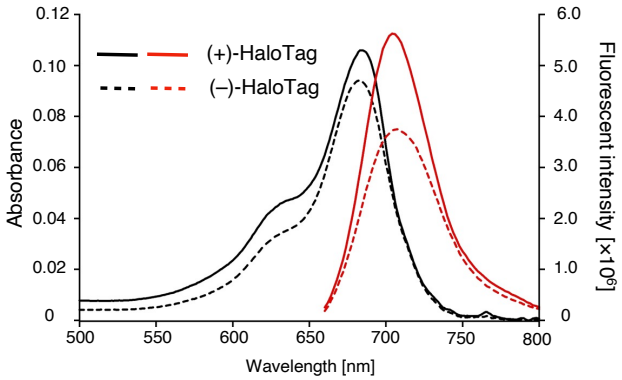

Fig. S15 Absorption (black) and fluorescence (red) spectra of *trans*-POR675-Halo measured in the presence (solid line) or absence (dashed line) of HaloTag protein after incubation for 3 h.

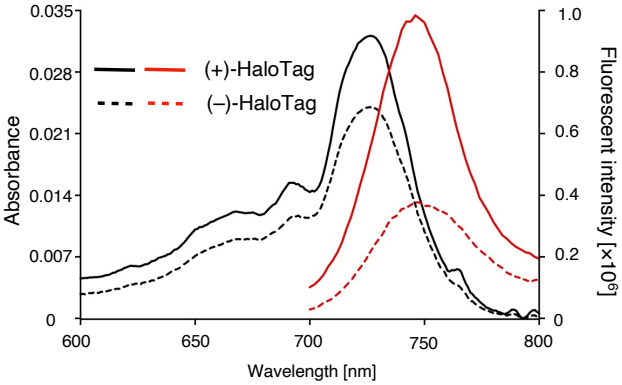

Fig. S16 Absorption (black) and fluorescence (red) spectra of *trans*-PORSA715-Halo measured in the presence (solid line) or absence (dashed line) of HaloTag protein after incubation for 3 h.

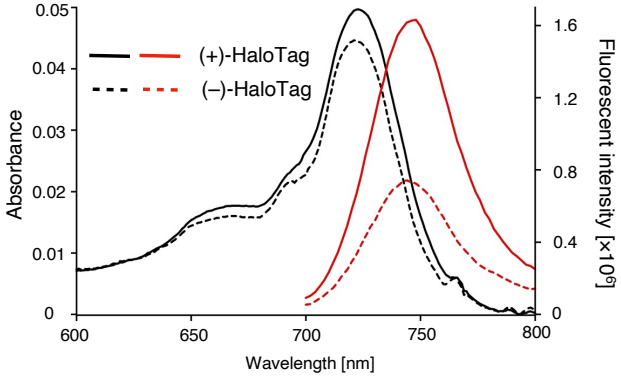

Fig. S17 Absorption (black) and fluorescence (red) spectra of *cis*-PORSA715-Halo measured in the presence (solid line) or absence (dashed line) of HaloTag protein after incubation for 3 h.

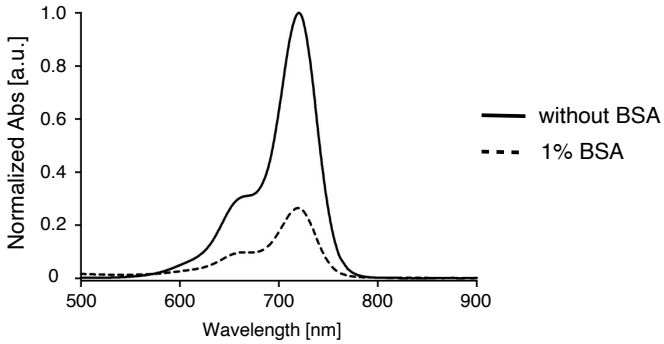

Fig. S18 Absorption spectra of *trans*-PORSA715 in 50 mM HEPES buffer without (solid line) and with (dashed line) 1% BSA. Spectra were normalized to those for without BSA.

4. Cell experiments

Cell culture. HeLa (RCB0007) and COS-7 (RCB0539) cells were purchased from RIKEN Cell Bank. Dulbecco's modified Eagle's medium (DMEM) with low glucose, *L*-glutamine, sodium pyruvate (Wako, 041-29775), fetal bovine serum (FBS, Biosera, 554-02155), and Antibiotic-Antimycotic (AA, Wako, 161-23181) were used for culture. Cells were cultured in DMEM containing 10% FBS and 1% AA at 37 °C in a humidified 5% CO_2 incubator. Two days before imaging, HeLa cells (5×10^4) or COS-7 cells (3×10^4) were seeded in non-coated glass-bottom dishes.

Transfection. The before day of imaging, transfection process was conducted by Lipofectamine™ 3000 Reagent (ThirmoFisher). 1.0 μL of Lipofectamine™ 3000 Reagent was diluted with 50 μL of Opti-MEM™ medium in a microtube. In the other microtube, 1.0 μL of P 3000™ Reagent and 1 μg of corresponding plasmid DNA (hH2B Halo-N1 for cell nucleus, β Tul Halo endo for microtubule, Sec61β-Halo or KDEL-Halo for ER, TOMM20-Halo for mitochondria) were diluted with 50 μL of Opti-MEM™ medium. Then, diluted DNA solution was added to lipid solution, mixed gently and incubated for 5 min at room temperature. The DNA-lipid complex was diluted with 1 mL of DMEM(+), which is for cell culturing, added to glass-bottom dish and incubated over night at 37 °C in a humidified 5% CO_2 incubator.

Cell imaging. FLUOVIEW FV3000 (Olympus) equipped with five excitation lasers (405, 488, 561, 640, and 730 nm), GaAsP PMT and GaAs PMT detectors, and TruFocus Red Z-Drift Compensator. The cell dish was mounted on a stage top incubator (Tokai Hit) maintained at 37 °C in an environment of humidified 5% CO_2. The images in multiple channels were recorded in a line-by-line.

Organelle labelling. After removal of the incubation medium from the glass-bottom dish, the HaloTag-expressing cells were washed with DMEM(+) three times and treated with each POR dye in DMEM(+) containing 0.1% DMSO in a CO_2 incubator. Labelling conditions: *trans/cis*-POR715-Halo, *trans*-POR675-Halo, and *trans/cis*-PORSA715-Halo: 100 nM for 2 h, *cis*-POR675-Halo and t*rans/cis*-POR645-Halo: 500 nM for 4 h with 10 μM Verapamil. For co-staining experiments, 100 nM TMR-Halo were used. Acquisition conditions are indicated in each figure caption.

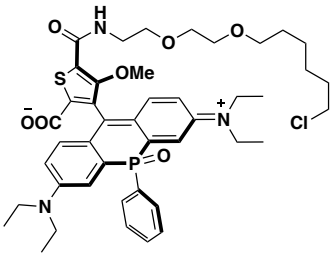

***trans*-POR715-Halo**

Cell type: HeLa
Staining condition: 100 nM (2 h) in DMEM (+)
Co-staining: 100 nM TMR-Halo

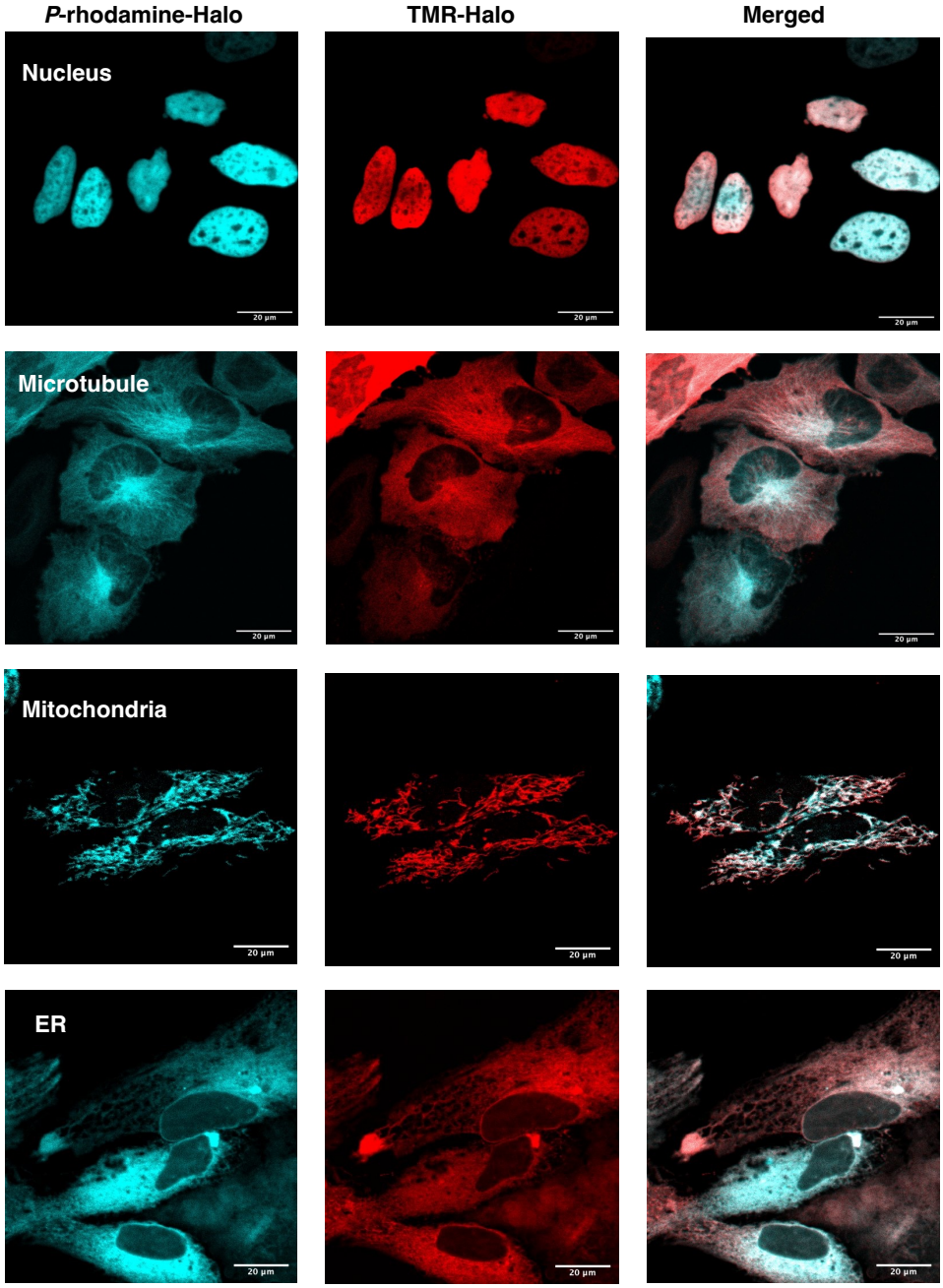

Fig. S19 Confocal images of HaloTag-expressing live HeLa cells labelled with *trans*-POR715-Halo (λ_{ex} = 730 nm, λ_{em} = 750–790 nm) and TMR-Halo (λ_{ex} = 561 nm, λ_{em} = 570–620 nm). HaloTag was expressed on the indicated organelle. Scale Bar = 20 μm.

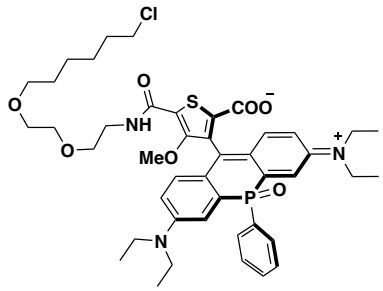

***cis*-POR715-Halo**

Cell type: HeLa
Staining condition: 100 nM (2 h) in DMEM (+)
Co-staining: 100 nM TMR-Halo

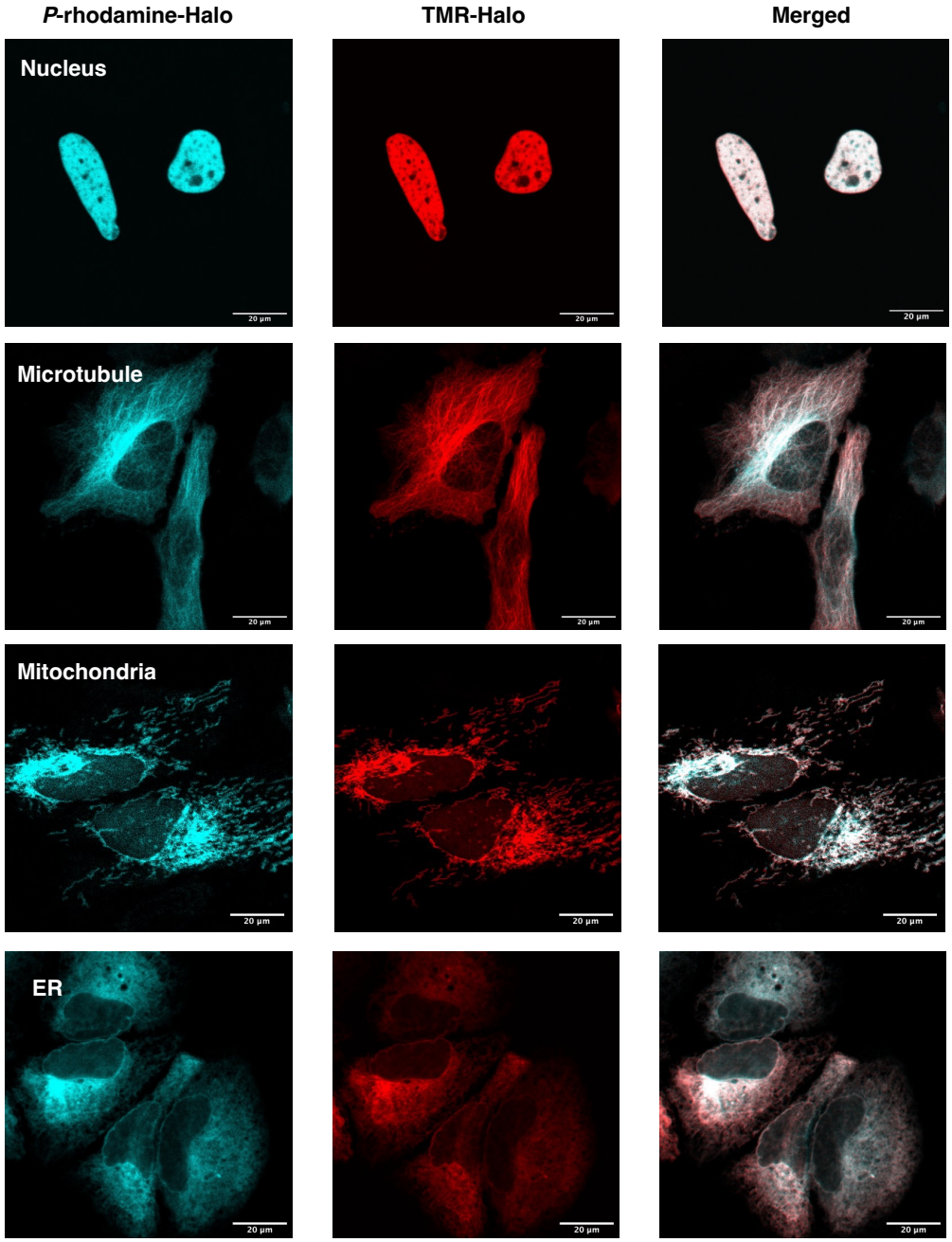

Fig. S20 Confocal images of HaloTag-expressing live HeLa cells labelled with *cis*-POR715-Halo (λ_{ex} = 730 nm, λ_{em} = 750–790 nm) and TMR-Halo (λ_{ex} = 561 nm, λ_{em} = 570–620 nm). HaloTag was expressed on the indicated organelle. Scale Bar = 20 μm.

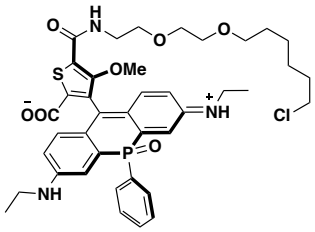

***trans*-POR675-Halo**

Cell type: HeLa
Additive: 10 μM Verapamil
Staining medium: 100 nM (2 h) in DMEM (+)
Co-staining: 100 nM TMR-Halo

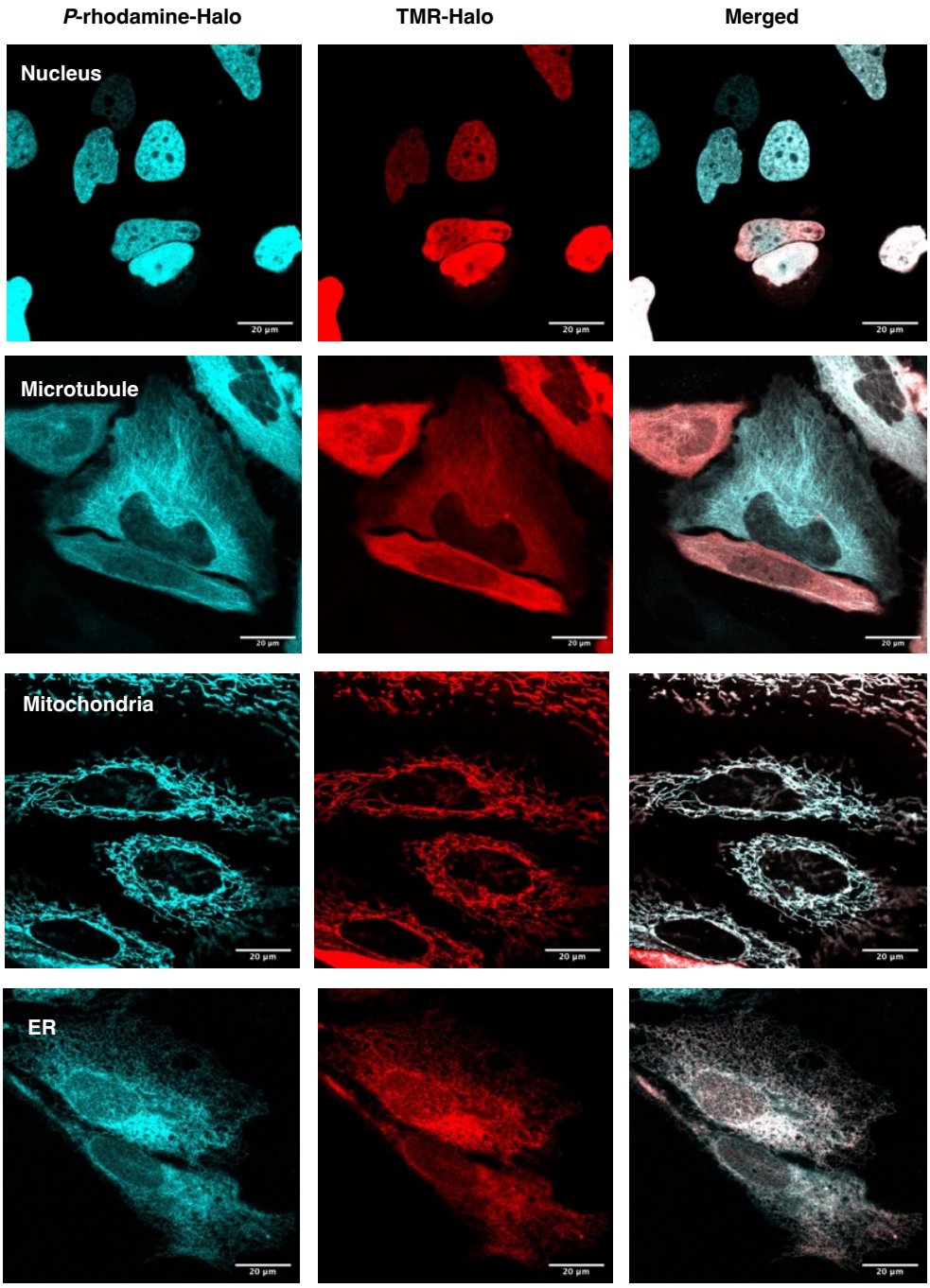

Fig. S21 Confocal images of HaloTag-expressing live HeLa cells labelled with *trans*-POR675-Halo (λ_{ex} = 640 nm, λ_{em} = 650–750 nm) and TMR-Halo (λ_{ex} = 561 nm, λ_{em} = 570–620 nm). HaloTag was expressed on the indicated organelle. Scale Bar = 20 μm.

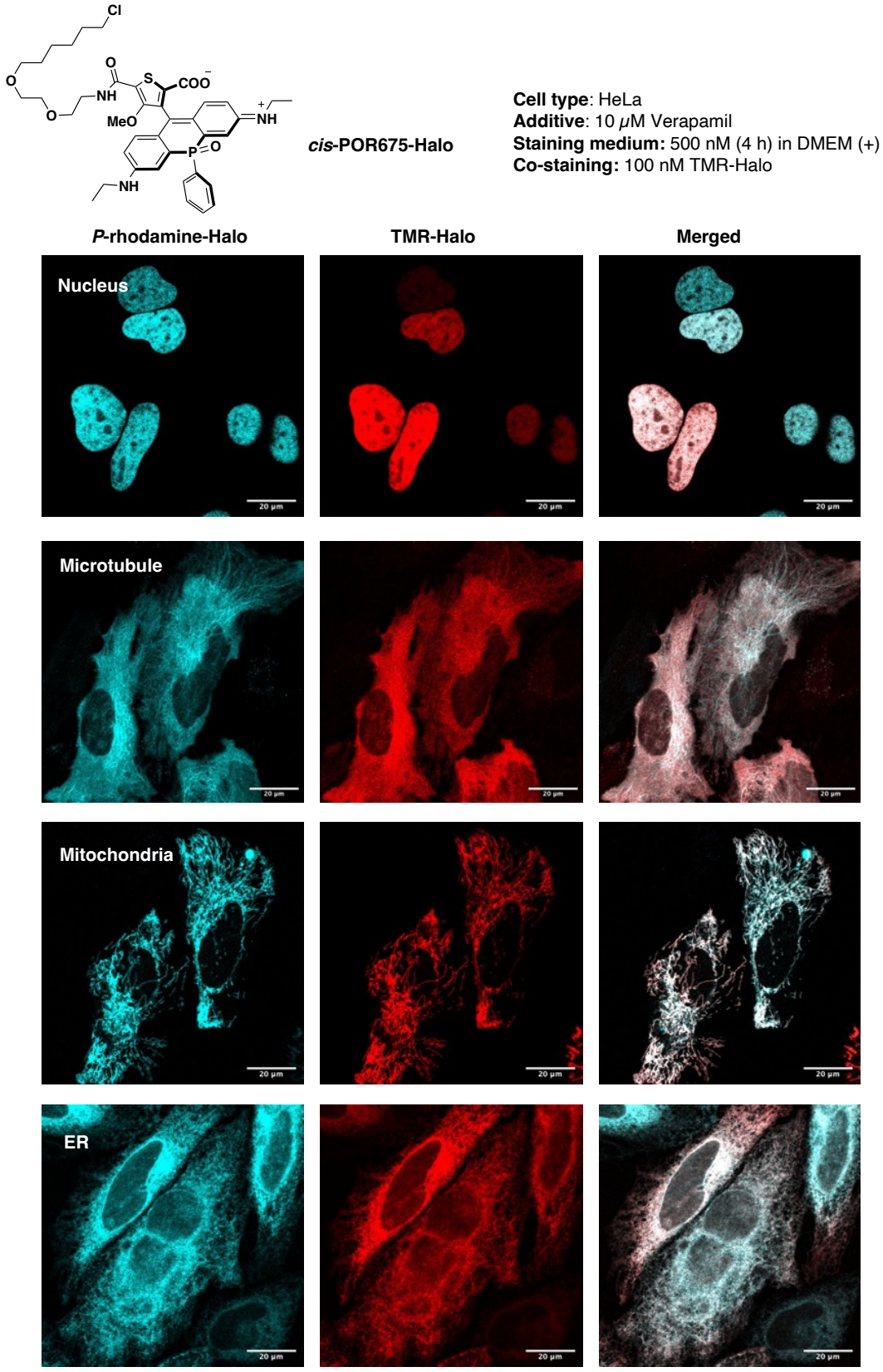

Fig. S22 Confocal images of HaloTag-expressing live HeLa cells labelled with *cis*-POR675-Halo (λ_{ex} = 640 nm, λ_{em} = 650–750 nm) and TMR-Halo (λ_{ex} = 561 nm, λ_{em} = 570–620 nm). HaloTag was expressed on the indicated organelle. Scale Bar = 20 μm.

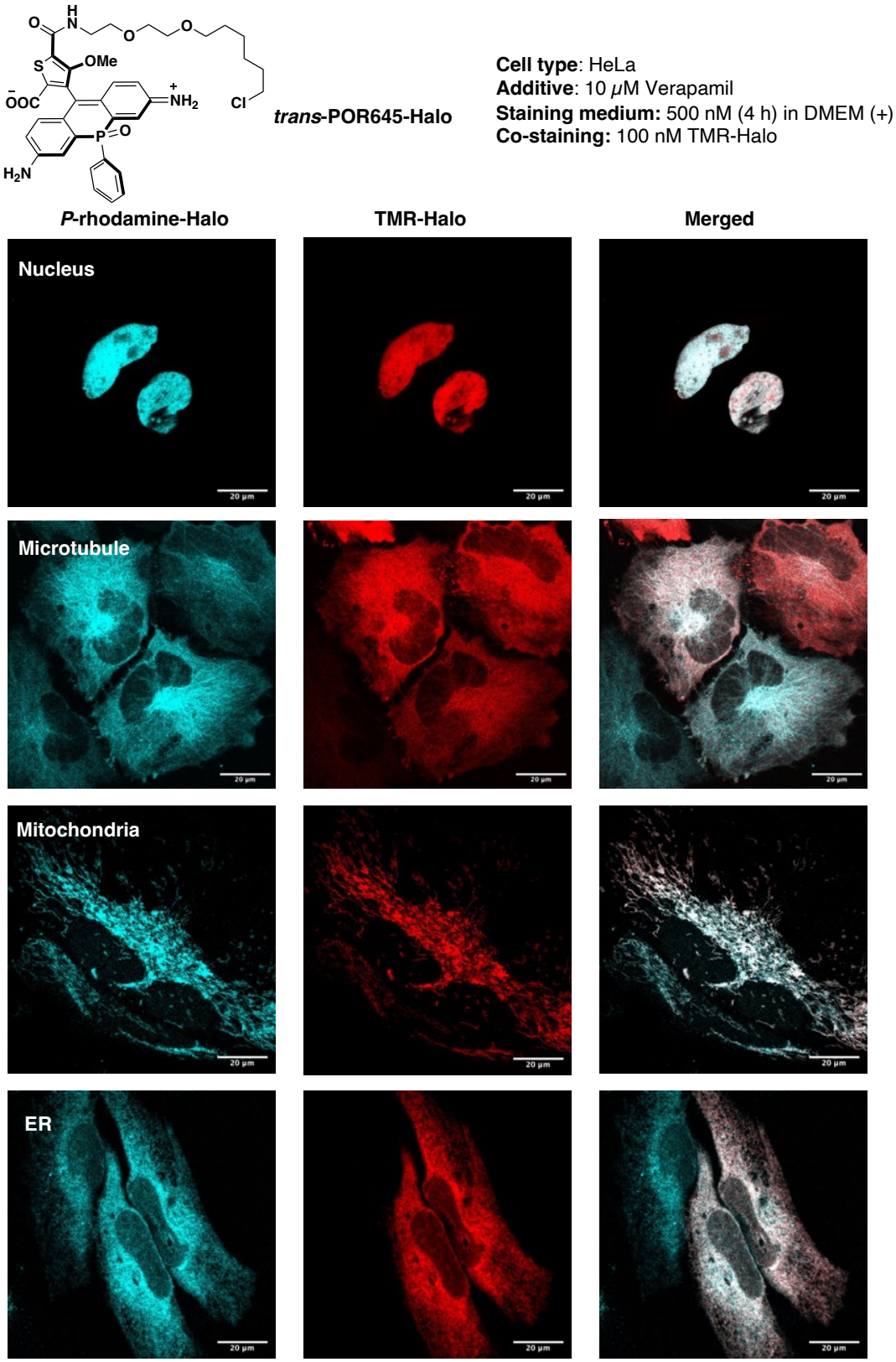

Fig. S23 Confocal images of HaloTag-expressing live HeLa cells labelled with *trans*-POR645-Halo (λ_{ex} = 640 nm, λ_{em} = 650–750 nm) and TMR-Halo (λ_{ex} = 561 nm, λ_{em} = 570–620 nm). HaloTag was expressed on the indicated organelle. Scale Bar = 20 μm.

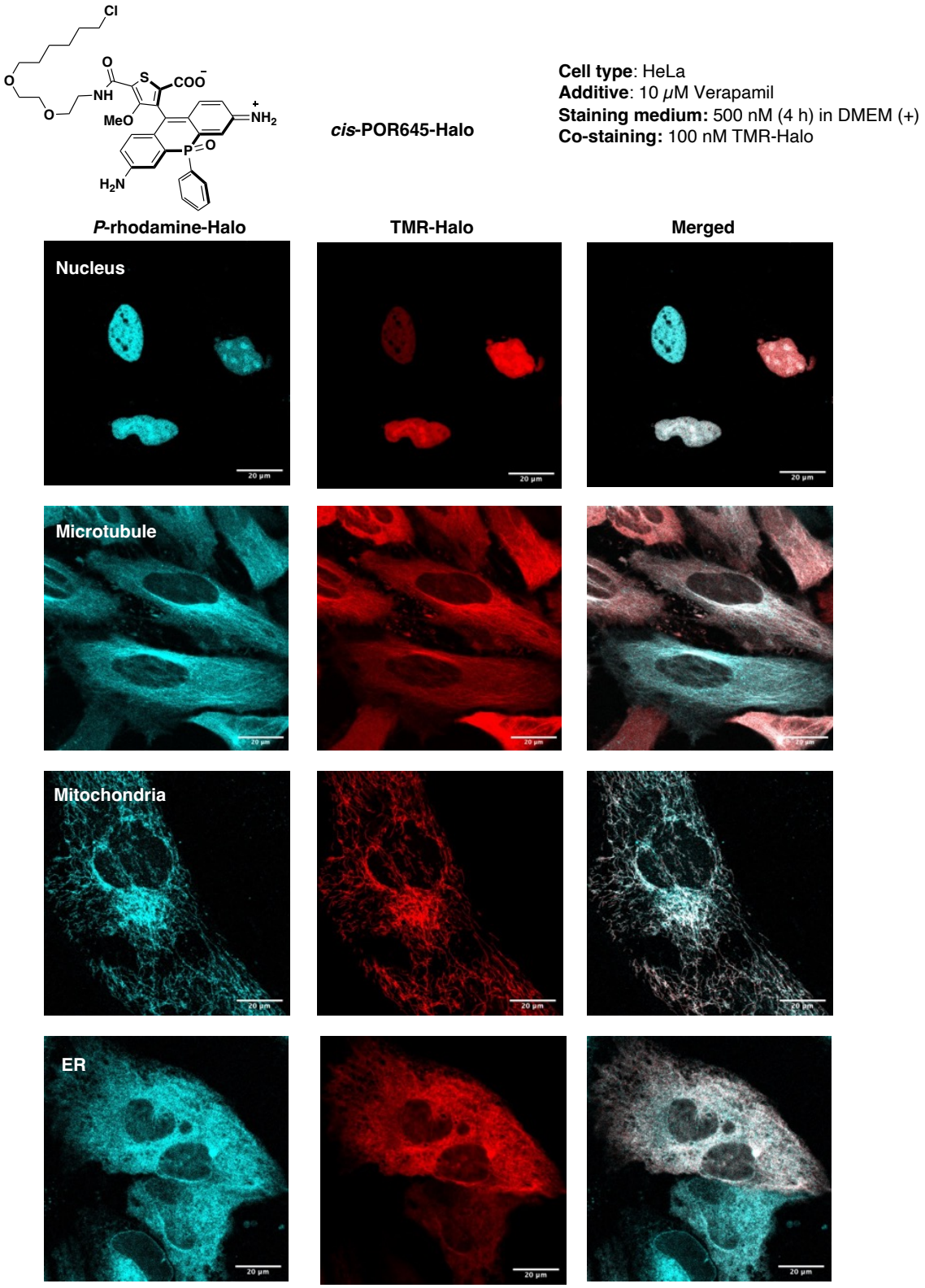

Fig. S24 Confocal images of HaloTag-expressing live HeLa cells labelled with *cis*-POR645-Halo (λ_{ex} = 640 nm, λ_{em} = 650–750 nm) and TMR-Halo (λ_{ex} = 561 nm, λ_{em} = 570–620 nm). HaloTag was expressed on the indicated organelle. Scale Bar = 20 μm.

Organelle labelling in stably HaloTag-expressing cells. After removal of the incubation medium from the glass-bottom dish, the cells were washed with DMEM(+) three times. HeLa stably expressing hH2B-HaloTag fusion protein were treated with POR dye in DMEM(+) containing 0.1% DMSO in a CO_2 incubator. Labelling conditions: *trans*-PORBT-Halo: 100 nM for 4 h, *trans*-POR715-Halo: 100 nM for 4 h, *trans*-POR675-Halo: 100 nM for 4 h, with 10 µM Verapamil and *trans*-POR645-Halo: 500 nM for 4 h with 10 µM Verapamil. Acquisition conditions are indicated in each figure caption.

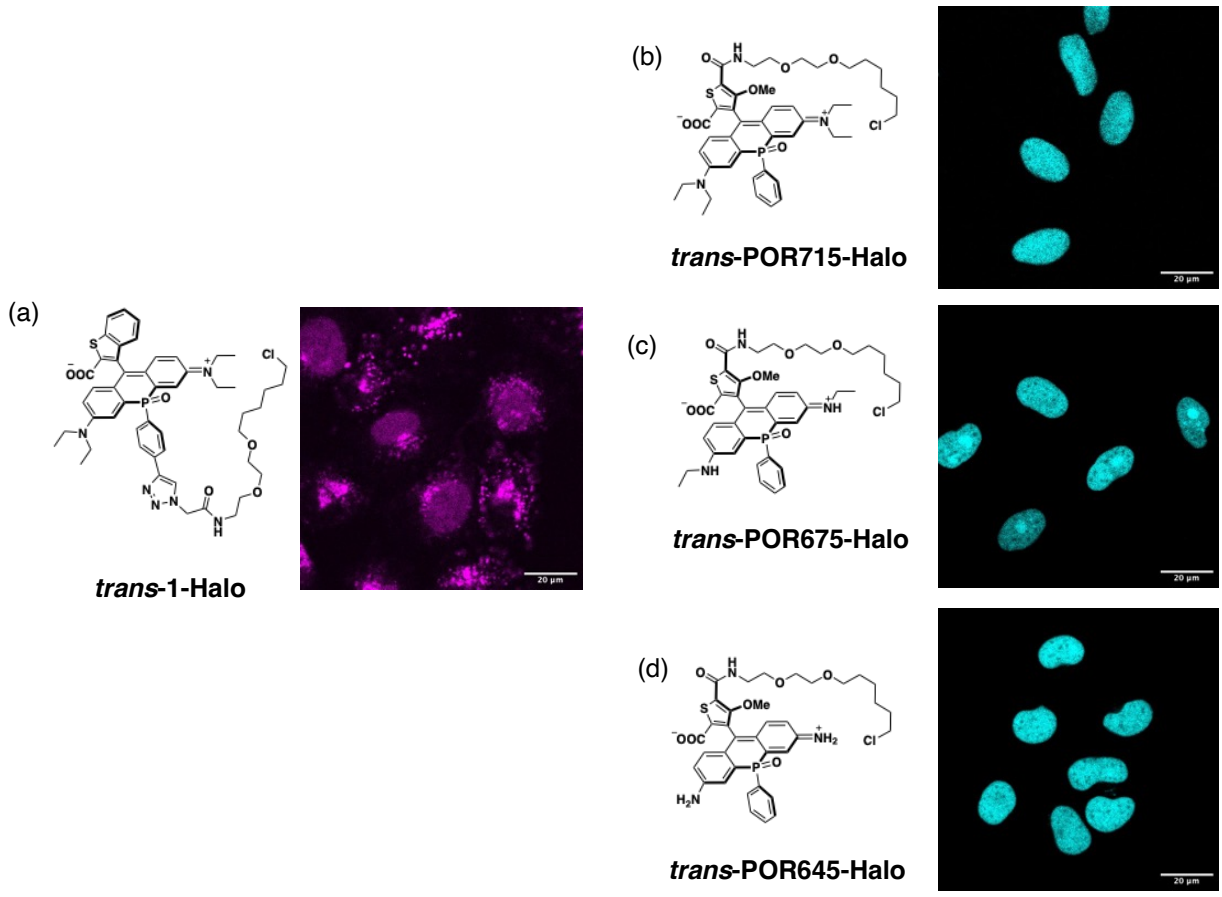

Fig. S25 Confocal images of live HeLa hH2B-HaloTag fusion protein-expressing cells (stably expression) stained with a) *trans*-PORBT-Halo, b) *trans*-POR715-Halo, c) *trans*-POR675-Halo, d) *trans*-POR645-Halo, (*trans*-1-Halo, *trans*-POR715-Halo: λ_{ex} = 730 nm, λ_{em} = 750–790 nm, *trans*-POR675-Halo, *trans*-POR645-Halo: λ_{ex} = 640 nm, λ_{em} = 650–750 nm,). Scale Bar = 20 µm.

STED imaging. COS-7 cells expressing β Tul Halo endo fused protein on microtubule were washed three times with DMEM(+). The cells were stained with *trans*-POR675-Halo (1 µM) with 10 µM Verapamil for 4 h in a CO_2 incubator. The STED images were obtained with Leica TCS SP8 STED 3X system (λ_{ex} = 670 nm, WLL; λ_{em} = 680–750 nm HyD detector; 100 × oil-immersion objective (*NA* 1.4), λ_{STED} = 775 nm) in a line-by-line sequential scan mode. For multi-color STED imaging, COS-7 cells were stained with *trans*-POR675-Halo (1

μM) and SiR-tubuline (1 μM) with 10 μM Verapamil for 4 h in a CO_2 incubator. The STED images were obtained with the same system (λ_{ex} = 670 nm, WLL; λ_{em} = 600–660 nm: SiR-tubuline, λ_{em} = 720–750 nm: *trans*-POR675-Halo). The STED images were deconvoluted using a Huygens software (Scientific Volume Imaging).

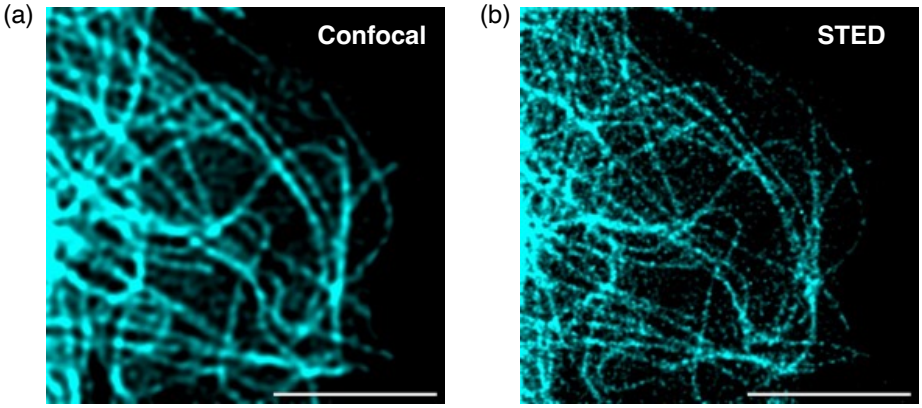

Fig. S26 a) Confocal and b) STED images of live COS-7 cells expressing β Tul Halo endo labelled with *trans*-POR675-Halo (λ_{ex} = 670 nm, λ_{em} = 680–750 nm). Scale Bar = 2 μm.

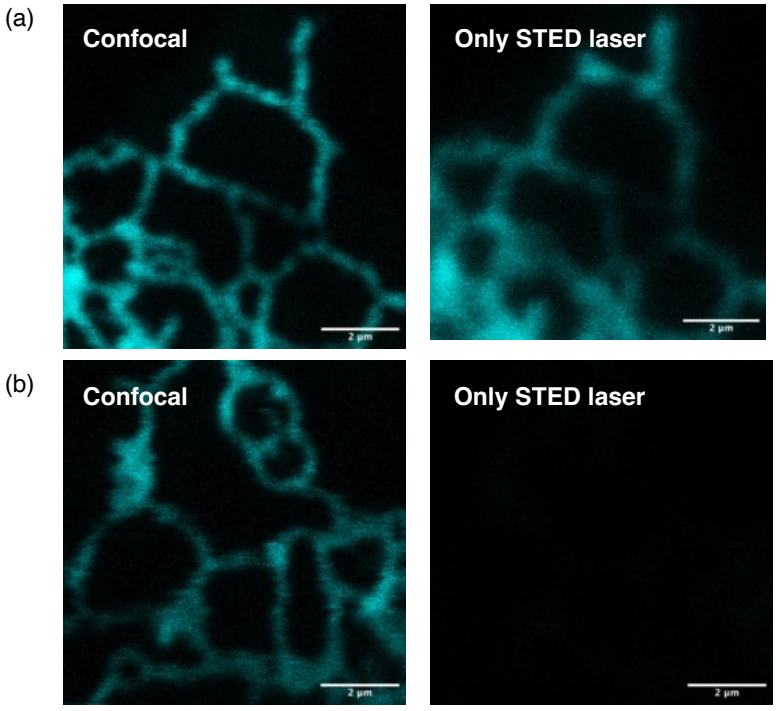

Fig. S27 Confocal and STED (0% excitation laser) images of live COS-7 cells expressing KDEL-HaloTag labelled with a) *trans*-POR715-Halo and b) *trans*-POR675-Halo (λ_{ex} = 670 nm, λ_{em} = 680–750 nm). Scale Bar = 2 μm.

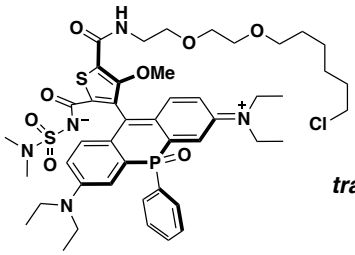

***trans*-PORSA715-Halo**

Cell type: HeLa
Staining condition: 100 nM (2 h) in DMEM (+)
Co-staining: 100 nM TMR-Halo

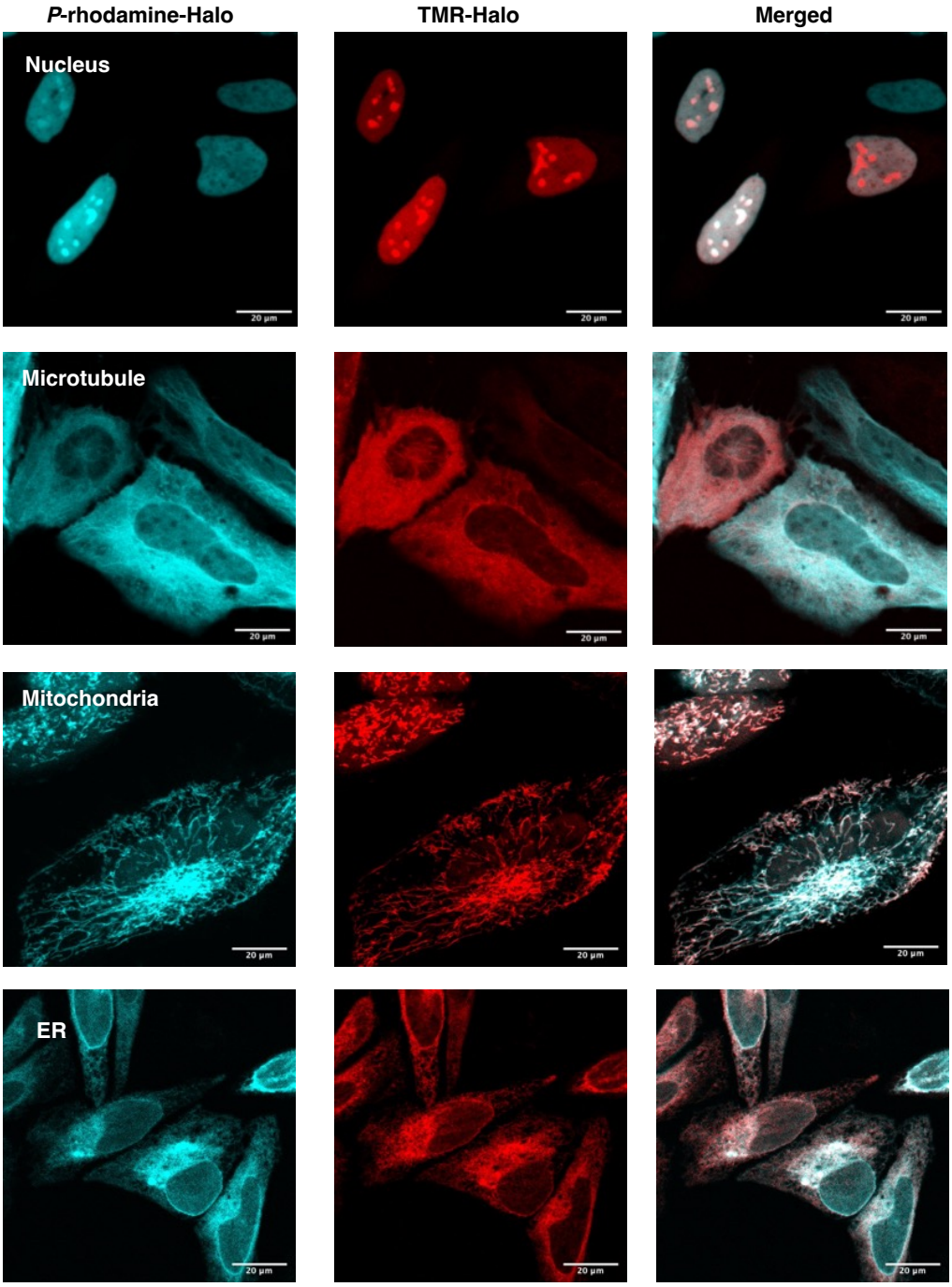

Fig. S28 Confocal images of live HeLa cells labelled with *trans*-PORSA715-Halo (λ_{ex} = 730 nm, λ_{em} = 750–790 nm) and TMR-Halo (λ_{ex} = 561 nm, λ_{em} = 570–620 nm). HaloTag was expressed on the indicated organelle. Scale Bar = 20 μm.

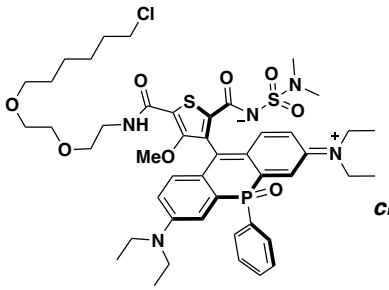

***cis*-PORSA715-Halo**

Cell type: HeLa
Staining condition: 100 nM (2 h) in DMEM (+)
Co-staining: 100 nM TMR-Halo

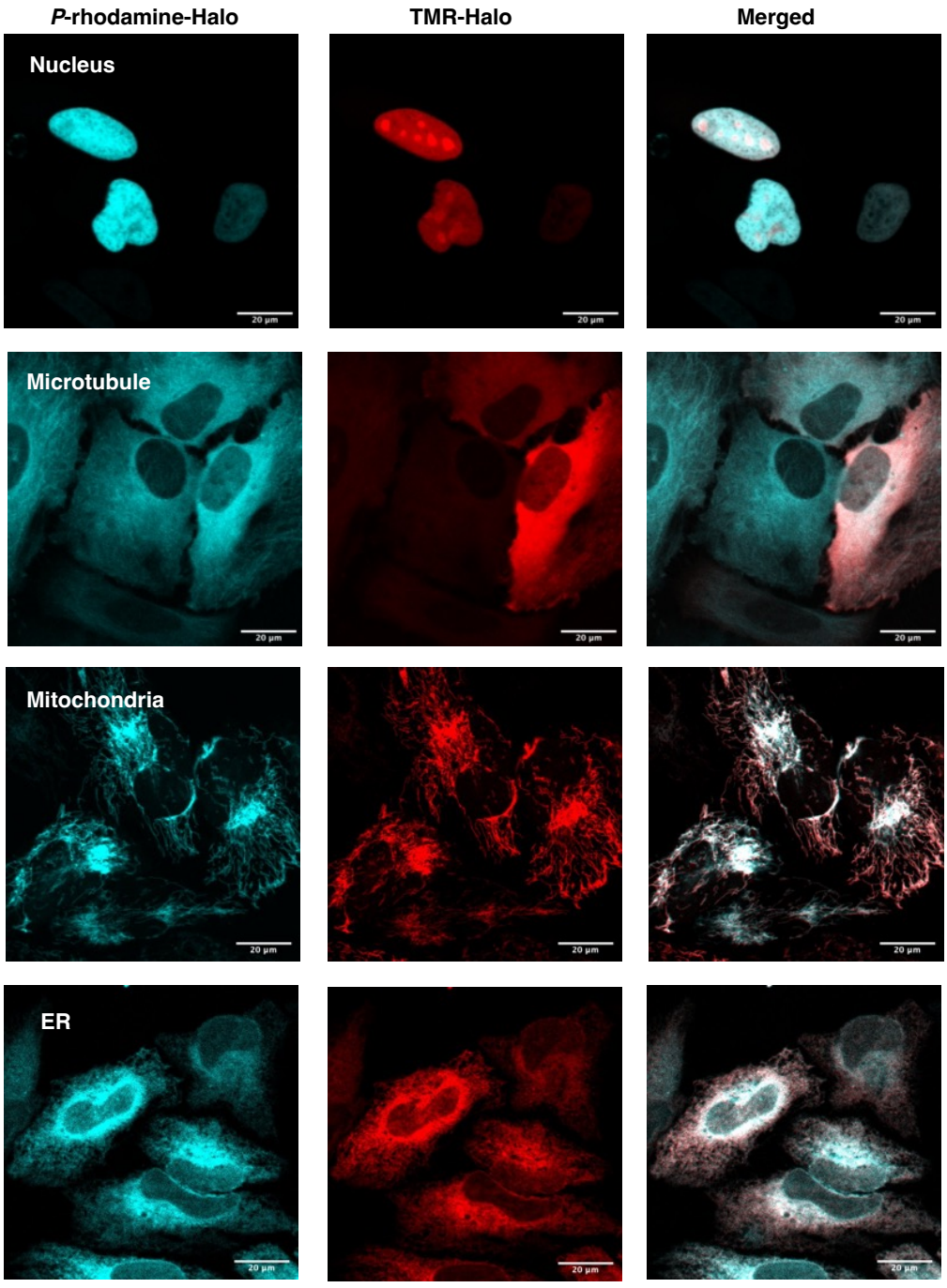

Fig. S29 Confocal images of live HeLa cells labelled with *cis*-PORSA715-Halo (λ_{ex} = 730 nm, λ_{em} = 750–790 nm) and TMR-Halo (λ_{ex} = 561 nm, λ_{em} = 570–620 nm). HaloTag was expressed on the indicated organelle. Scale Bar = 20 μm.

Time dependent labelling in living cells. HeLa cells transiently expressing hH2B-HaloTag were washed three times with DMEM(+). The medium was replaced with DMEM(+) containing 200 nM of *trans*-POR715-Halo or *trans*-PORSA715-Halo or JF_{646}-Halo in the presence of 0.1% DMSO. Cells were then incubated for 10 min at 37 °C in a humidified 5% CO_2 incubator. Images were taken every 10 min. The fluorescence intensity recorded from the nucleus at each time point was normalized to maximum intensity. Microscopy conditions: FLUOVIEW FV3000 (Olympus), λ_{ex} = 730 nm, λ_{em} = 750–790 nm for POR-Halo and λ_{ex} = 640 nm, λ_{em} = 650–750 nm for JF_{646}-Halo. For each dye, 5 cells were included for calculation in ImageJ.

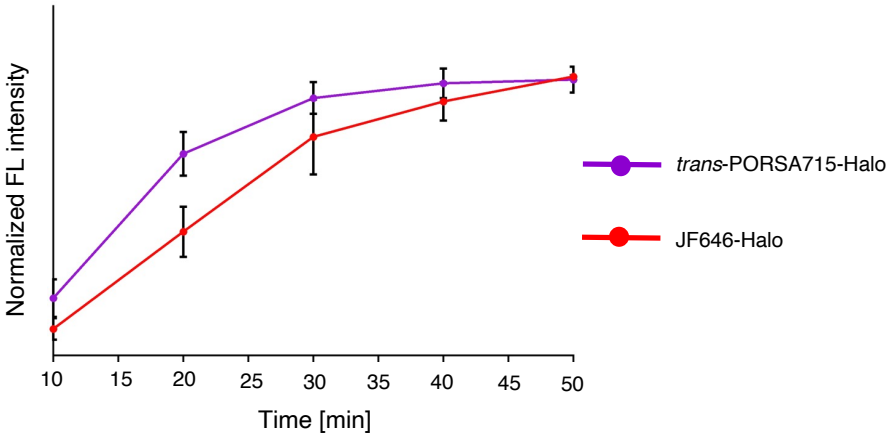

Fig. S30 Normalized fluorescence intensities of *trans*-PORSA715-Halo (purple) and JF_{646}-Halo (red) at different time points in live HeLa cells transiently expressing hH2B-HaloTag. Error bars show the standard deviation (n = 5).

Competitive staining of *trans*-PORSA715-Halo with TMR-Halo. For the control experiment, HeLa cells expressing hH2B-HaloTag were washed three times with DMEM(+). The medium was replaced with DMEM (+) containing 500 nM of *trans*-PORSA715-Halo or TMR-Halo in the presence of 0.1% DMSO, and the cells were incubated for 3 h at 37 °C in a humidified 5% CO_2 incubator. After washing with dye-free medium three times, images were acquired. Subsequently, for the competitive experiment, cells were incubated with DMEM(+) containing two dyes (500 nM *trans*-PORSA715-Halo and 500 nM TMR-Halo). Experimental conditions were identical to the control. After washing with dye-free medium three times, images for each dye were recorded. The occupancy of the dye was calculated by dividing the fluorescence intensities calculated for the competitive experiment by those for the control (n > 25 cells). The similar experiment was also conducted using JF_{646}-Halo instead of *trans*-PORSA715-Halo. Acquisition conditions: for *trans*-PORSA715-Halo; λ_{ex} = 730 nm, λ_{em} = 750–790 nm, for TMR: λ_{ex} = 561 nm, λ_{em} = 570–670 nm, for JF_{646}-Halo; λ_{ex} = 640 nm, λ_{em} = 650–750 nm.

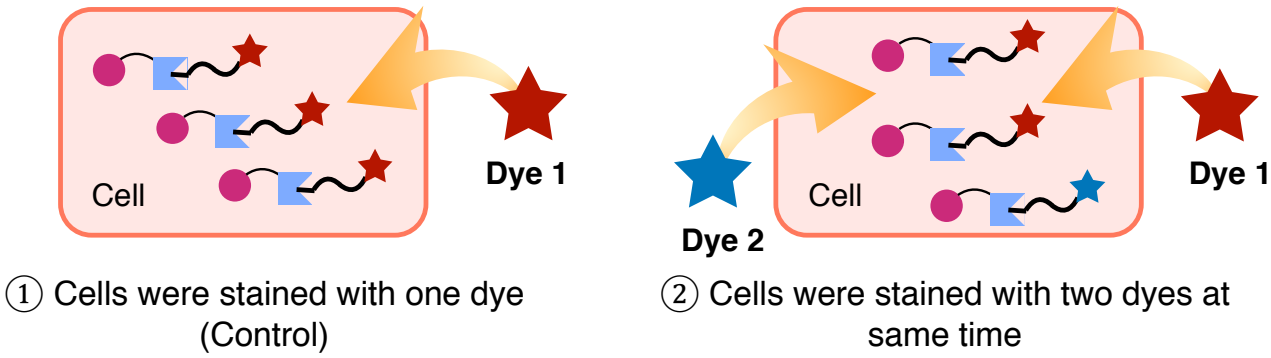

Fig. S31 The protocol of competitive staining experiments.

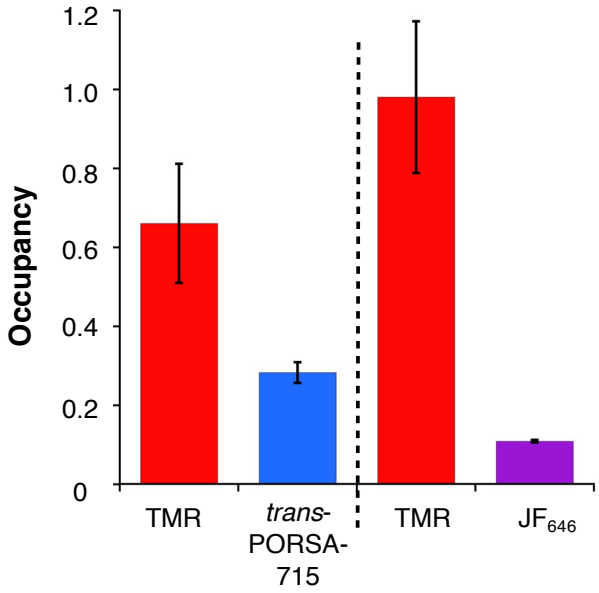

Fig. S32 Competitive staining of *trans*-PORSA715-Halo or JF_{646}-Halo with TMR-Halo.

Analysis of labelling efficiency. HeLa cells transiently expressing hH2B-HaloTag were washed three times with DMEM(+). The medium was then replaced with DMEM(+) containing 200 nM of *trans*-PORSA715-Halo or JF_{646}-Halo, along with 0.1% DMSO, and incubated for 1 h at 37 °C in a 5% CO_2 incubator. Subsequently, the cells were further labelled with 500 nM TMR-Halo for 1 h at 37 ºC. As a control, cells were labelled with only 500 nM TMR-Halo for 1 h at 37 ºC. The occupancy of HaloTag protein by *trans*-PORSA715-Halo or JF_{646}-Halo was estimated by normalizing the fluorescence intensity of TMR to the control (n > 85 cells).

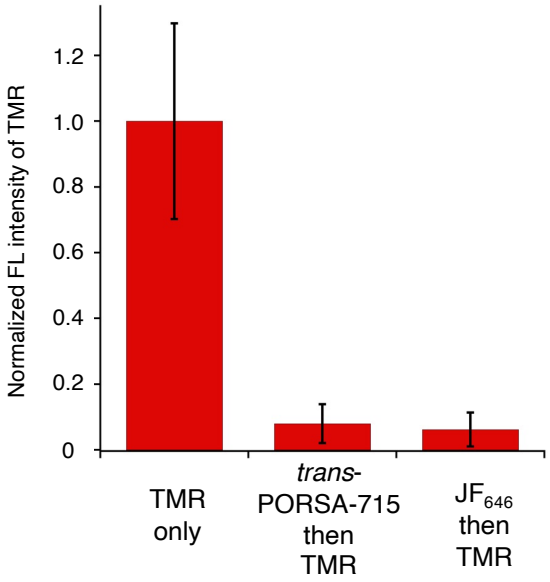

Fig. S33 Labelling efficiency for HaloTag ligands by pulse-chase analysis. HeLa cells transiently expressing hH2B-HaloTag were labelled with 200 nM *trans*-PORSA715-Halo or JF_{646}-Halo (pulse) in a culture medium for 1 h, then treated with 500 nM TMR-Halo (chase) for 1 h. The fluorescence intensities of the cell nuclei were measured and normalized to the control. Error bars show the standard deviation ($n > 85$).

Low concentration labelling. HeLa cells expressing hH2B-HaloTag or *β*-tubulin-HaloTag were washed three times with DMEM(+) and the medium was replaced with DMEM(+) containing 10 nM of *trans*-PORSA715-Halo in the presence of 0.1% DMSO. The cells were incubated for 2 h at 37 °C in a humidified 5% CO_2 incubator, washed with DMEM(+) three times, and imaged (λ_{ex} = 730 nm, λ_{em} = 750–790 nm).

Time lapse imaging. HeLa cells expressing hH2B-HaloTag or TOMM20-HaloTag were washed three times with DMEM(+), incubated with 100 nM *trans*-PORSA715-Halo in DMEM(+) containing 0.1% DMSO for 3 h at 37 °C in a humidified 5% CO_2 incubator, and imaged (λ_{ex} = 730 nm, λ_{em} = 750–790 nm). For nucleus: 1000 images with a frame interval of 90 s. For mitochondria: 10000 images with a frame interval of 33.3 ms (resonant scanning mode). The images were deconvoluted using a Huygens software (Scientific Volume Imaging).

5. References

[1] A. Kessler, C. M. Coleman, P. Charoenying, D. F. O'Shea, *J. Org. Chem.*, 2004, **69**, 7836–7846.

[2] N. Hergué, P. Frère, J. Roncali, *Org. Biomol. Chem.*, 2011, **9**, 588–595.

[3] M. Grzybowski, M. Taki, K. Senda, Y. Sato, T. Ariyoshi, Y. Okada, R. Kawakami, T. Imamura and S. Yamaguchi, *Angew. Chem. Int. Ed.,* 2018, **57**, 10137–10141.

[4] A. Fukazawa, S. Suda, M. Taki, E. Yamaguchi, M. Grzybowski, Y. Sato, T. Higashiyama and S. Yamaguchi, *Chem. Commun.,* 2016, **52**, 1120–1123.

[5] Y. Zhang, M-k. So, A. M. Loening, H. Yao, S. S. Gambhir, J. Rao, *Angew. Chem. Int. Ed.*, 2006, **45**, 4936–4940.

[6] K. Hanaoka, Y. Kagami, W. Piao, T. Myochin, K. Numasawa, Y. Kuriki, T. Ikeno, T. Ueno, T. Komatsu, T. Terai, T. Nagano, Y. Urano, *Chem. Commun.*, 2018, **54**, 6939–6942.

[7] Y. Zhao and D. G. Truhlar, *Theor. Chem. Account* 2008, **120**, 215–241.

[8] a) R. Ditchfield, W. J. Hehre and J. A. Pople, *J. Chem. Phys.* 1971, **54**, 724–728; b) W. J. Hehre, R. Ditchfield and J. A. Pople, *J. Chem. Phys.* 1972, **56**, 2257–2261; c) P. C. Hariharan and J. A. Pople, *Theor. Chim. Acta,* 1973, **28**, 213–222; d) M. M. Francl, W. J. Pietro, W. J. Hehre, J. S. Binkley, M. S. Gordon, D. J. DeFrees and J. A. Pople, *J. Chem. Phys.* 1982, **77**, 3654–3665.

[9] A. V. Marenich, C. J. Cramer, D. G. Truhlar, *J. Phys. Chem. B*, 2009, **113**, 6378–6696.

[10] Gaussian 16, Revision B.01, M. J. Frisch, G. W. Trucks, H. B. Schlegel, G. E. Scuseria, M. A. Robb, J. R. Cheeseman, G. Scalmani, V. Barone, G. A. Petersson, H. Nakatsuji, X. Li, M. Caricato, A. V. Marenich, J. Bloino, B. G. Janesko, R. Gomperts, B. Mennucci, H. P. Hratchian, J. V. Ortiz, A. F. Izmaylov, J. L. Sonnenberg, D. Williams-Young, F. Ding, F. Lipparini, F. Egidi, J. Goings, B. Peng, A. Petrone, T. Henderson, D. Ranasinghe, V. G. Zakrzewski, J. Gao, N. Rega, G. Zheng, W. Liang, M. Hada, M. Ehara, K. Toyota, R. Fukuda, J. Hasegawa, M. Ishida, T. Nakajima, Y. Honda, O. Kitao, H. Nakai, T. Vreven, K. Throssell, J. A. Montgomery, Jr., J. E. Peralta, F. Ogliaro, M. J. Bearpark, J. J. Heyd, E. N. Brothers, K. N. Kudin, V. N. Staroverov, T. A. Keith, R. Kobayashi, J. Normand, K. Raghavachari, A. P. Rendell, J. C. Burant, S. S. Iyengar, J. Tomasi, M. Cossi, J. M. Millam, M. Klene, C. Adamo, R. Cammi, J. W. Ochterski, R. L. Martin, K. Morokuma, O. Farkas, J. B. Foresman, and D. J. Fox, Gaussian, Inc., Wallingford CT, 2016.

[11] F. E. Critchfield, J. A. Gibson Jr., J. L. Hall, *J. Am. Chem. Soc.,* 1953*,* **75**, 1991-1992.

[12] A. N. Butkevich, *Org. Lett.*, 2021, **23**, 2604-2609.

6. NMR spectra

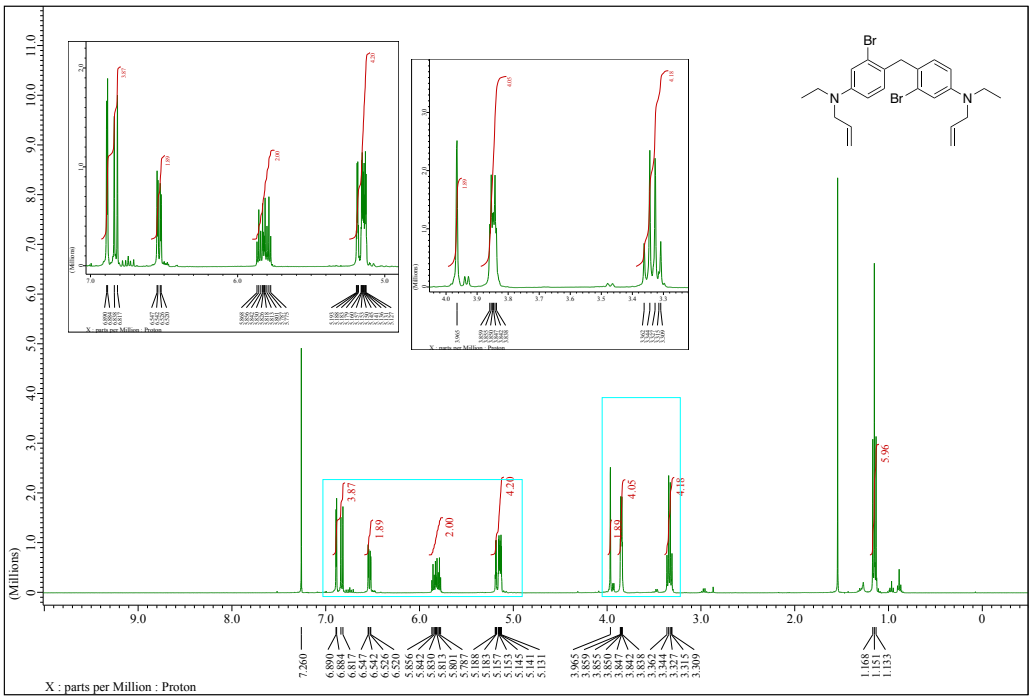

^{1}H NMR spectrum of **3** (400 MHz, $CDCl_3$)

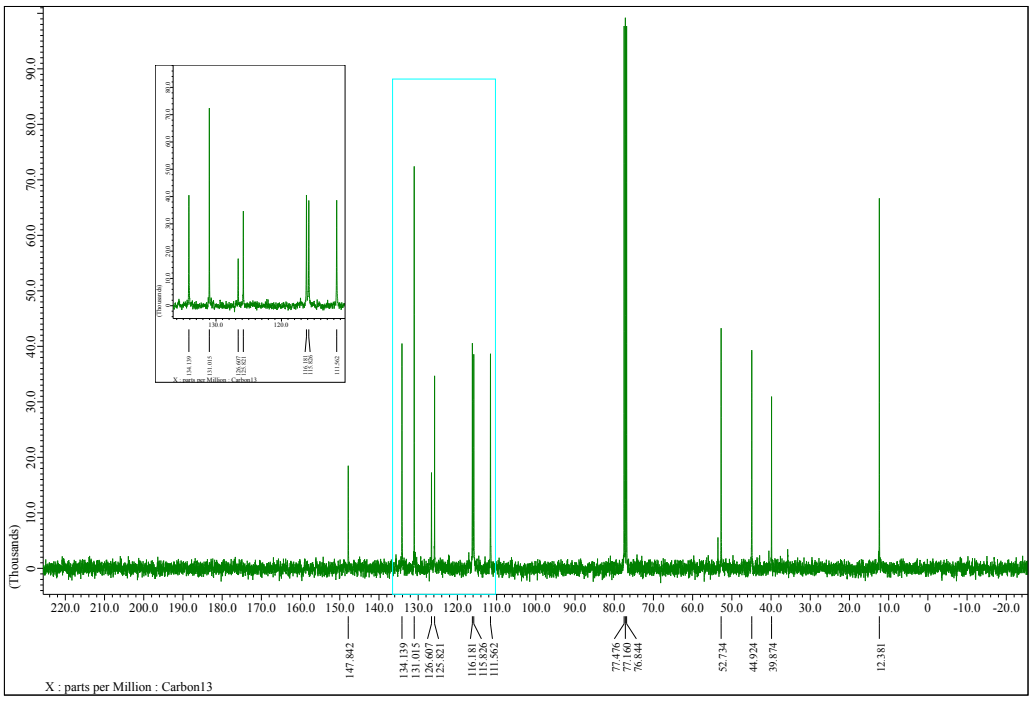

^{13}C NMR spectrum of **3** (100 MHz, $CDCl_3$)

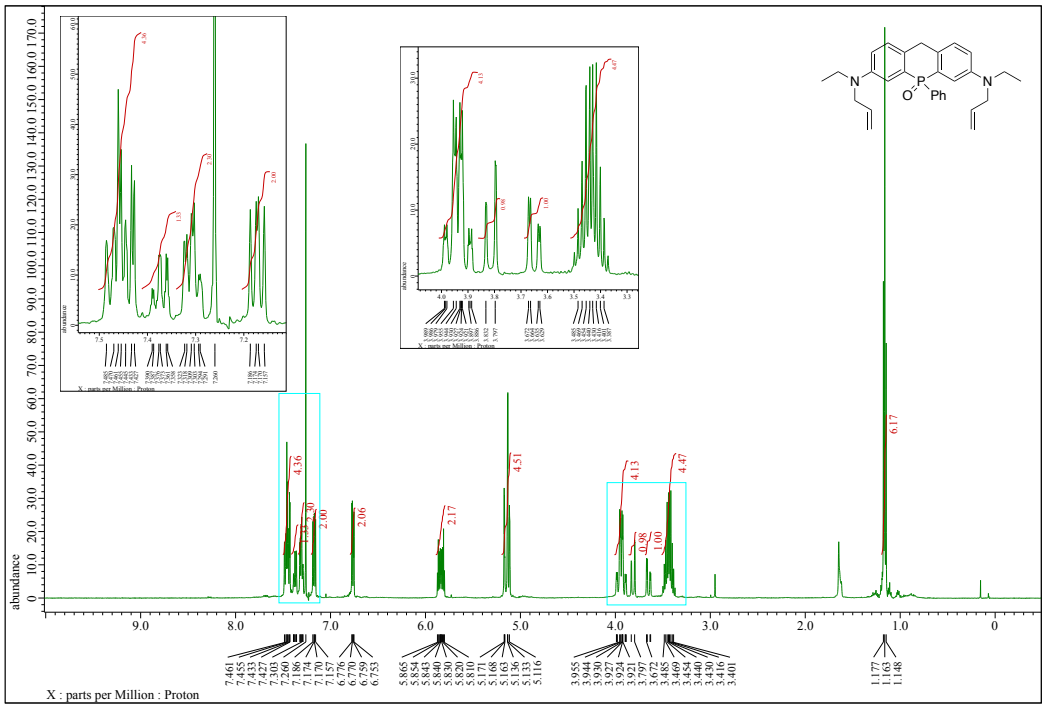

^{1}H NMR spectrum of **4** (500 MHz, $CDCl_3$)

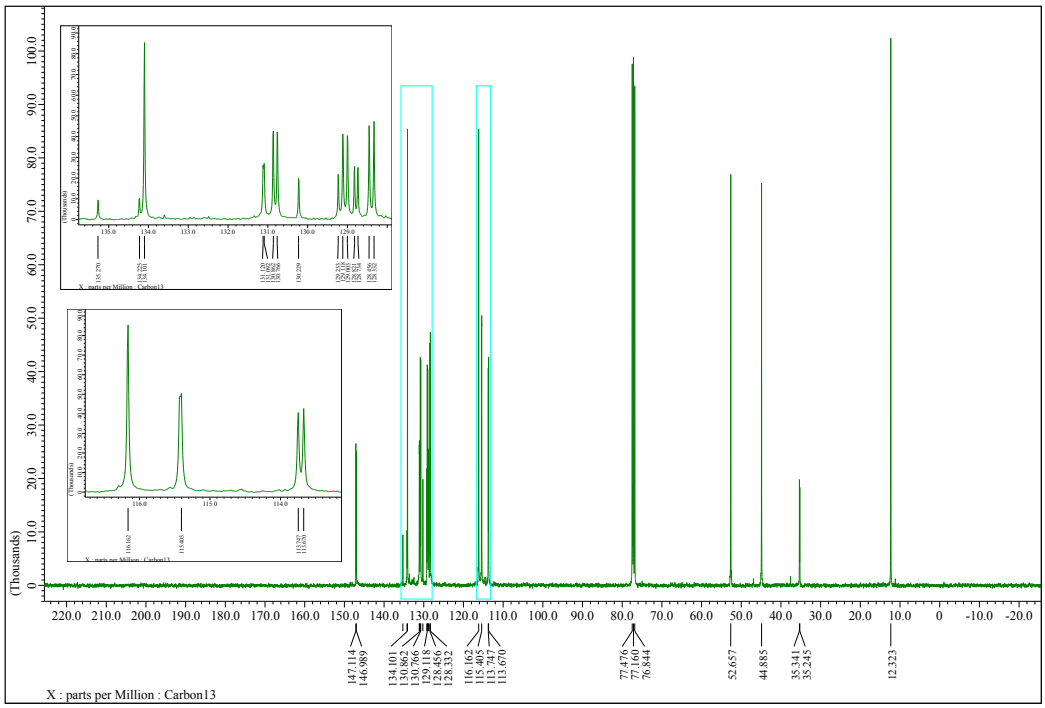

^{13}C NMR spectrum of **4** (100 MHz, $CDCl_3$)

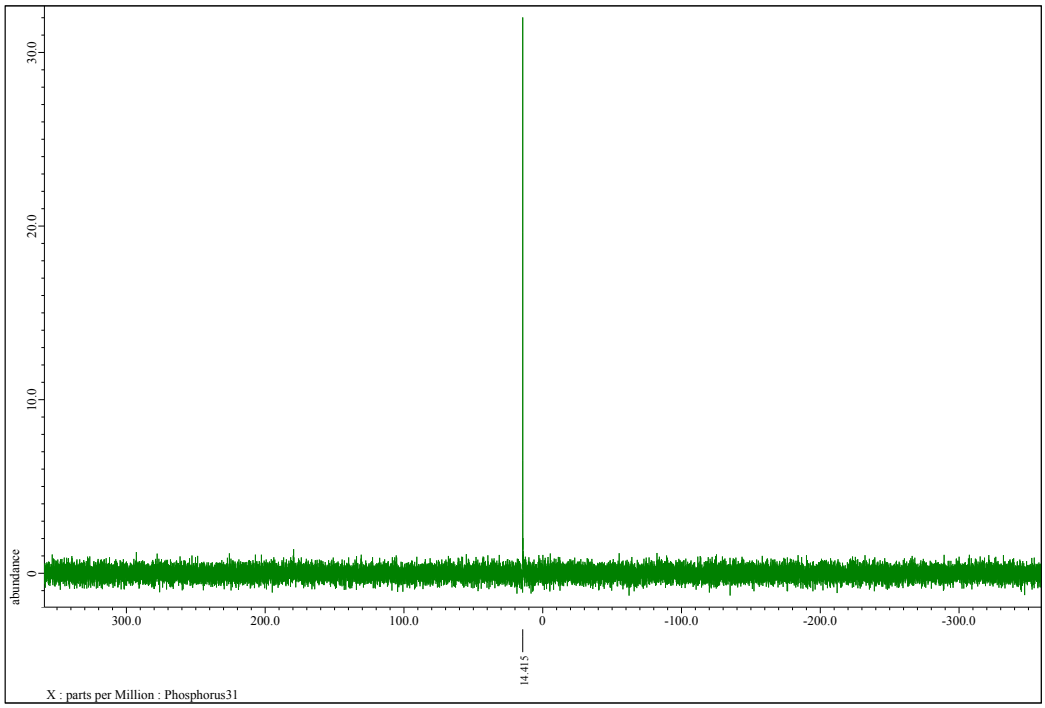

^{31}P NMR spectrum of **4** (202 MHz, $CDCl_3$)

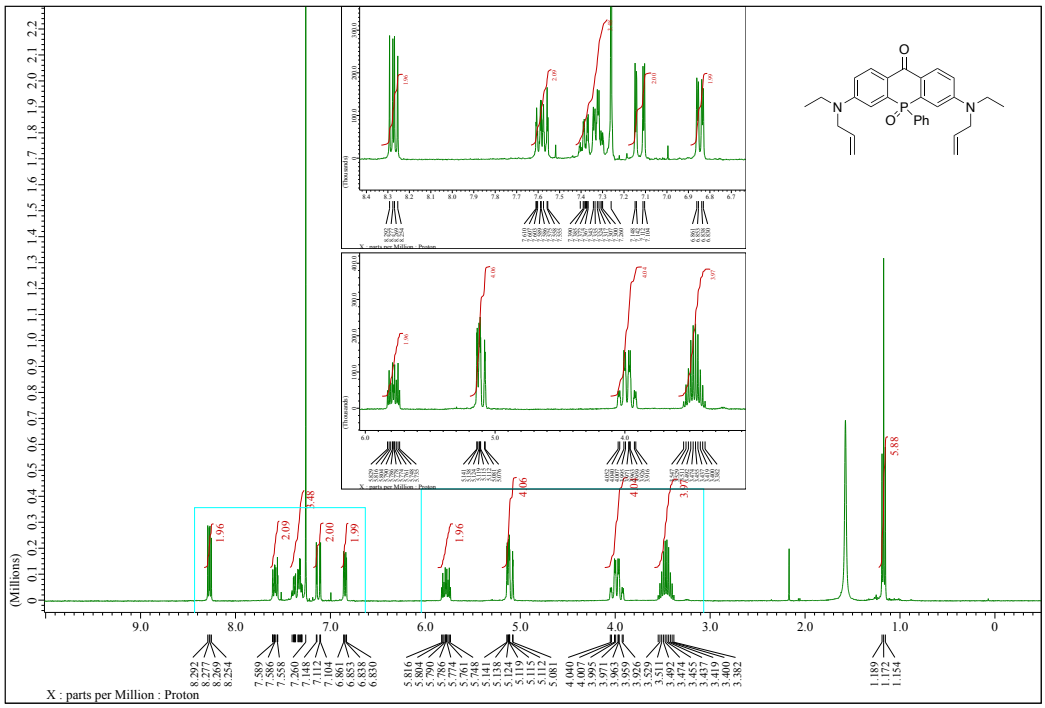

^{1}H NMR spectrum of **5** (400 MHz, $CDCl_3$)

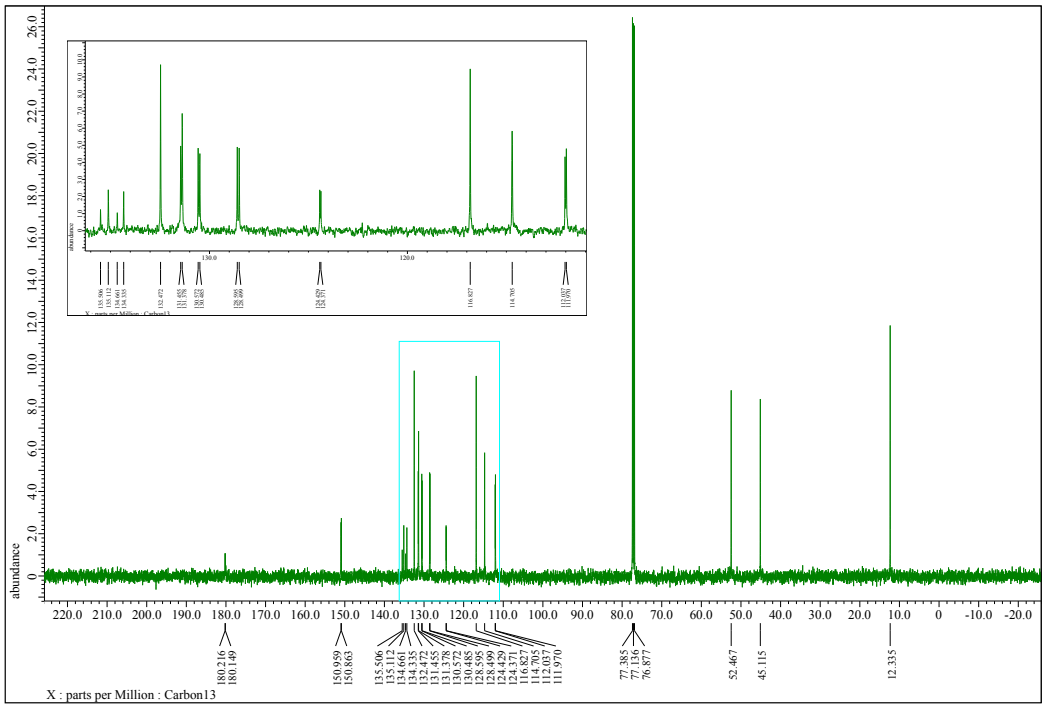

^{13}C NMR spectrum of **5** (125 MHz, $CDCl_3$)

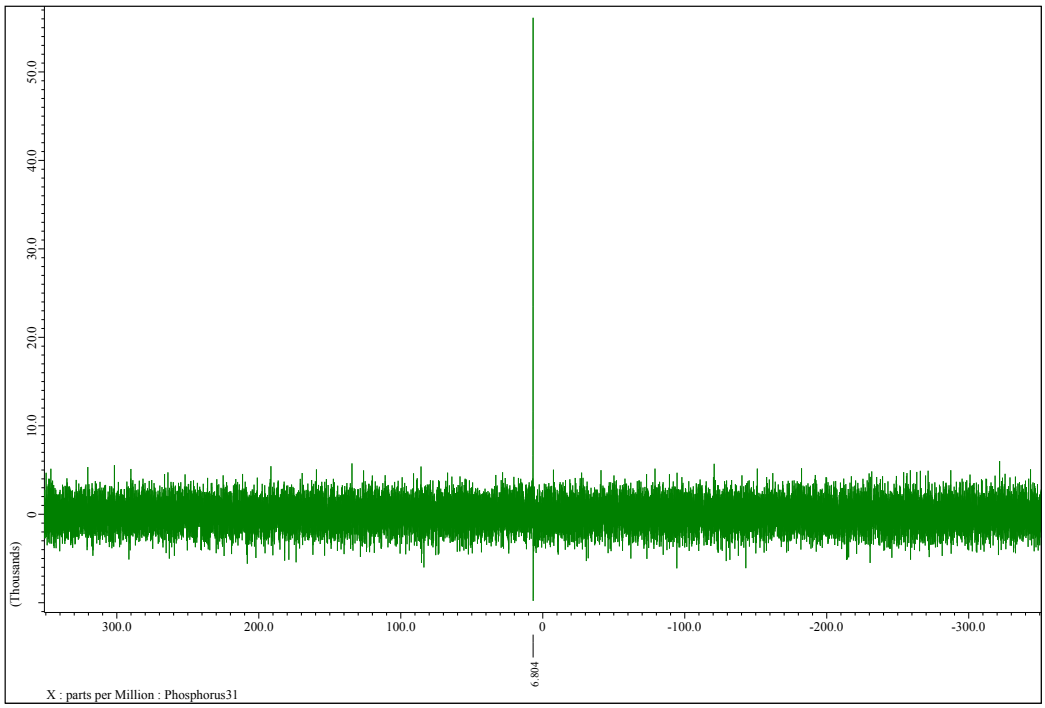

^{31}P NMR spectrum of **5** (162 MHz, $CDCl_3$)

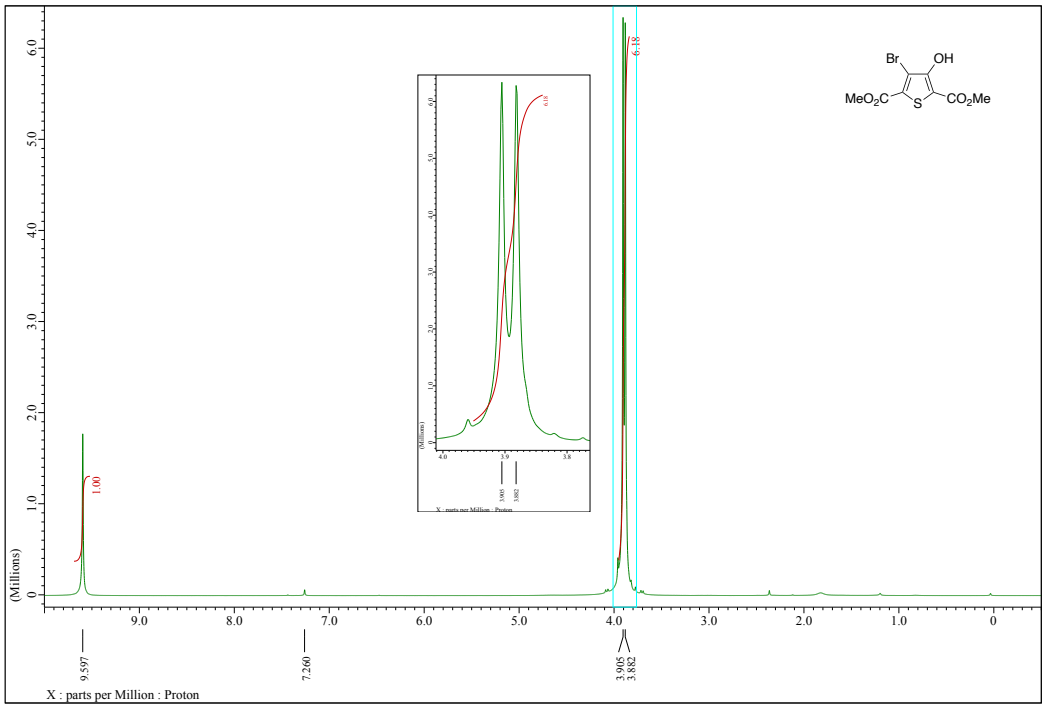

^{1}H NMR spectrum of **7** (400 MHz, $CDCl_3$)

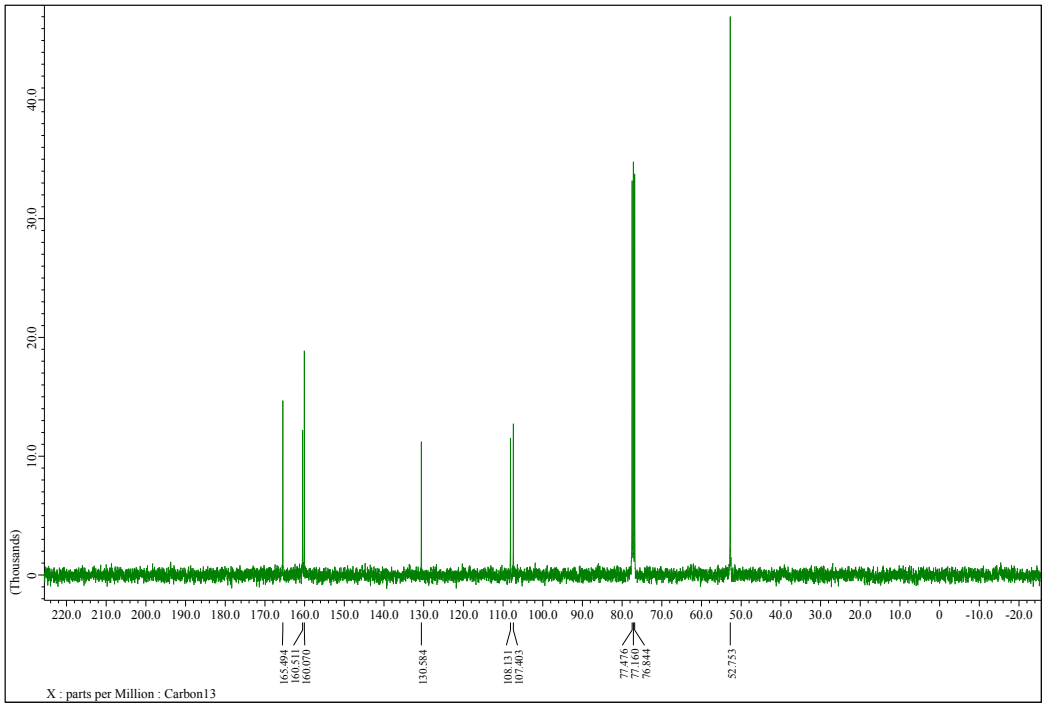

^{13}C NMR spectrum of **7** (100 MHz, $CDCl_3$)

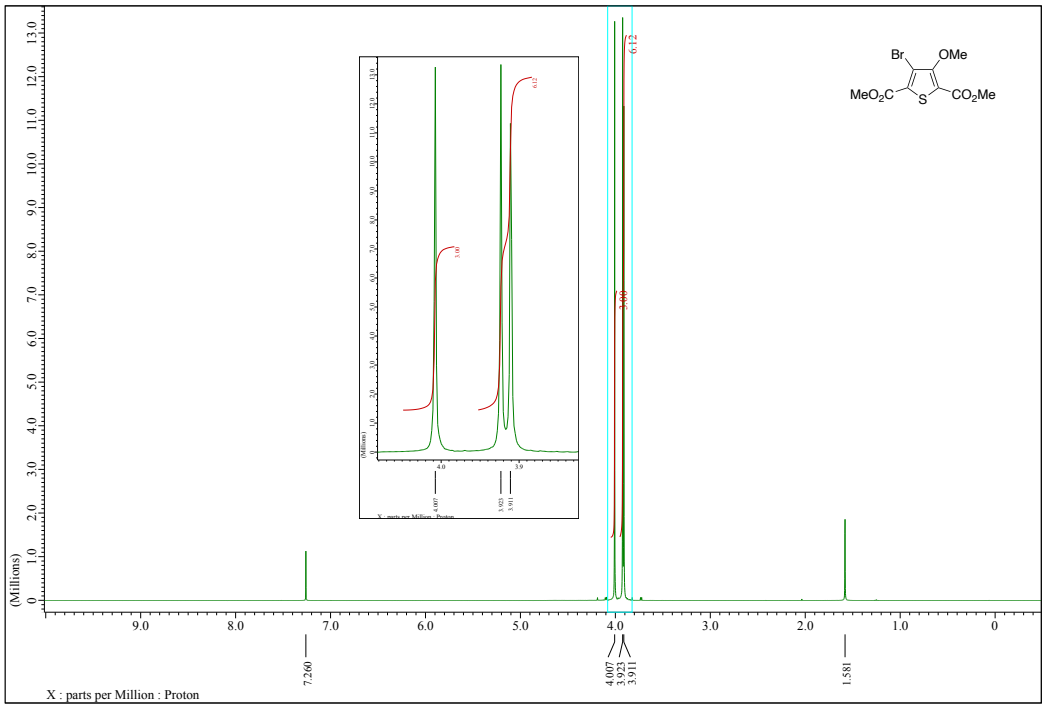

^{1}H NMR spectrum of **8** (400 MHz, $CDCl_3$)

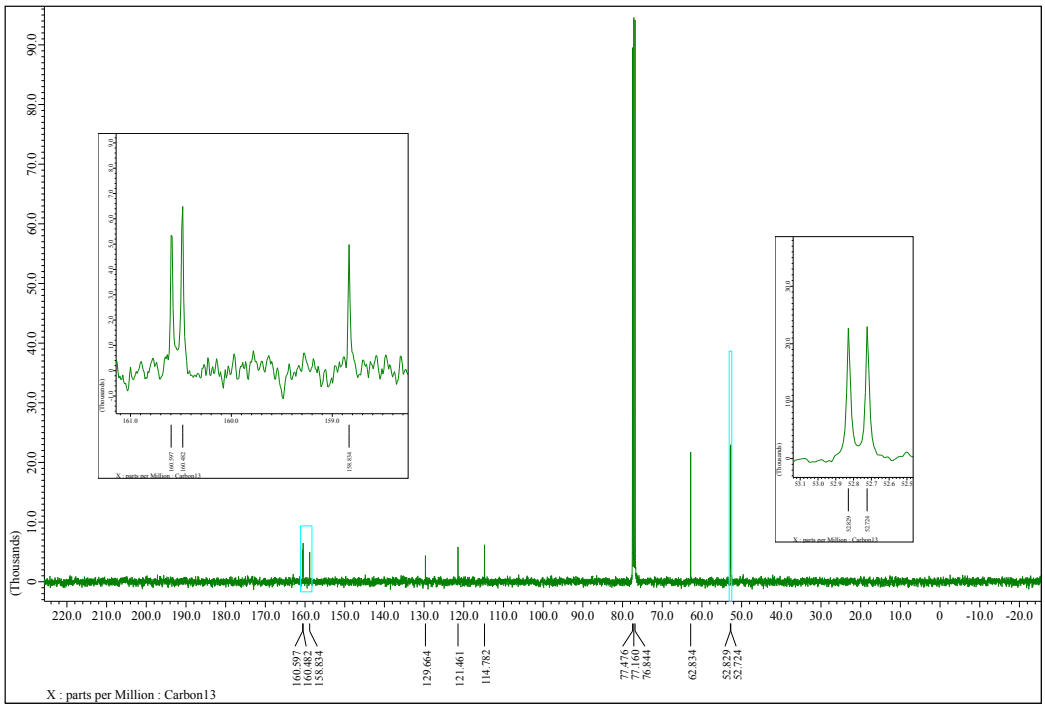

^{13}C NMR spectrum of **8** (100 MHz, $CDCl_3$)

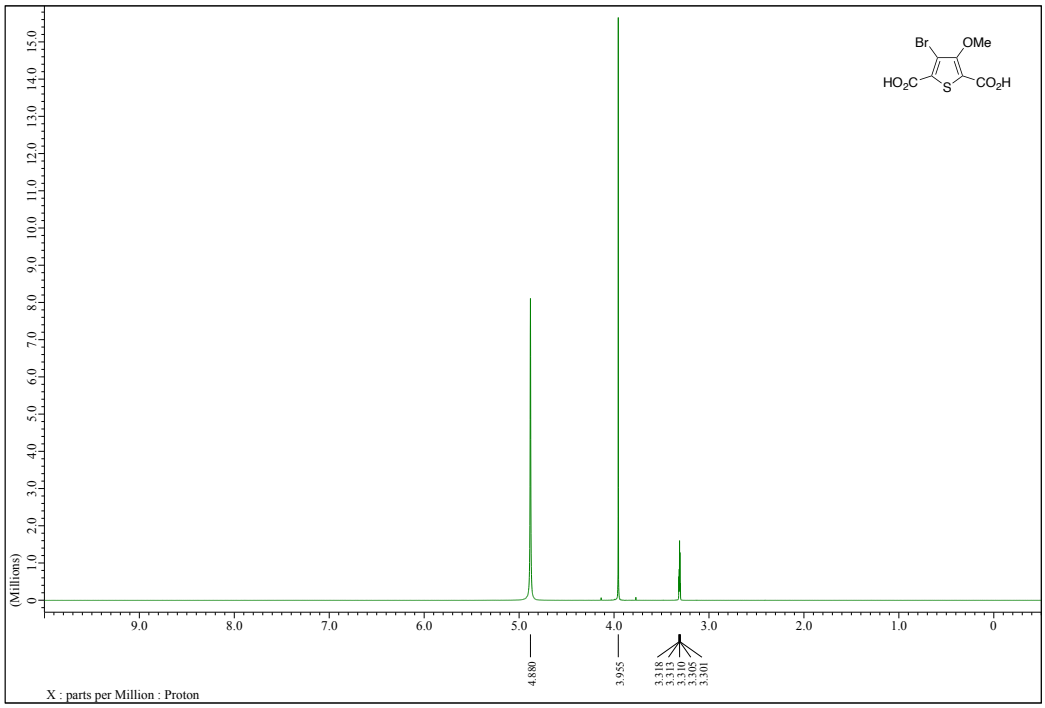

^{1}H NMR spectrum of **9** (400 MHz, CD_3OD)

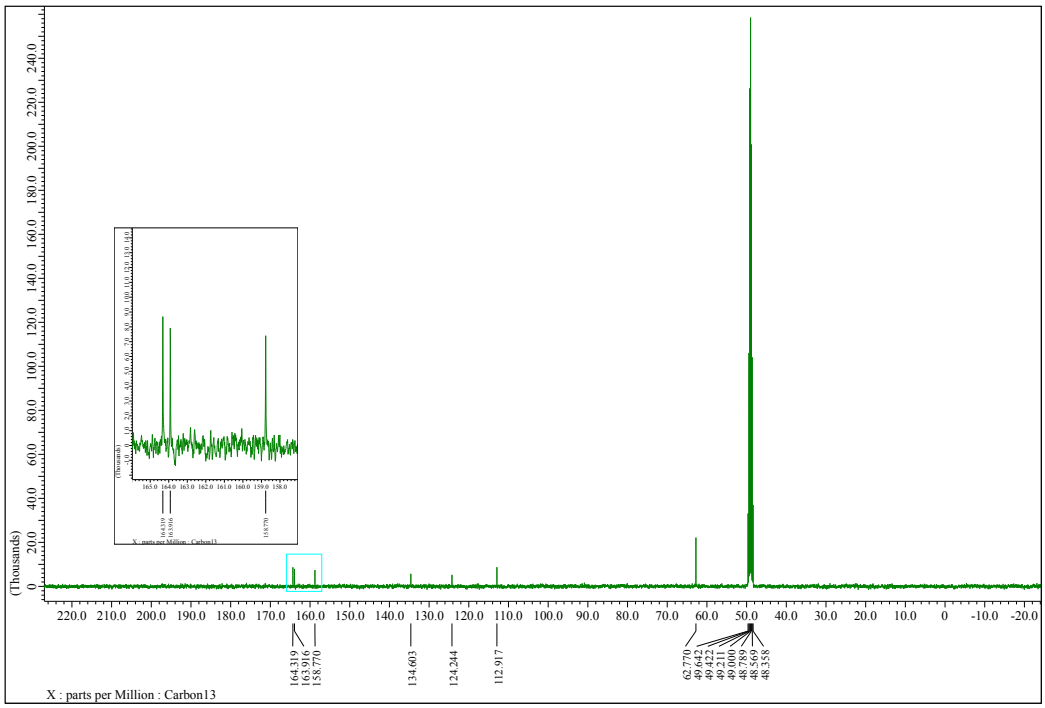

^{13}C NMR spectrum of **9** (100 MHz, CD_3OD)

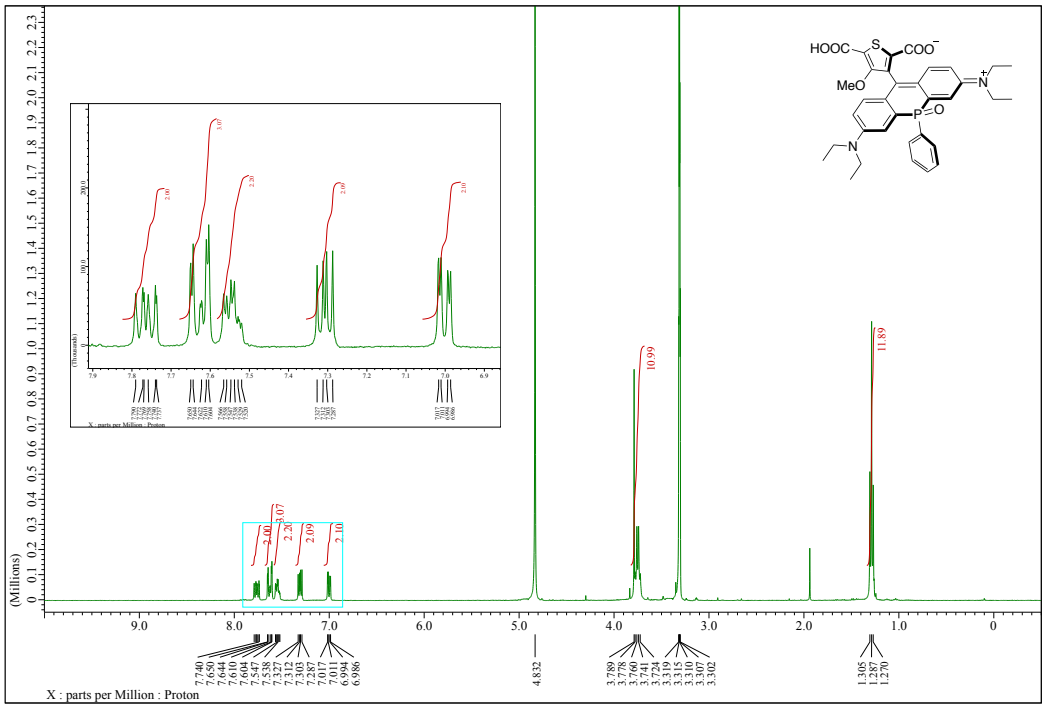

^{1}H NMR spectrum of ***cis*-POR715** (400 MHz, CD_3OD)

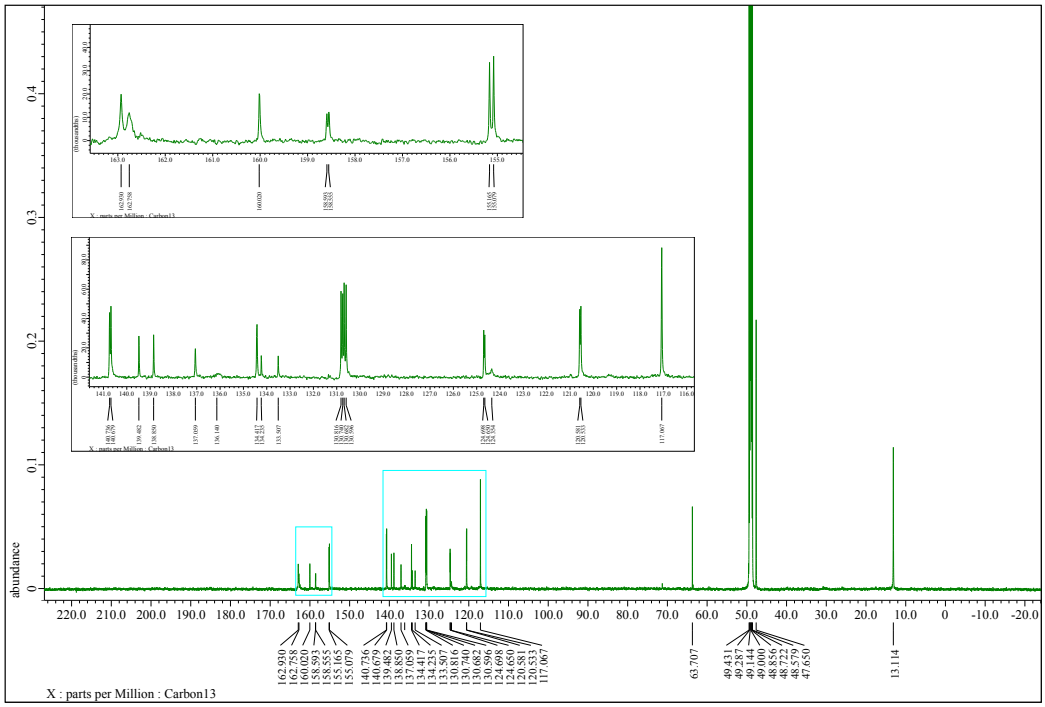

^{13}C NMR spectrum of ***cis*-POR715** (150 MHz, CD_3OD)

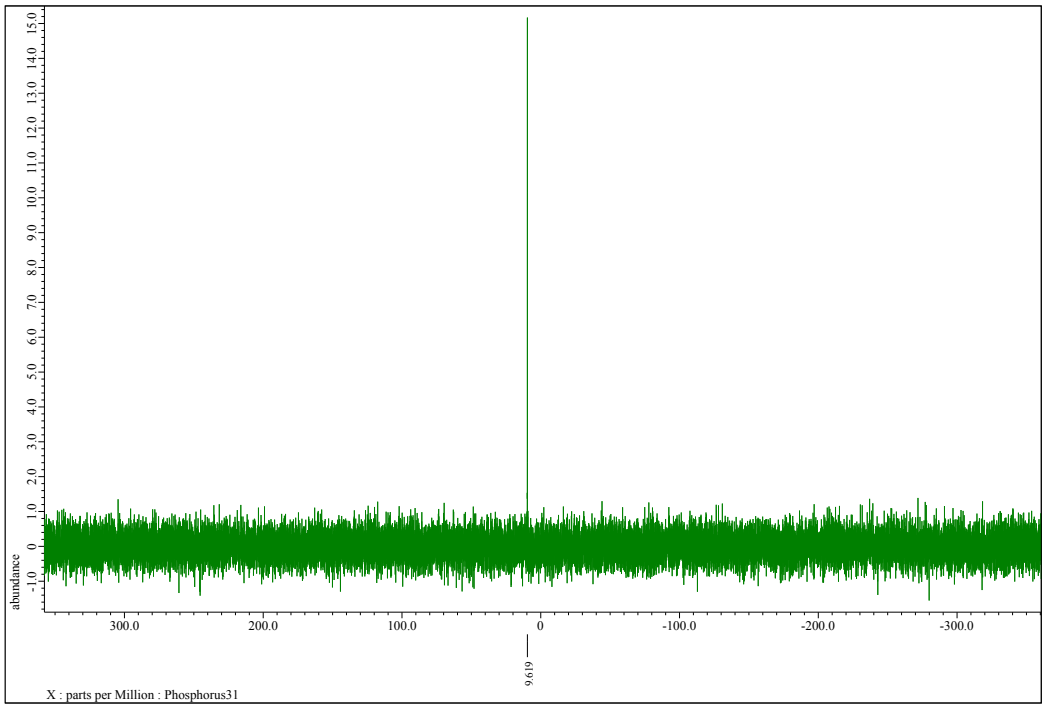

^{31}P NMR spectrum of ***cis*-POR715** (202 MHz, CD_3OD)

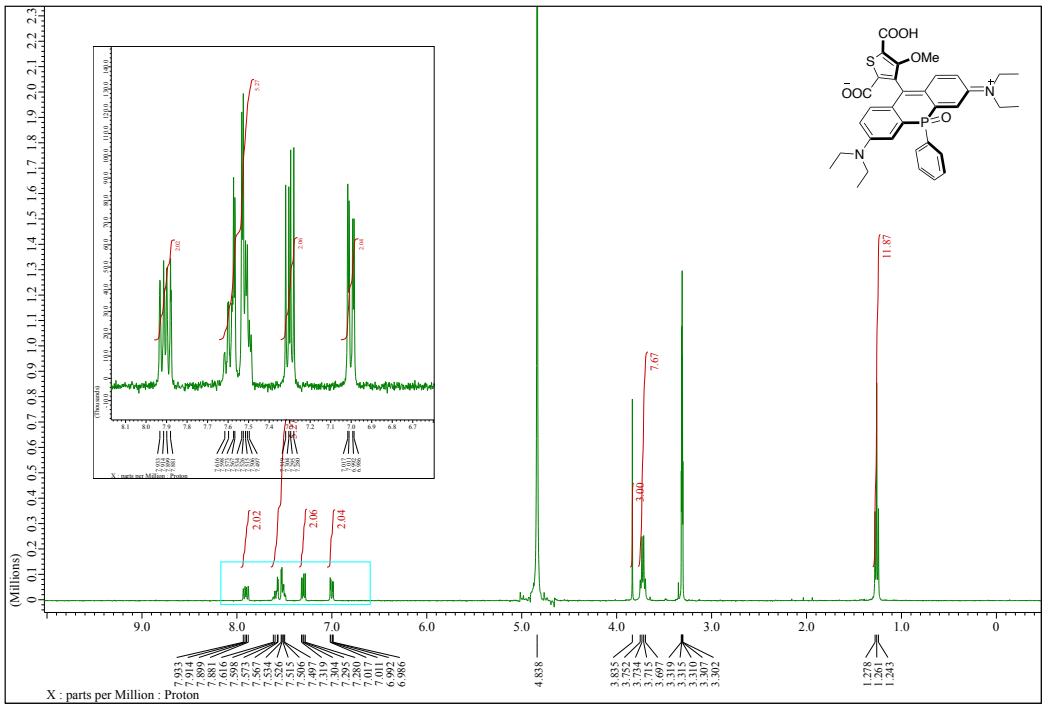

^{1}H NMR spectrum of ***trans*-POR715** (400 MHz, CD_3OD)

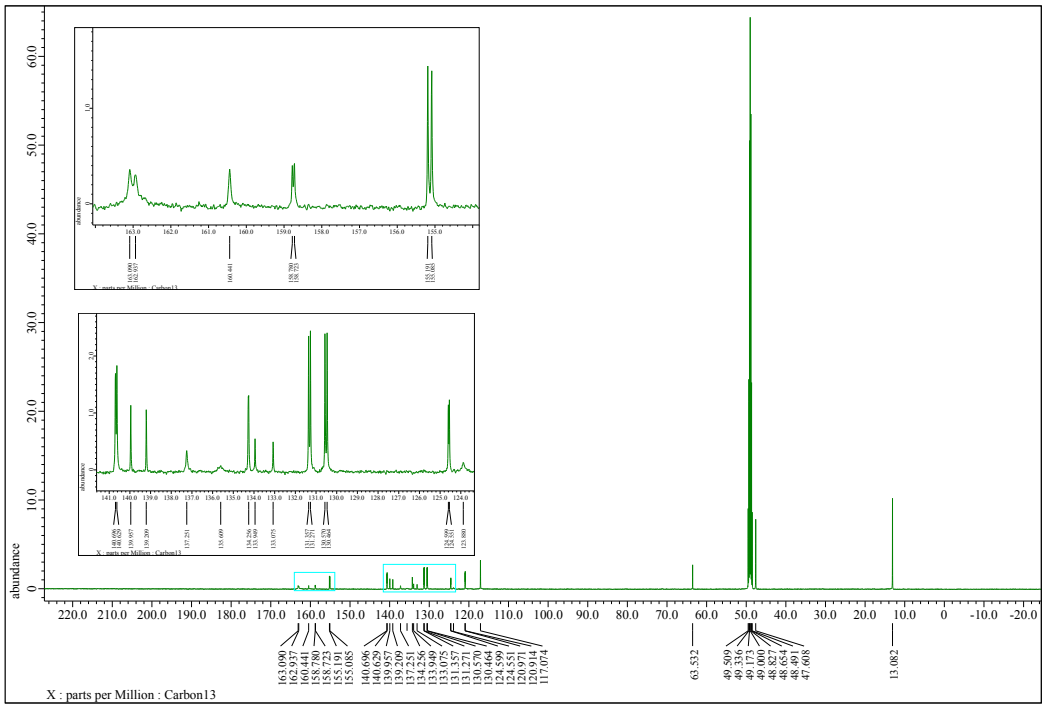

^{13}C NMR spectrum of ***trans*-POR715** (125 MHz, CD_3OD)

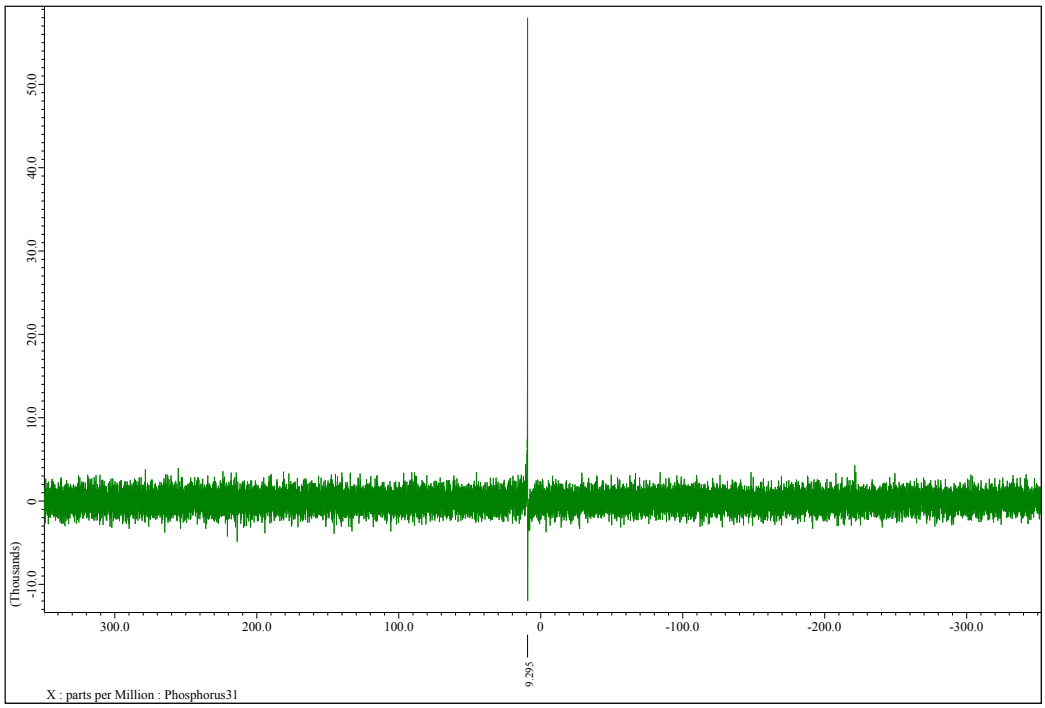

^{31}P NMR spectrum of ***trans*-POR715** (162 MHz, CD_3OD)

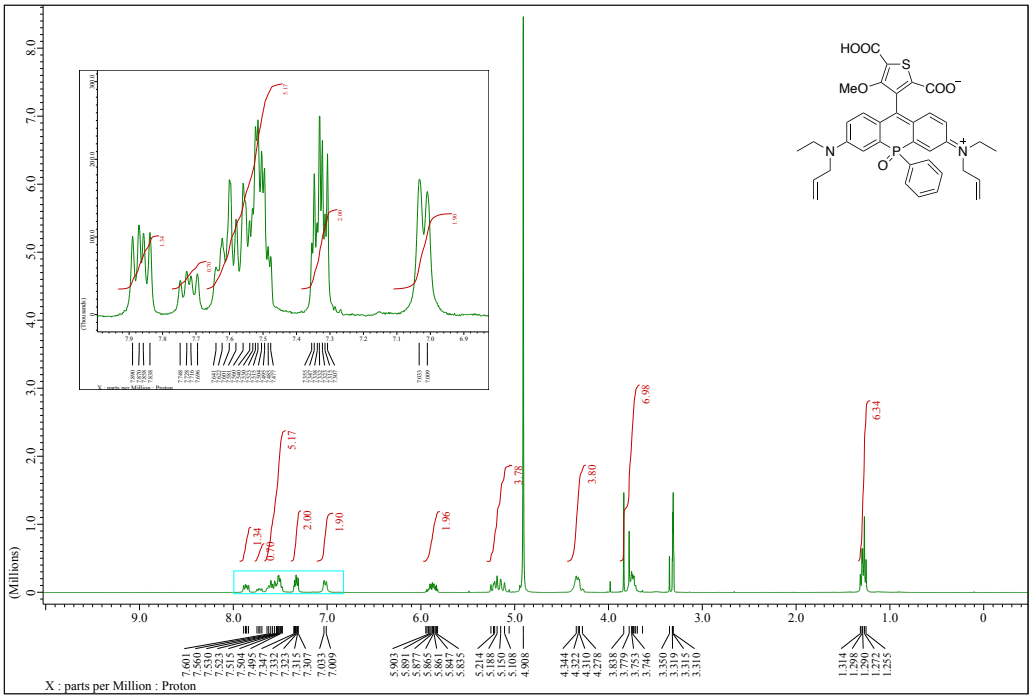

^{1}H NMR spectrum of **11** (400 MHz, CD_3OD)

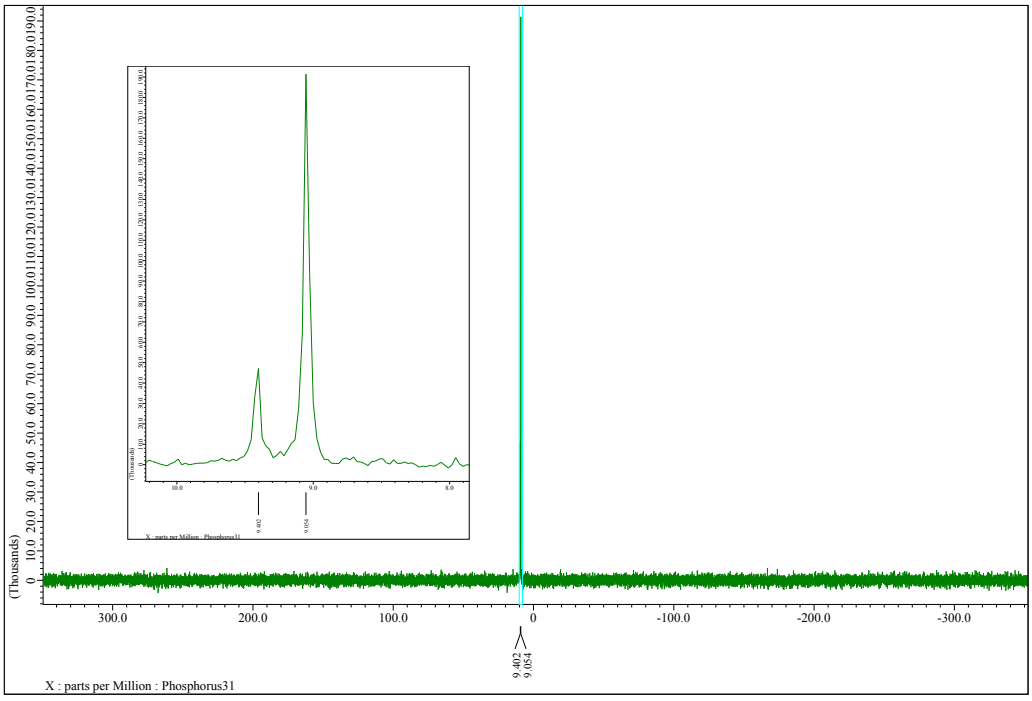

^{31}P NMR spectrum of **11** (162 MHz, CD_3OD)

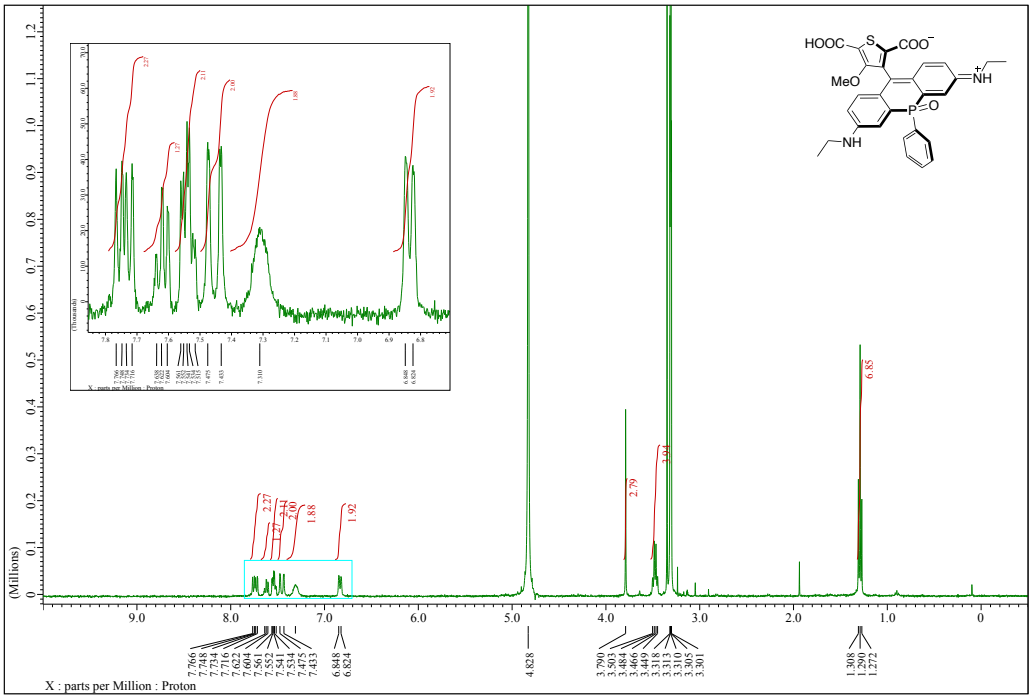

^{1}H NMR spectrum of ***cis*-POR675** (400 MHz, CD_3OD)

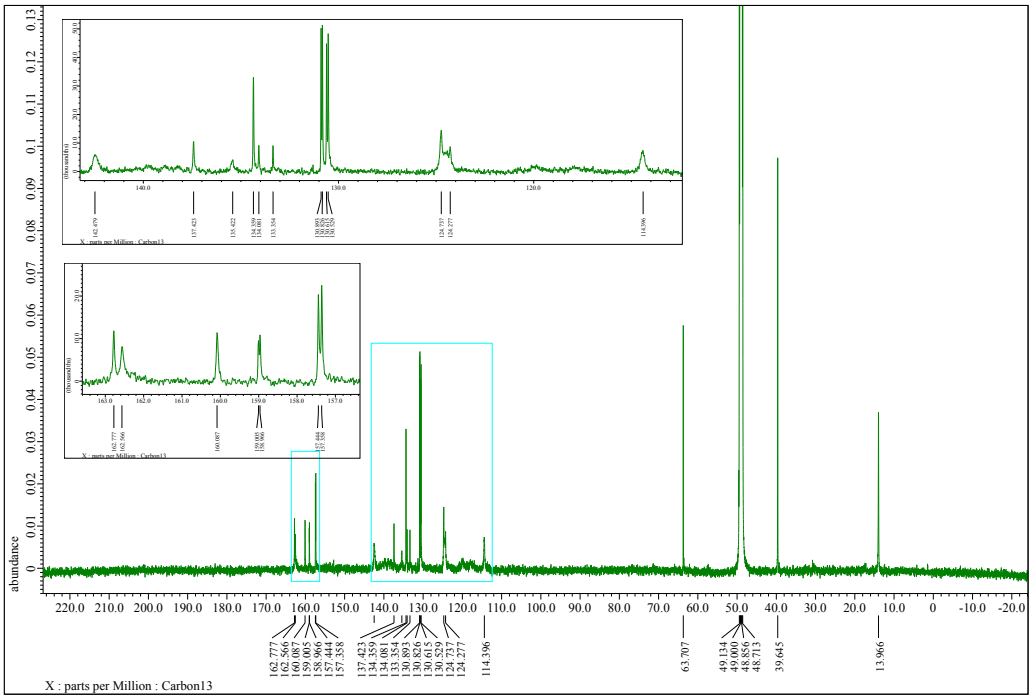

^{13}C NMR spectrum of ***cis*-POR675** (150 MHz, CD_3OD)

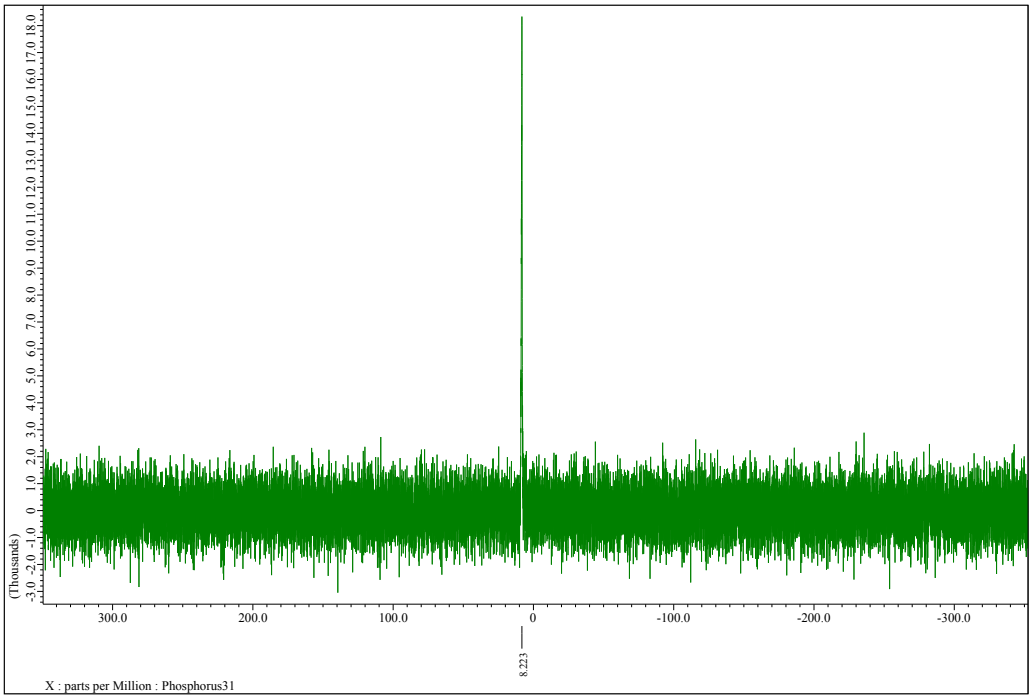

^{31}P NMR spectrum of ***cis*-POR675** (162 MHz, CD_3OD)

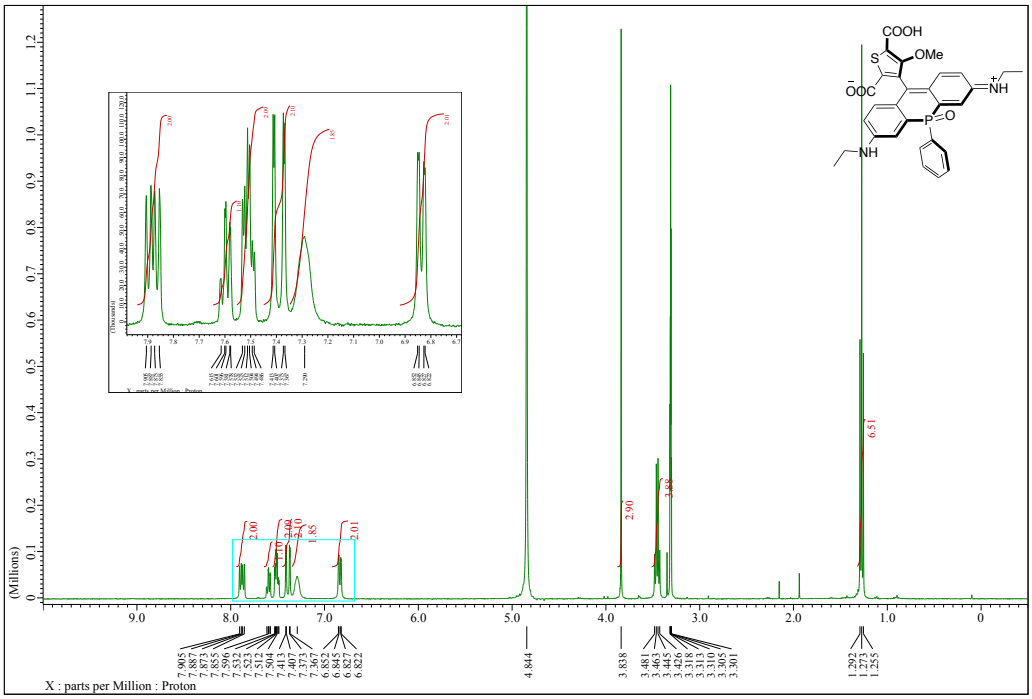

^{1}H NMR spectrum of ***trans*-POR675** (400 MHz, CD_3OD)

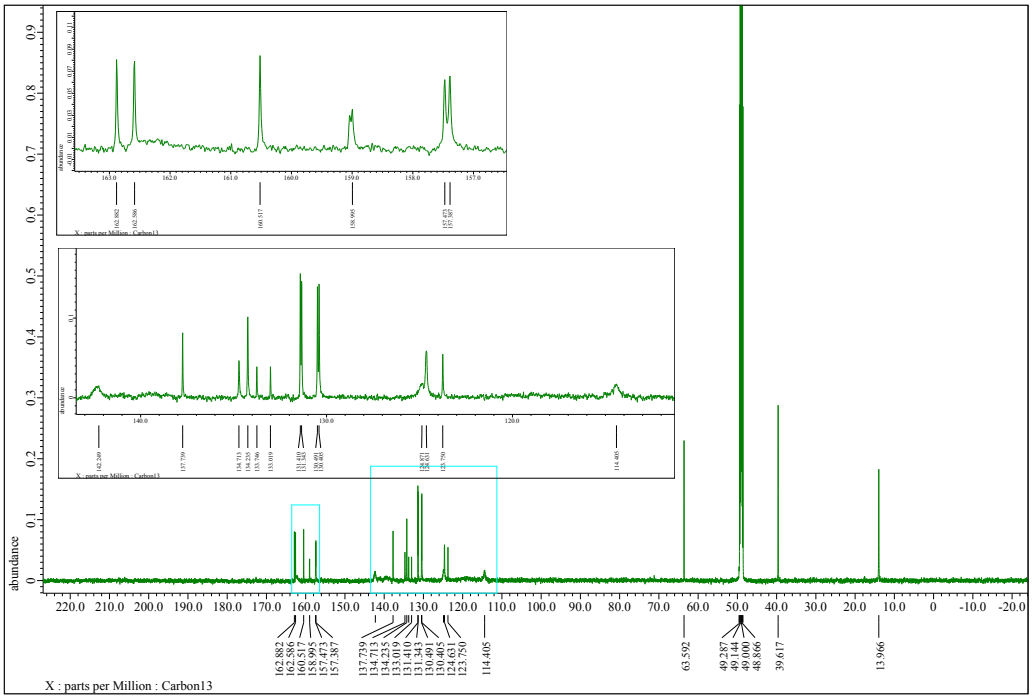

^{13}C NMR spectrum of ***trans*-POR675** (150 MHz, CD_3OD)

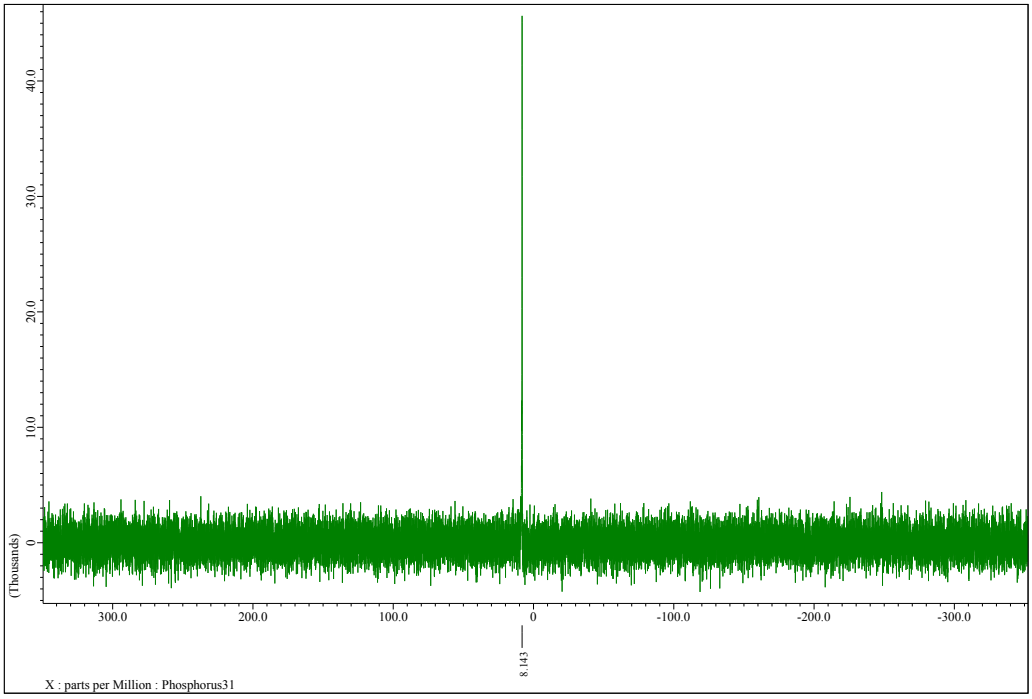

^{31}P NMR spectrum of ***trans*-POR675** (162 MHz, CD_3OD)

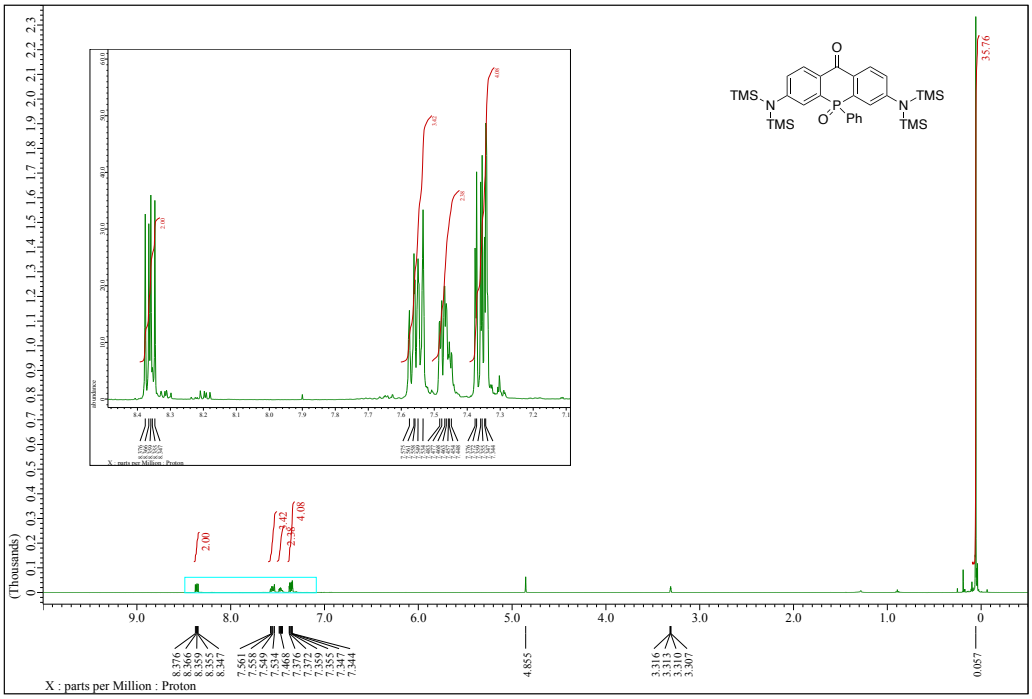

^{1}H NMR spectrum of **13** (500 MHz, CD_3OD)

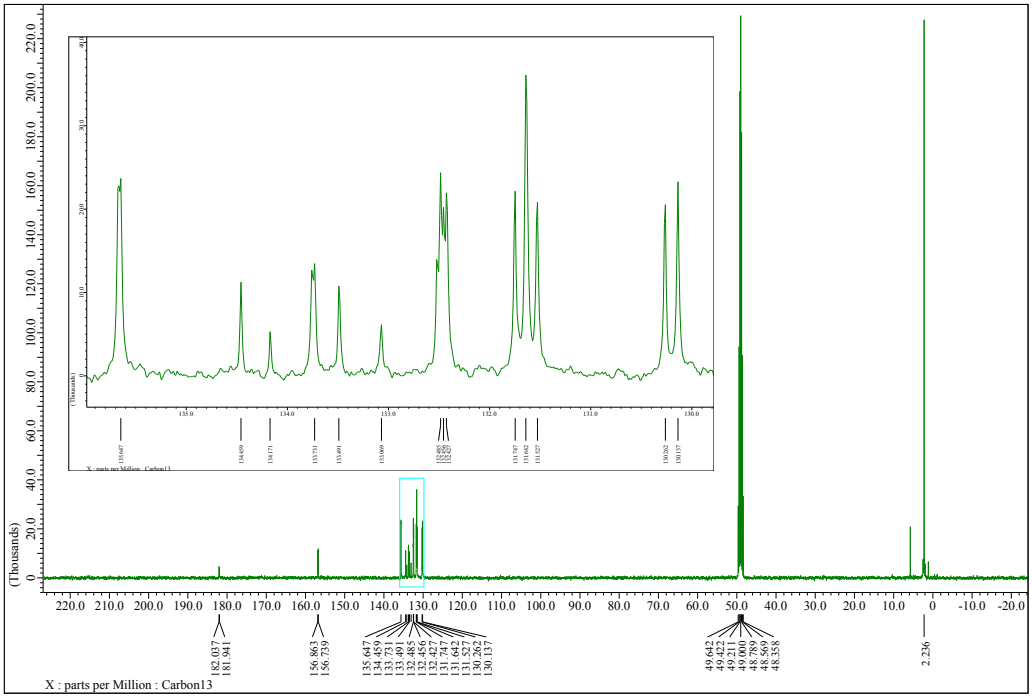

^{13}C NMR spectrum of **13** (100 MHz, CD_3OD)

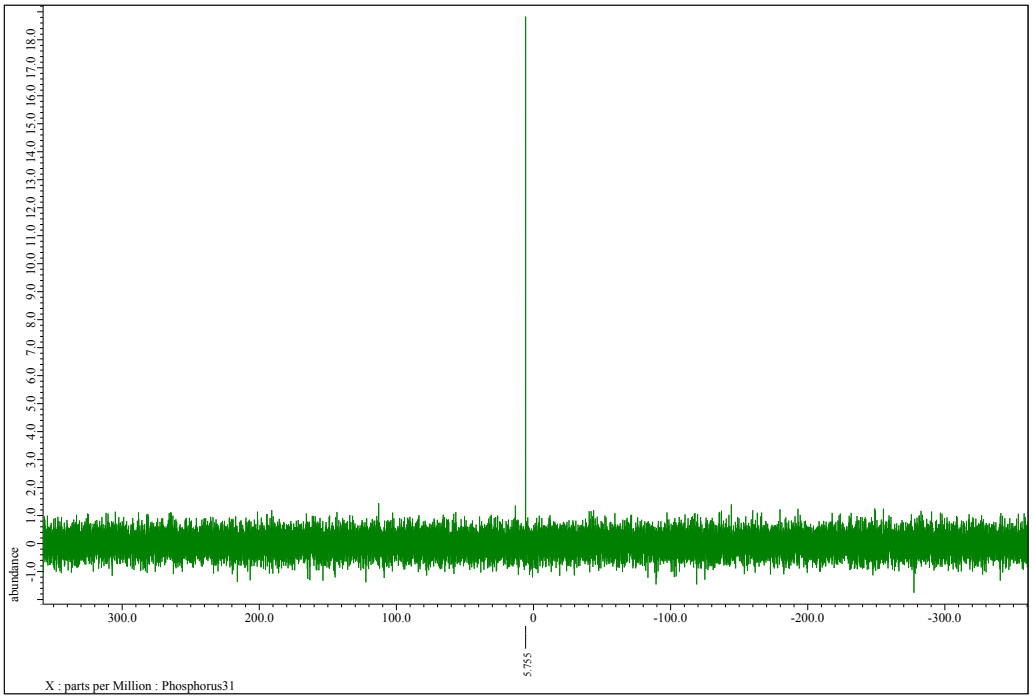

^{31}P NMR spectrum of **13** (202 MHz, CD_3OD)

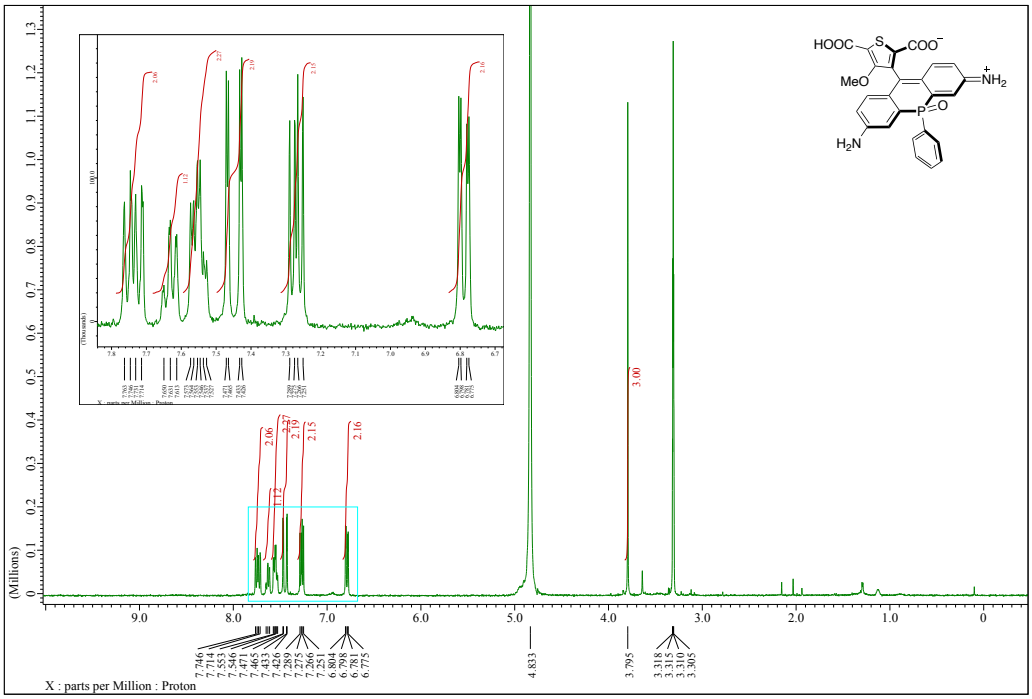

^{1}H NMR spectrum of ***cis*-POR645** (400 MHz, CD_3OD)

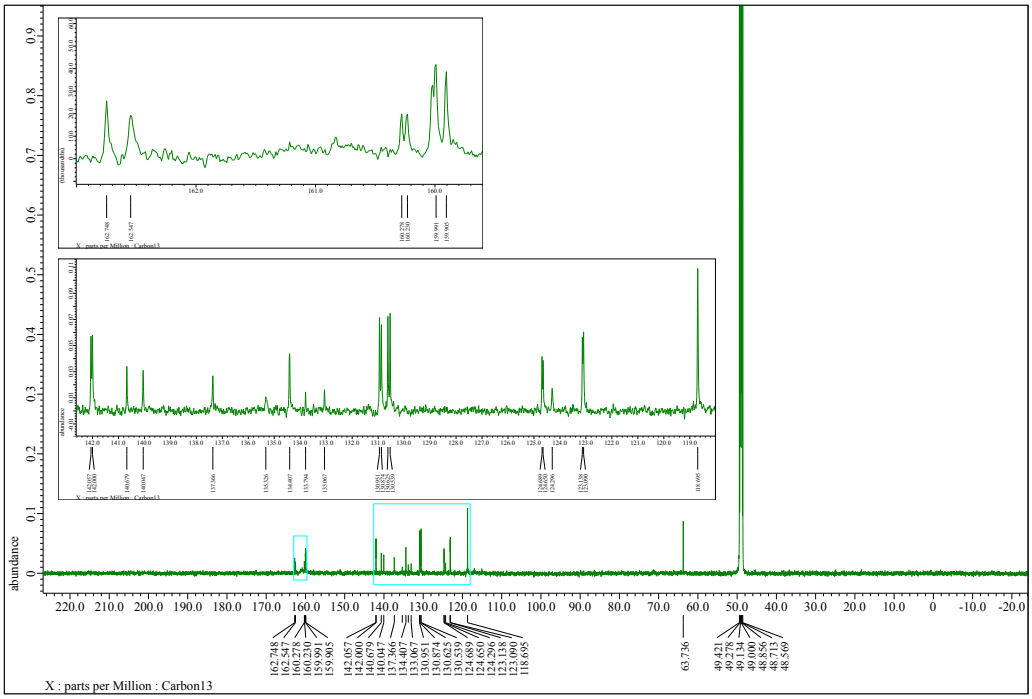

^{13}C NMR spectrum of ***cis*-POR645** (150 MHz, CD_3OD)

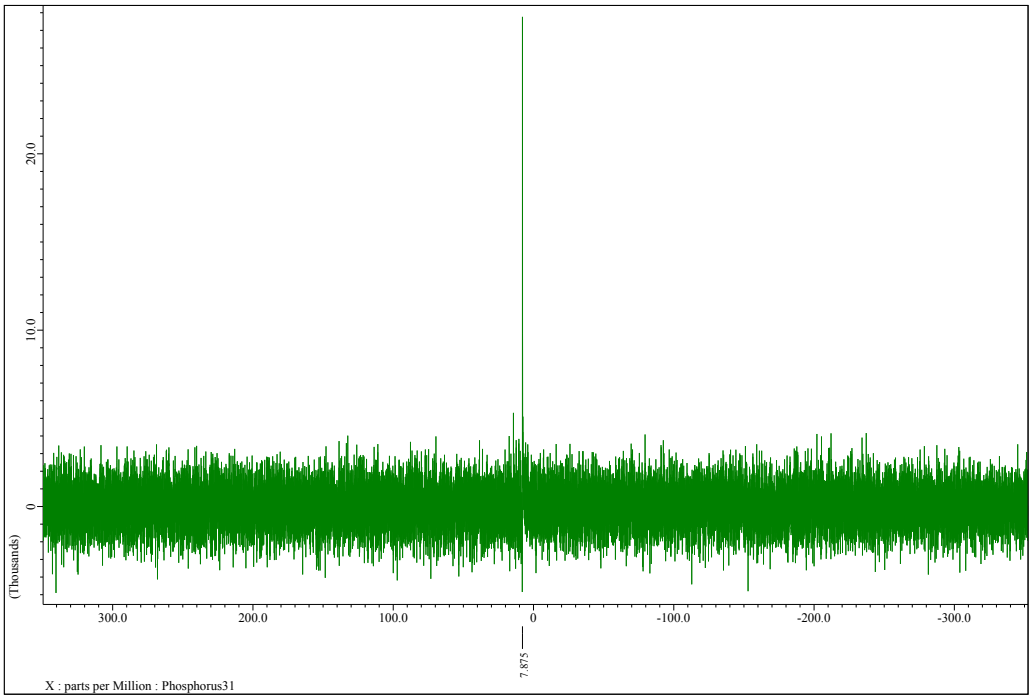

^{31}P NMR spectrum of ***cis*-POR645** (162 MHz, CD_3OD)

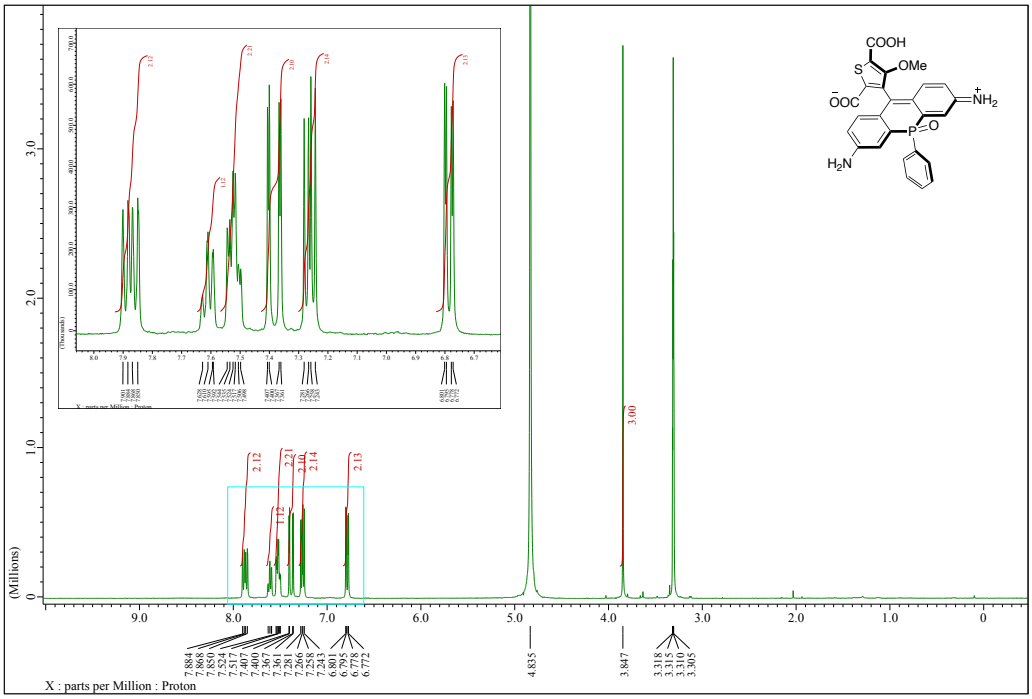

^{1}H NMR spectrum of ***trans*-POR645** (400 MHz, CD_3OD)

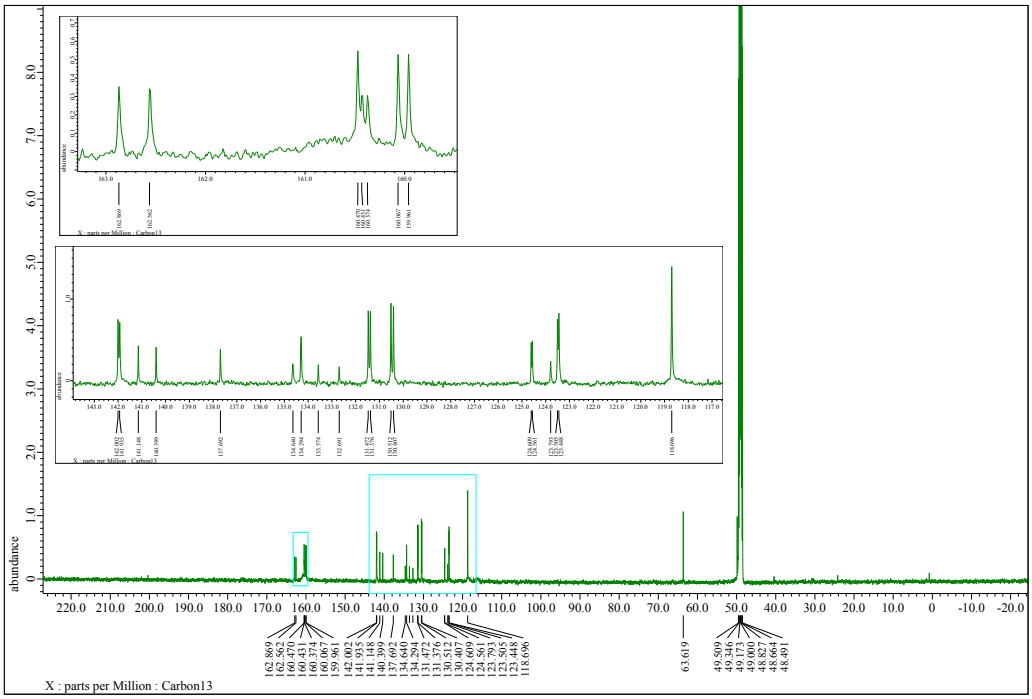

^{13}C NMR spectrum of ***trans*-POR645** (125 MHz, CD_3OD)

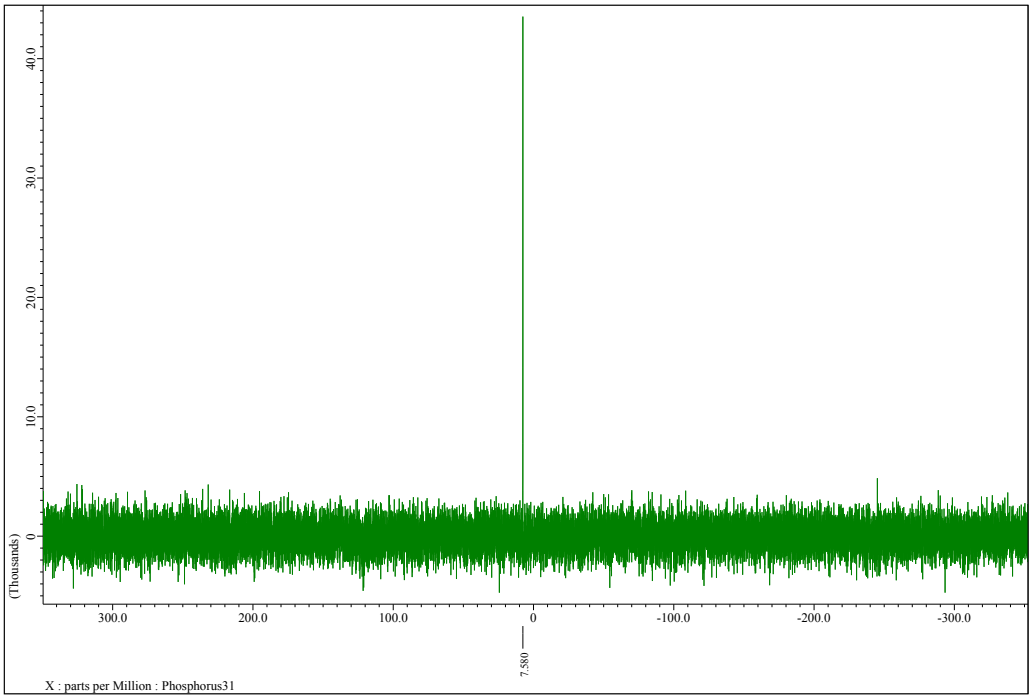

^{31}P NMR spectrum of ***trans*-POR645** (162 MHz, CD_3OD)

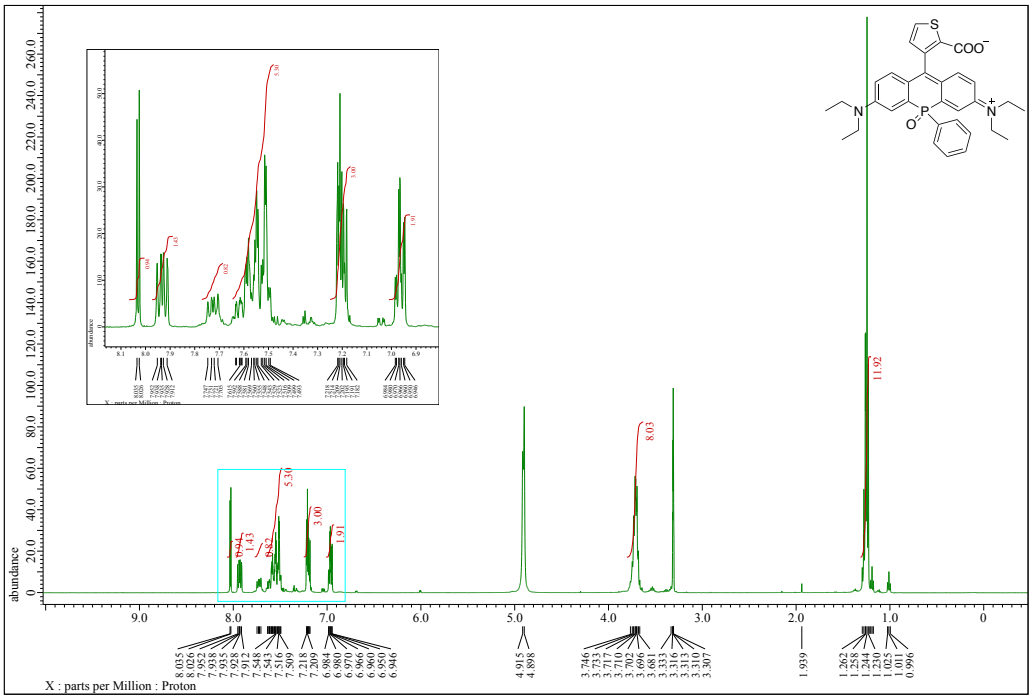

^{1}H NMR spectrum of **14** (500 MHz, CD_3OD)

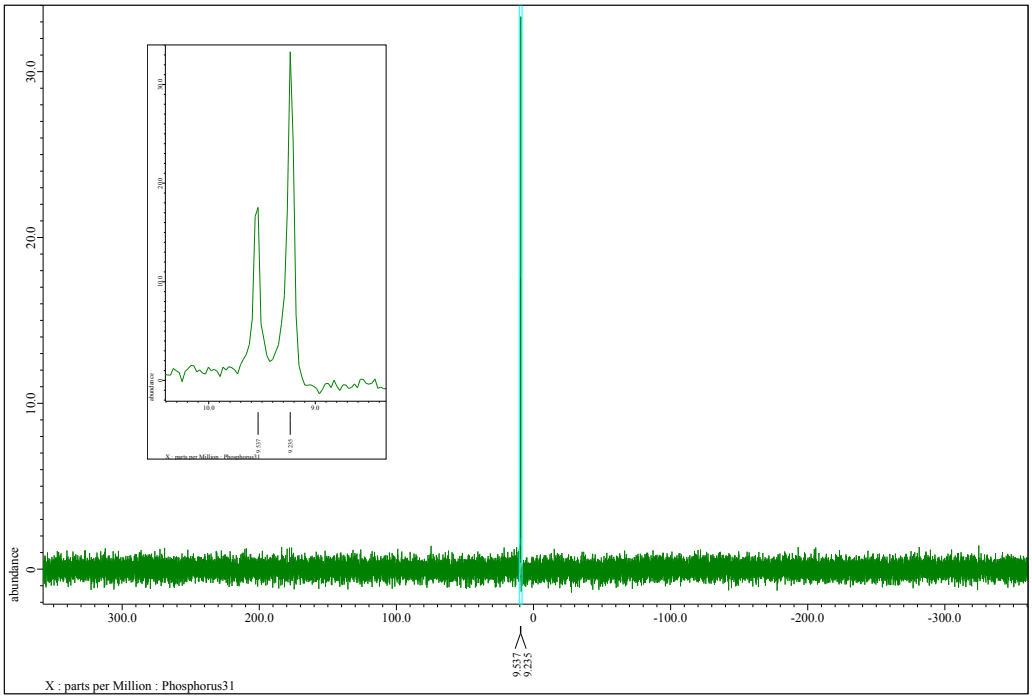

^{31}P NMR spectrum of **14** (202 MHz, CD_3OD)

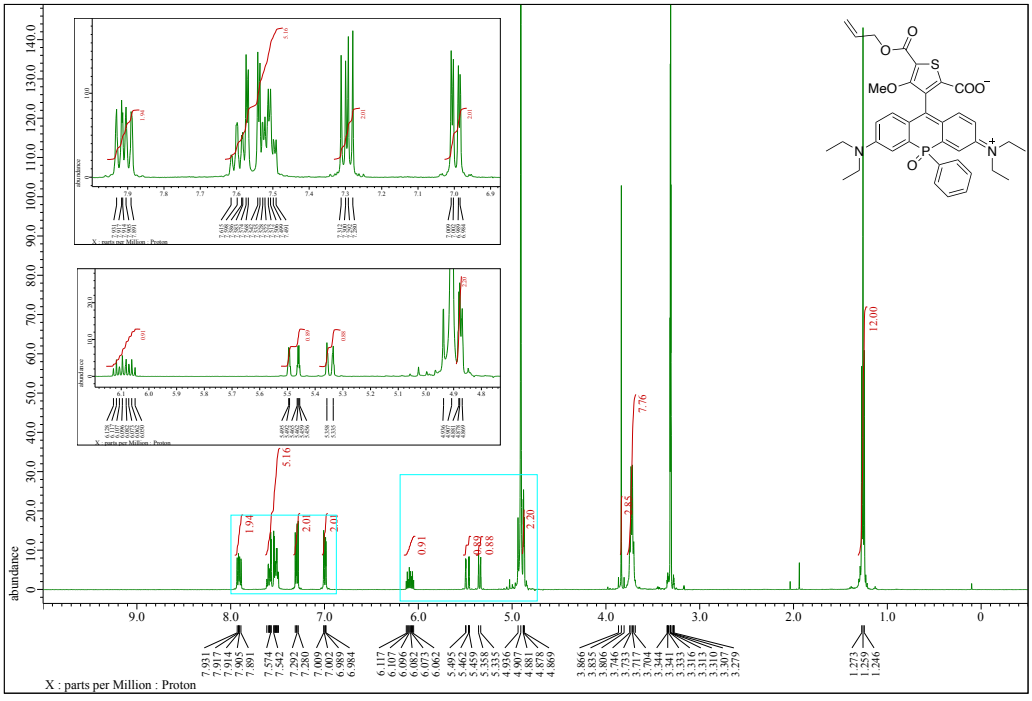

^{1}H NMR spectrum of **15** (500 MHz, CD_3OD)

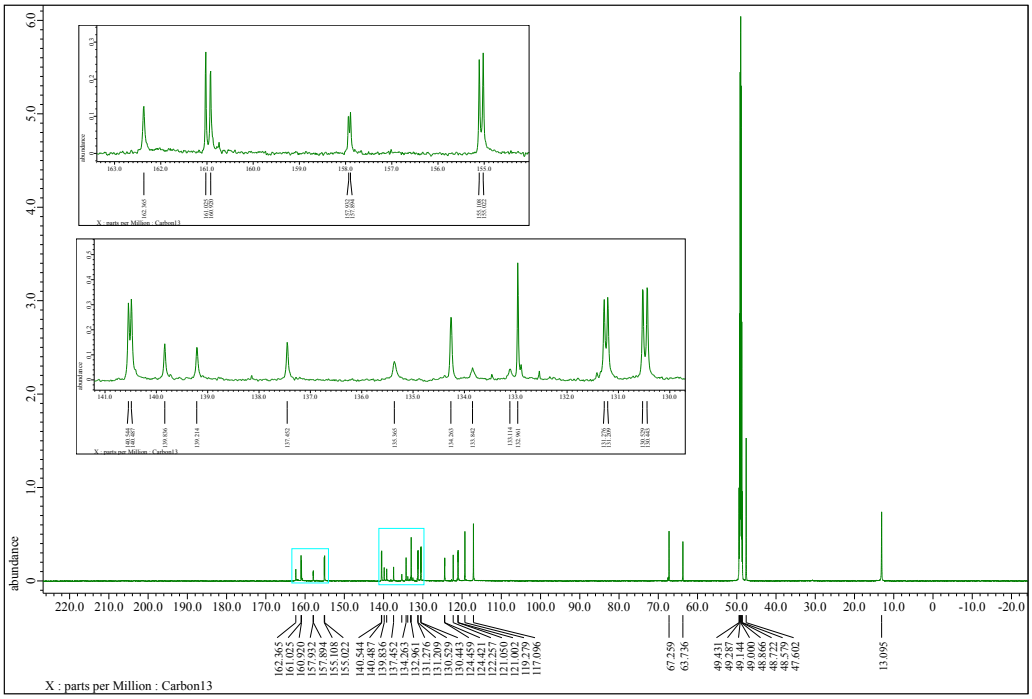

^{13}C NMR spectrum of **15** (150 MHz, CD_3OD)

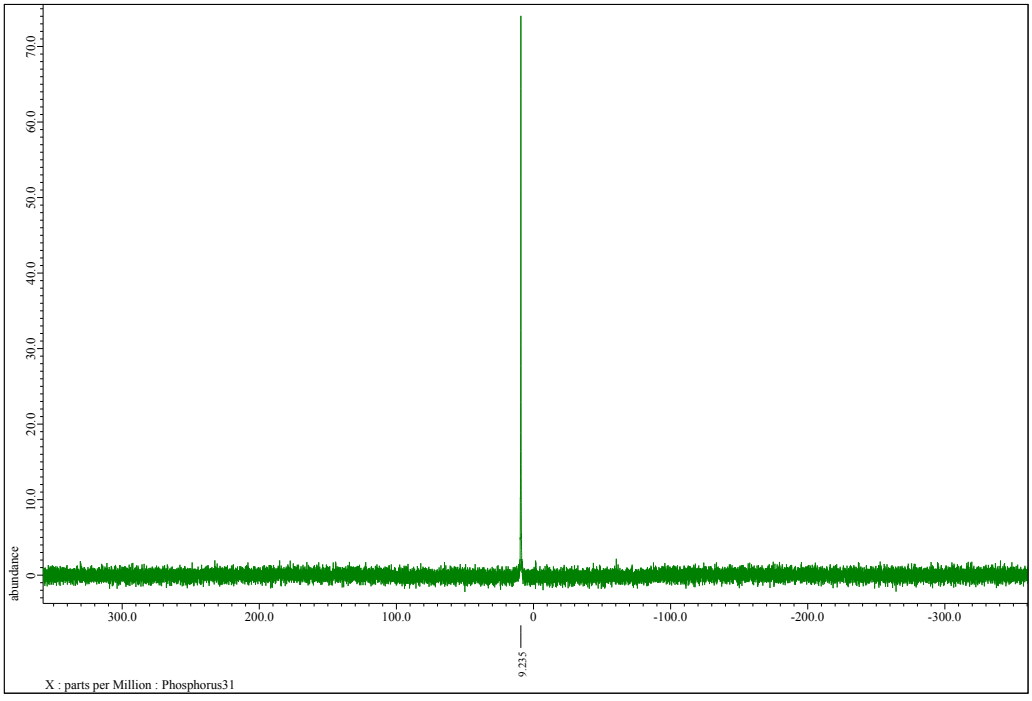

^{31}P NMR spectrum of **15** (202 MHz, CD_3OD)

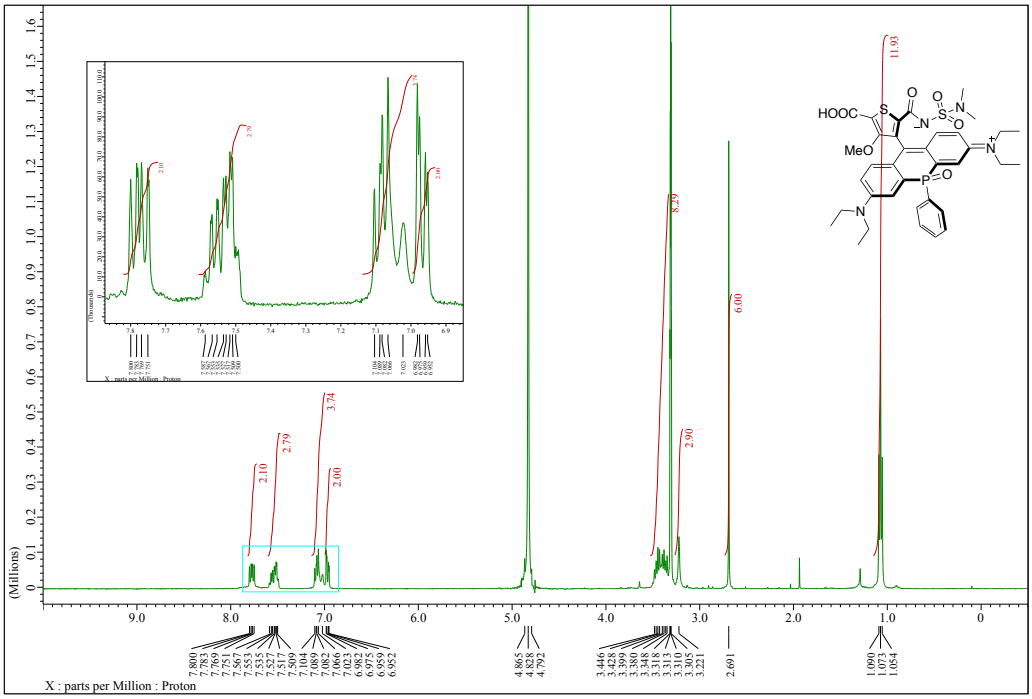

^{1}H NMR spectrum of ***cis*-PORSA715** (400 MHz, CD_3OD)

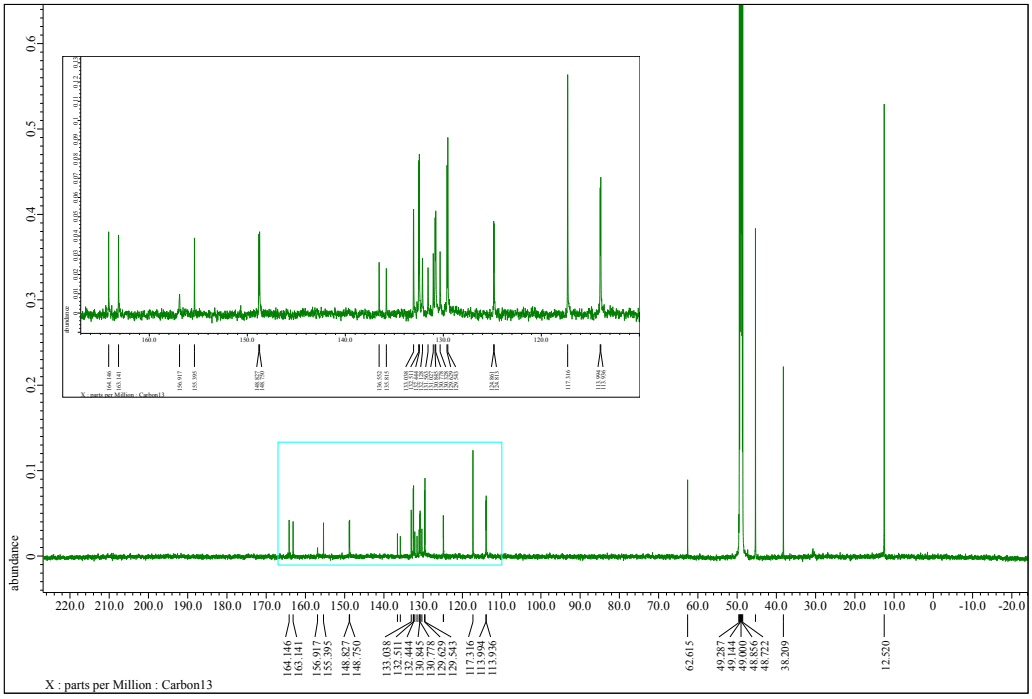

^{13}C NMR spectrum of ***cis*-PORSA715** (150 MHz, CD_3OD)

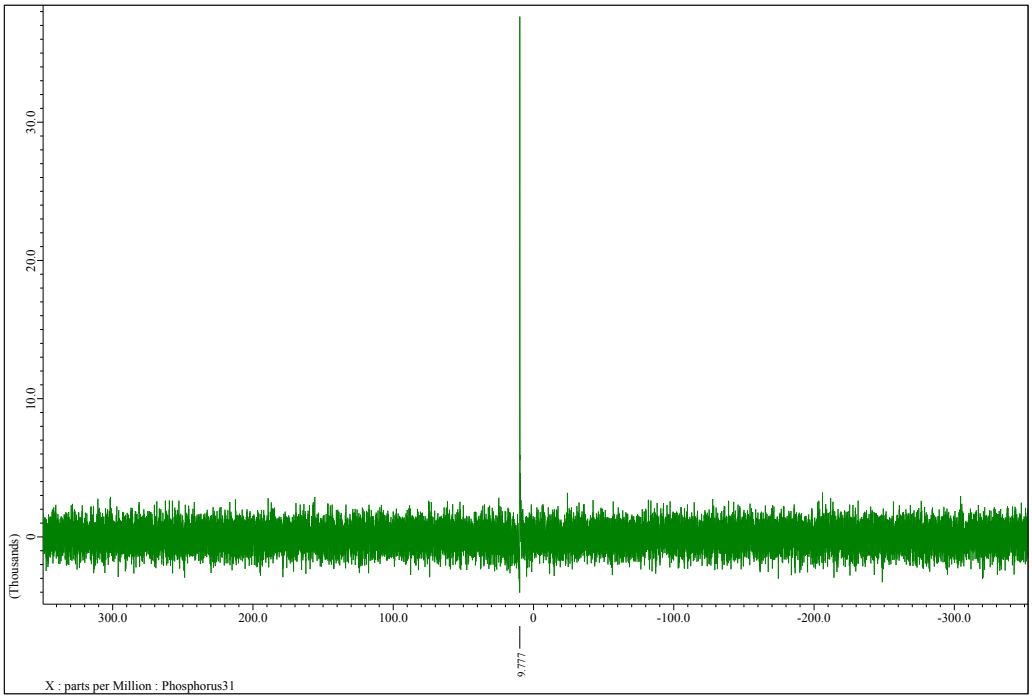

^{31}P NMR spectrum of ***cis*-PORSA715** (162 MHz, CD_3OD)

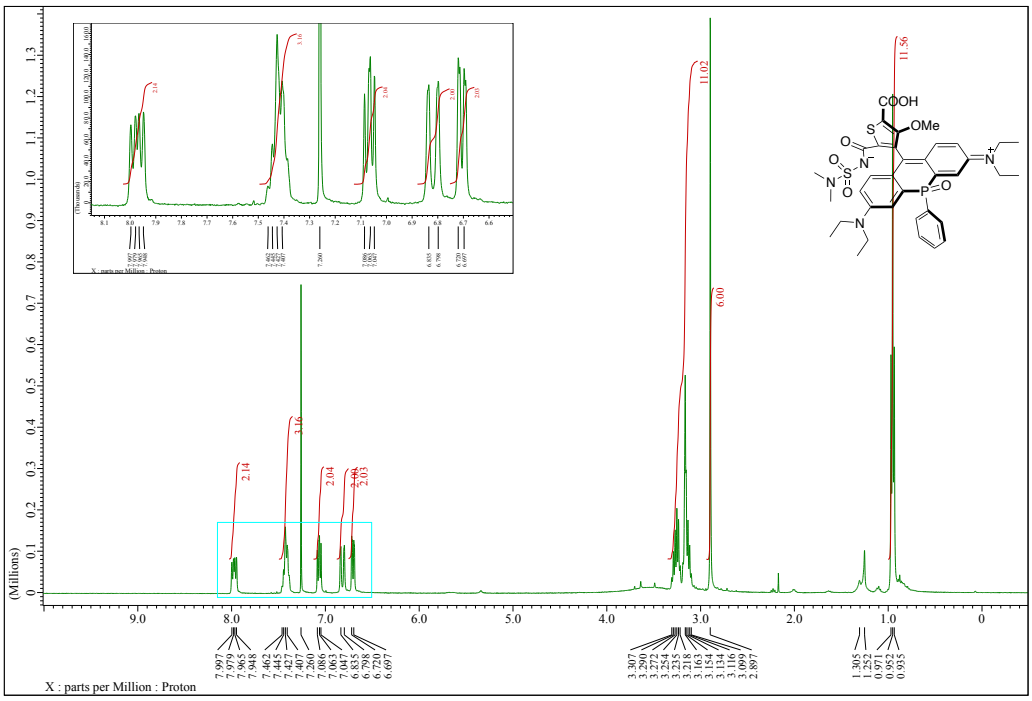

^{1}H NMR spectrum of ***trans*-PORSA715** (400 MHz, $CDCl_3$)

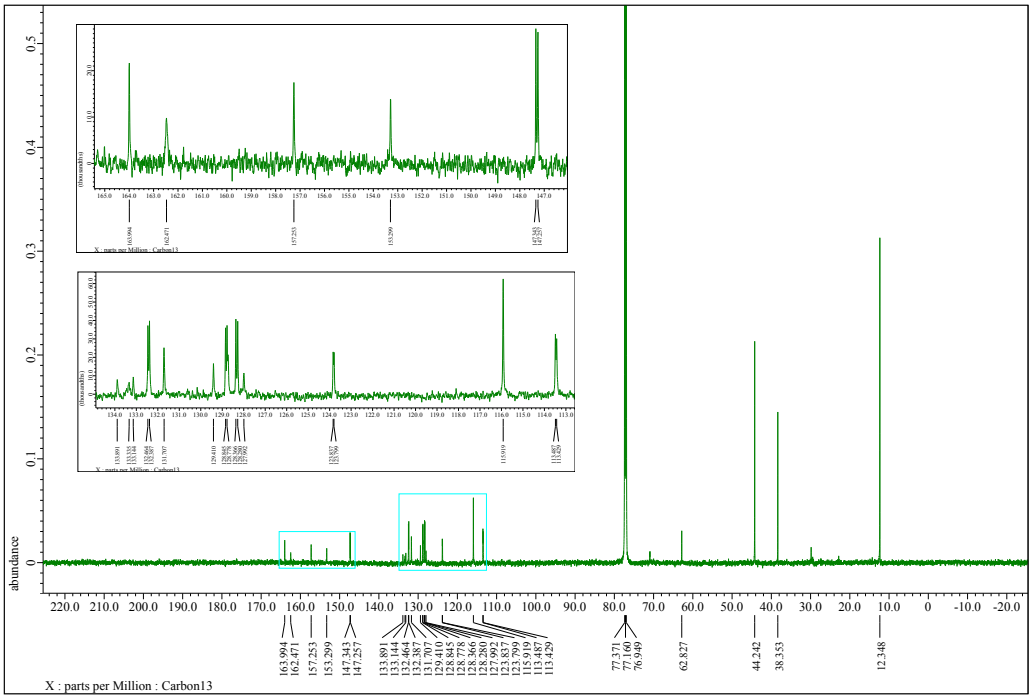

^{13}C NMR spectrum of ***trans*-PORSA715** (150 MHz, $CDCl_3$)

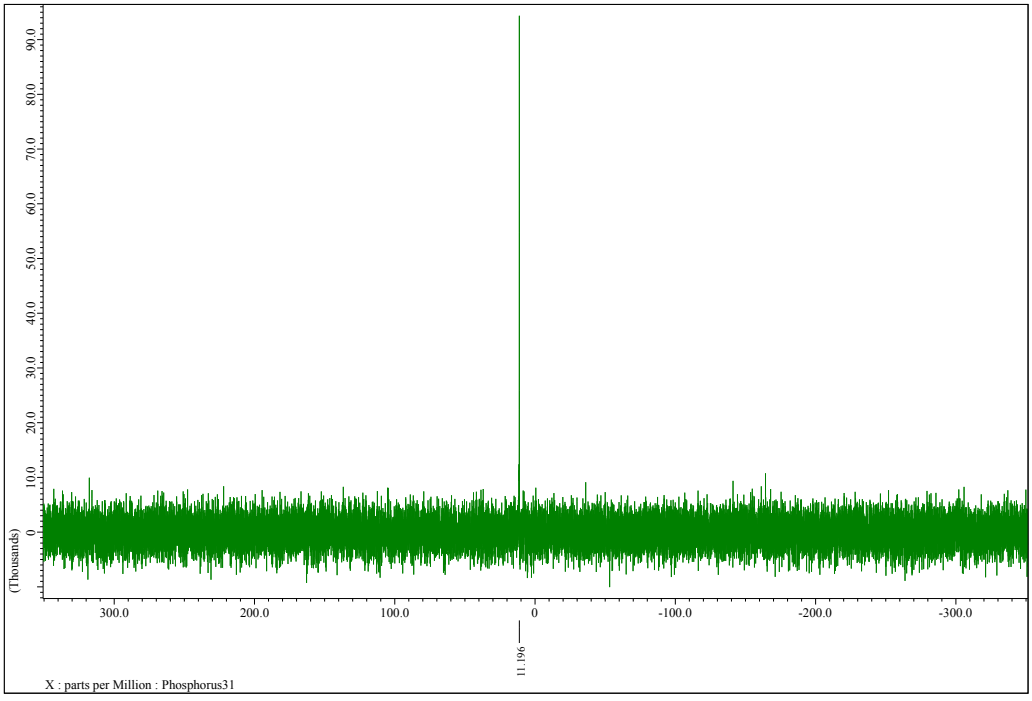

^{31}P NMR spectrum of ***trans*-PORSA715** (162 MHz, $CDCl_3$)

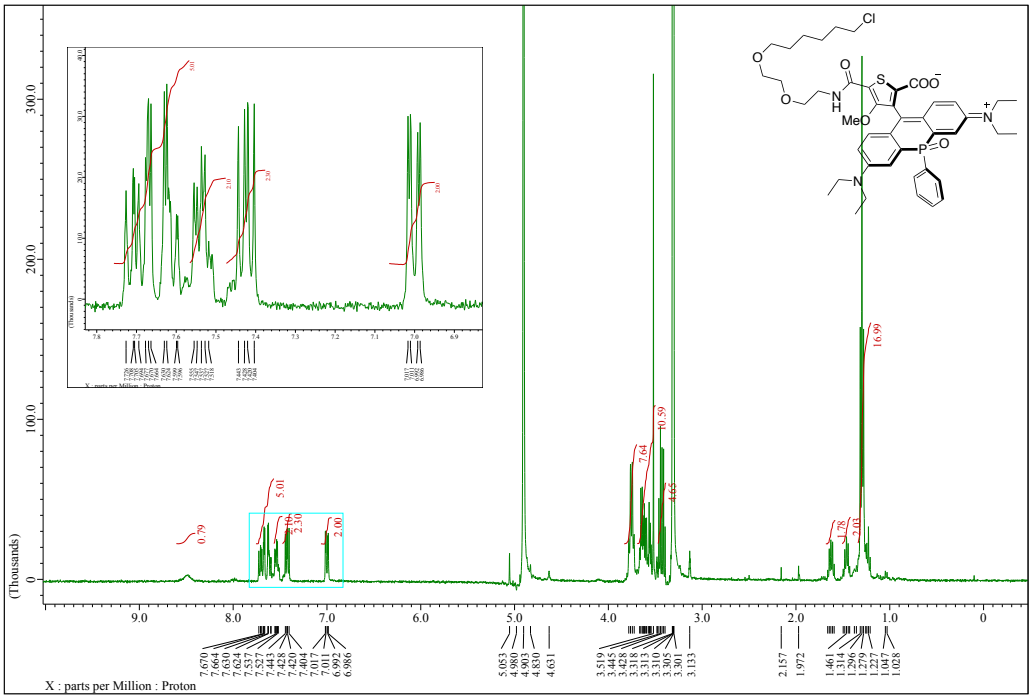

^{1}H NMR spectrum of ***cis*-POR715-Halo** (400 MHz, CD_3OD)

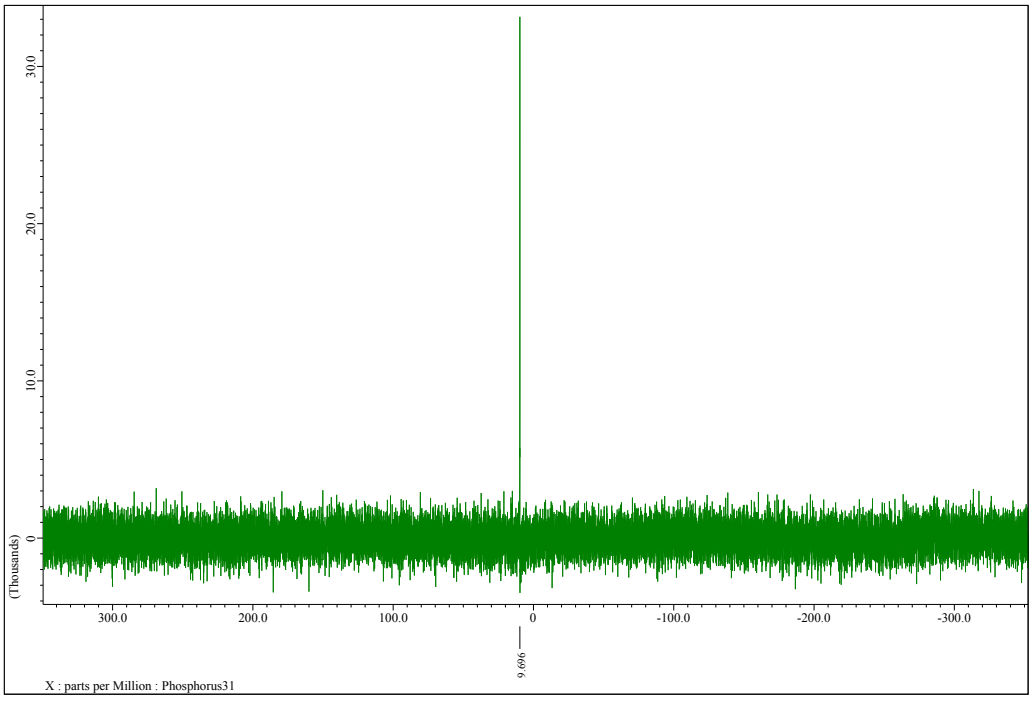

^{31}P NMR spectrum of ***cis*-POR715-Halo** (162 MHz, CD_3OD)

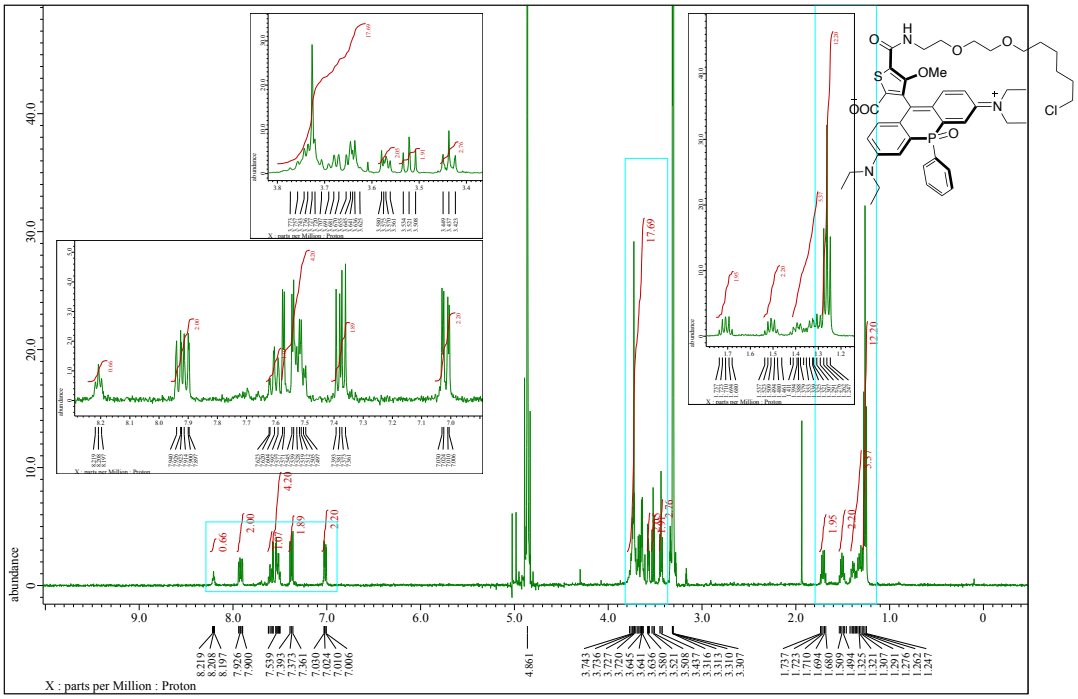

^{1}H NMR spectrum of ***trans*-POR715-Halo** (500 MHz, CD_3OD)

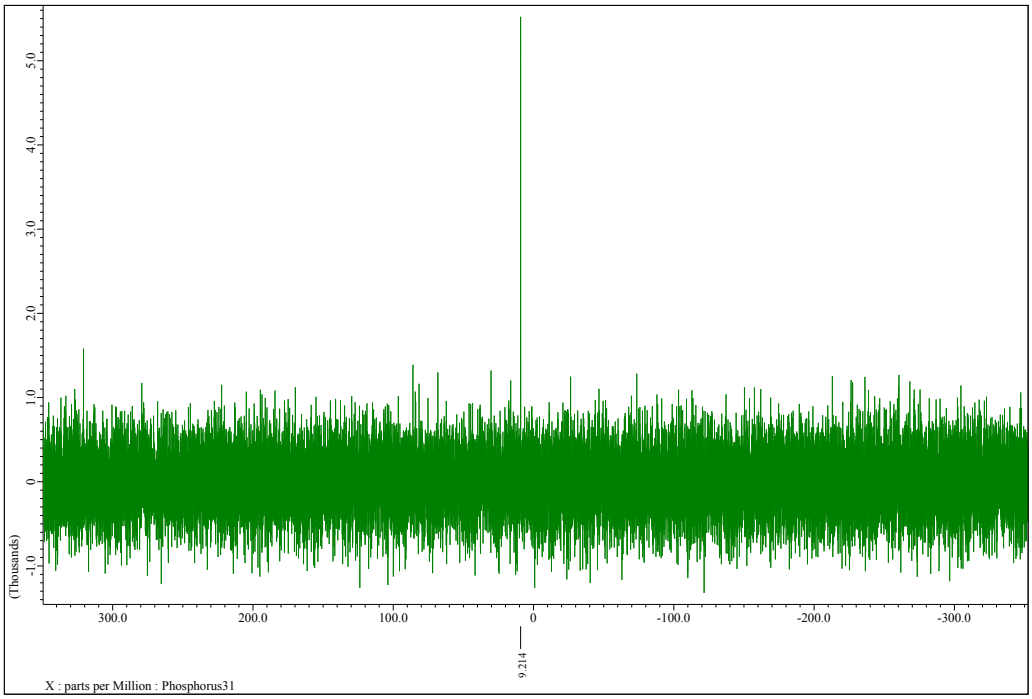

^{31}P NMR spectrum of ***trans*-POR715-Halo** (162 MHz, CD_3OD)

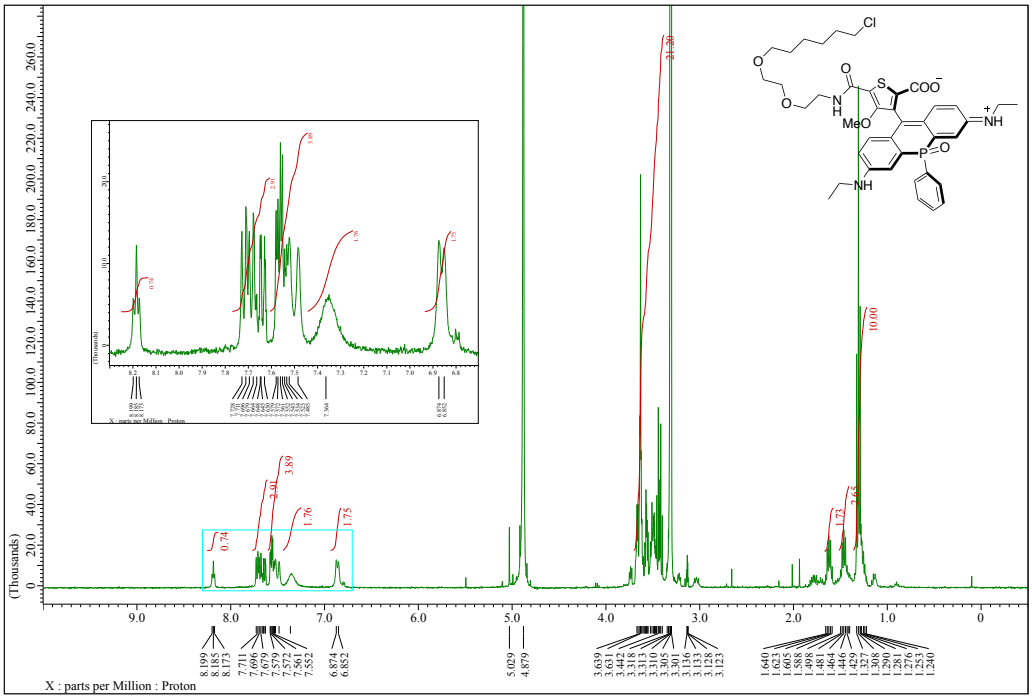

^{1}H NMR spectrum of ***cis*-POR675-Halo** (400 MHz, CD_3OD)

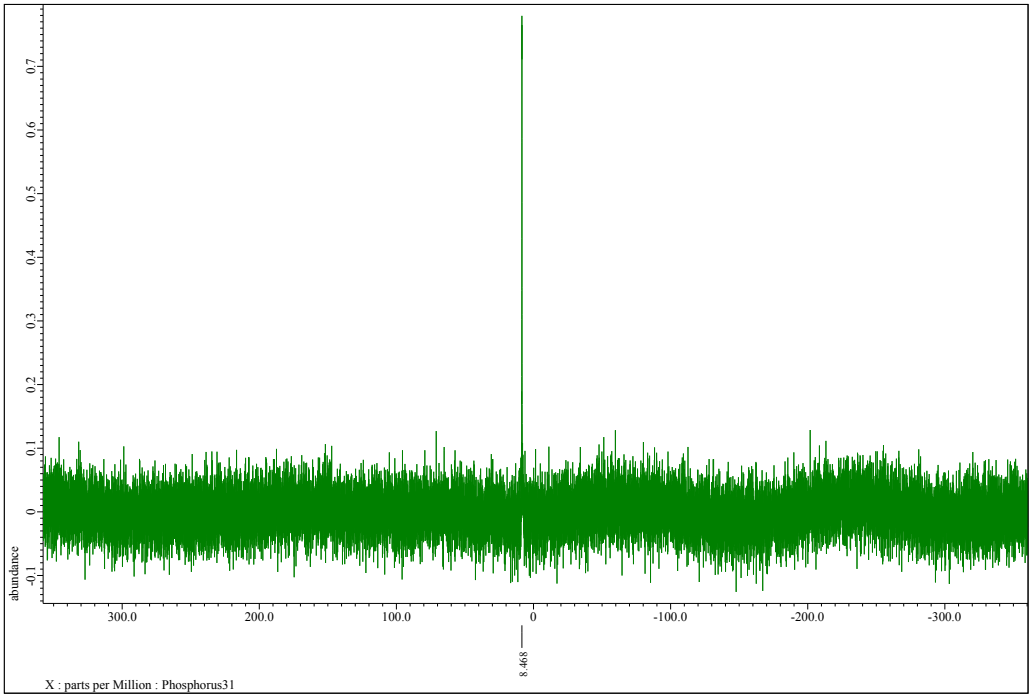

^{31}P NMR spectrum of ***cis*-POR675-Halo** (202 MHz, CD_3OD)

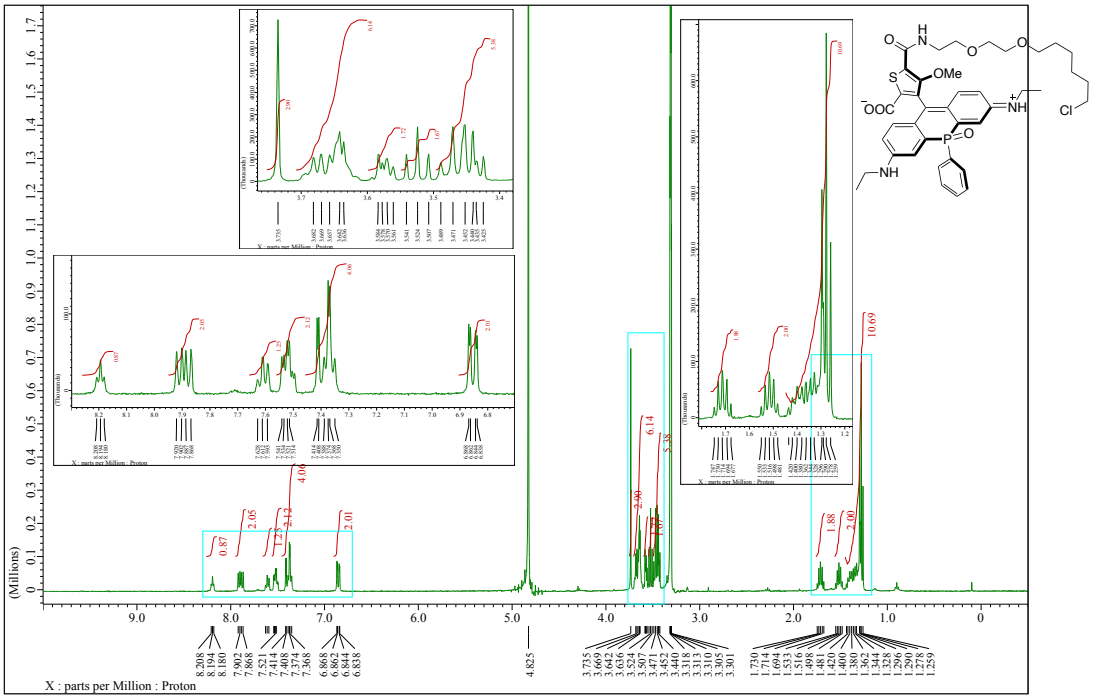

^{1}H NMR spectrum of ***trans*-POR675-Halo** (400 MHz, CD_3OD)

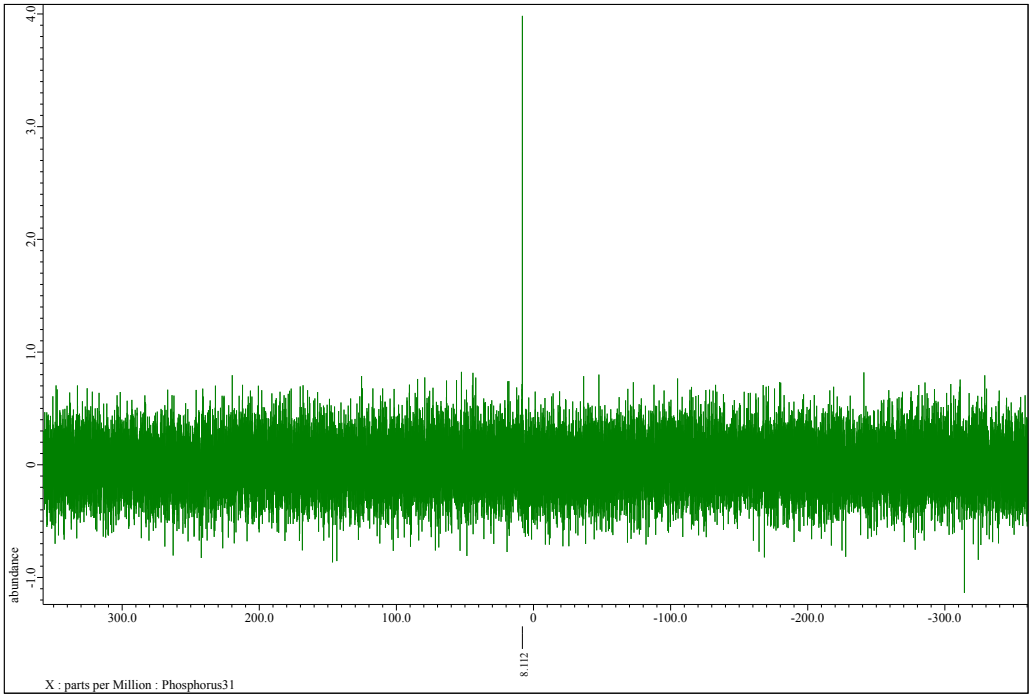

^{31}P NMR spectrum of ***trans*-POR675-Halo** (202 MHz, CD_3OD)

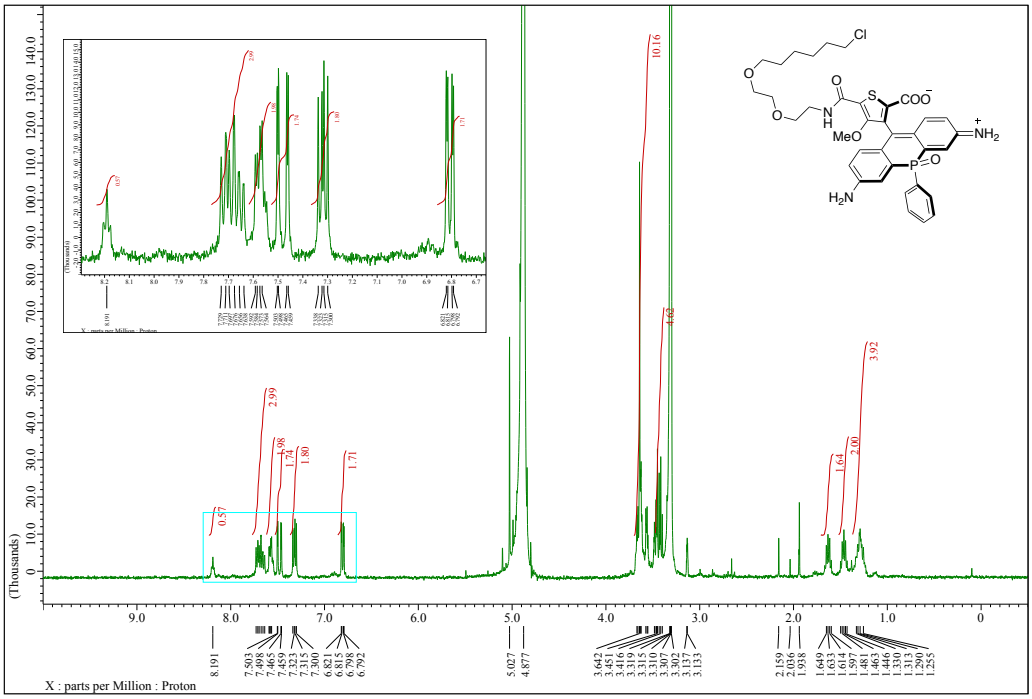

^{1}H NMR spectrum of ***cis*-POR645-Halo** (400 MHz, CD_3OD)

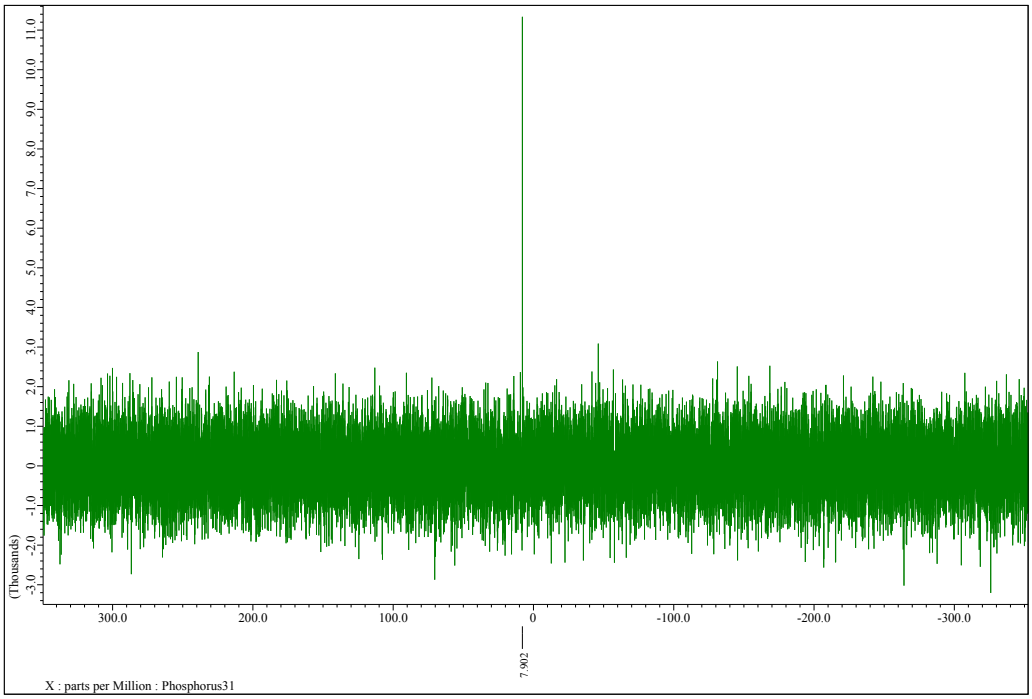

^{31}P NMR spectrum of ***cis*-POR645-Halo** (162 MHz, CD_3OD)

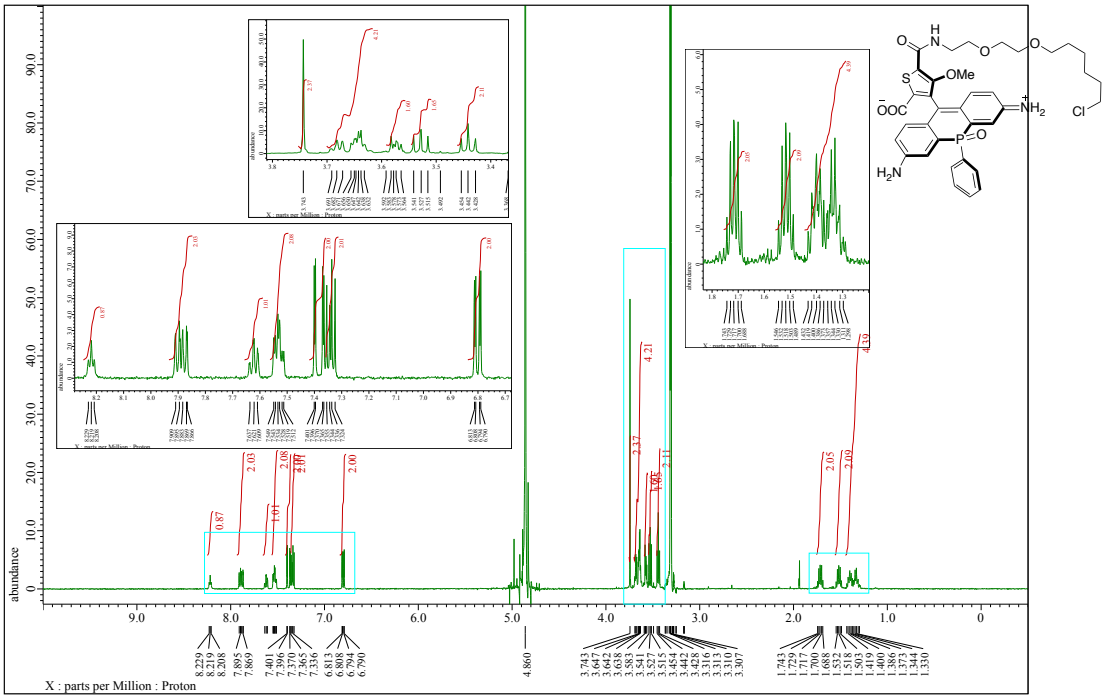

^{1}H NMR spectrum of ***trans*-POR645-Halo** (500 MHz, CD_3OD)

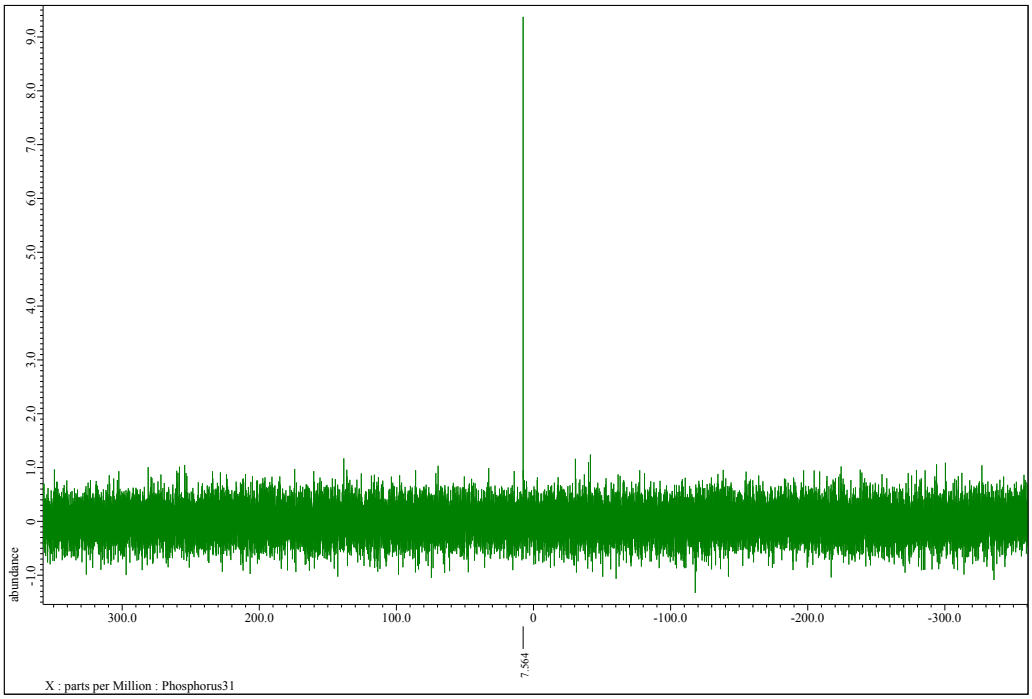

^{31}P NMR spectrum of ***trans*-POR645-Halo** (202 MHz, CD_3OD)

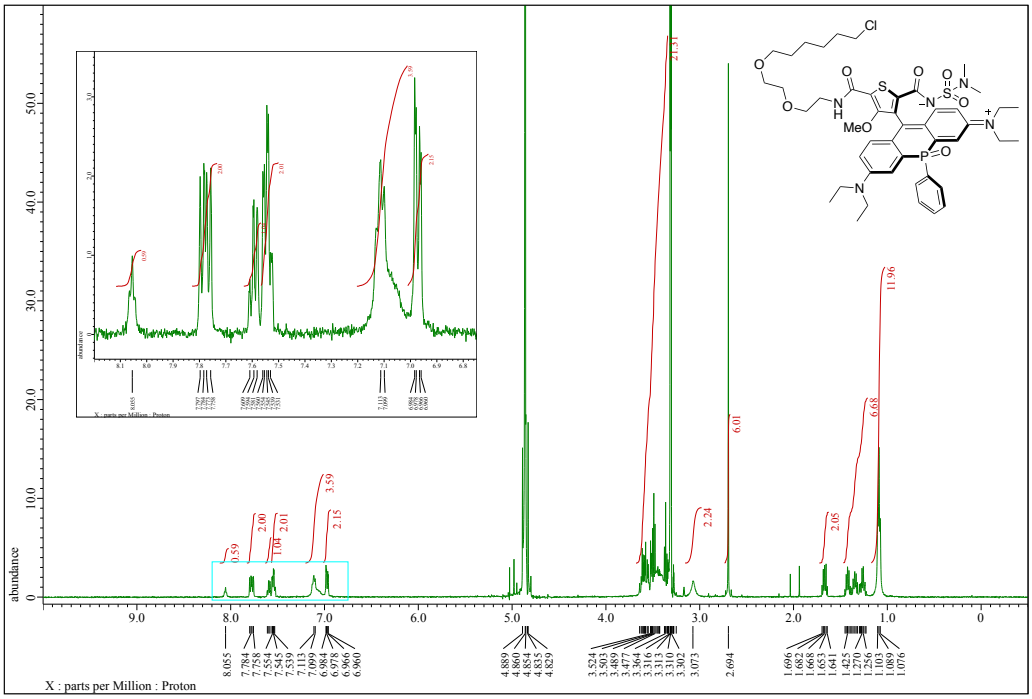

^{1}H NMR spectrum of ***cis*-PORSA715-Halo** (500 MHz, CD_3OD)

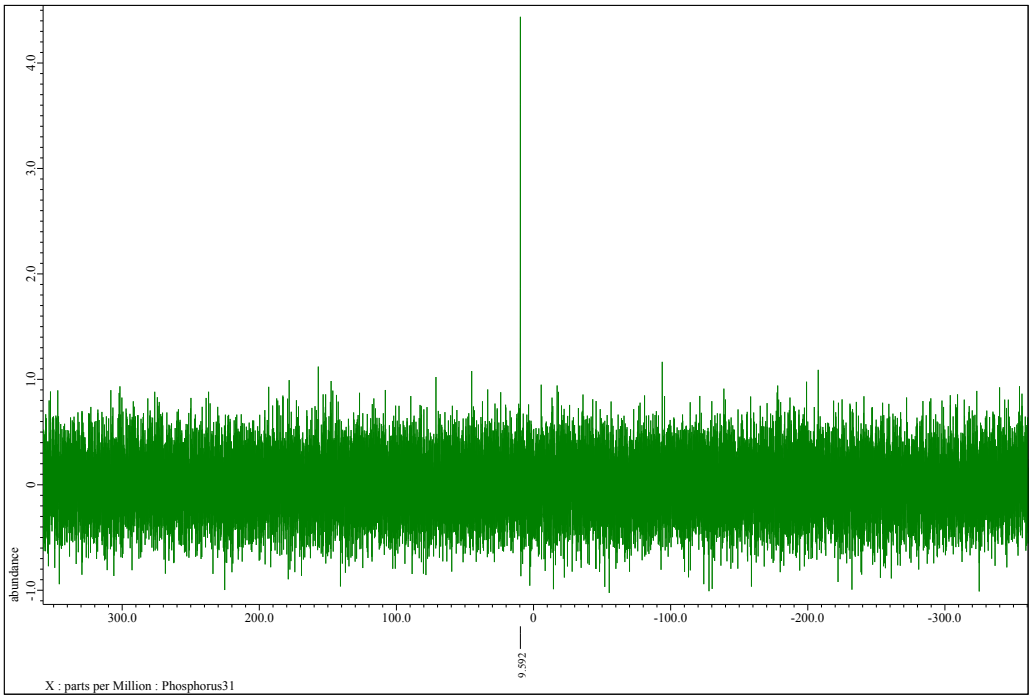

^{31}P NMR spectrum of ***cis*-PORSA715-Halo** (202 MHz, CD_3OD)

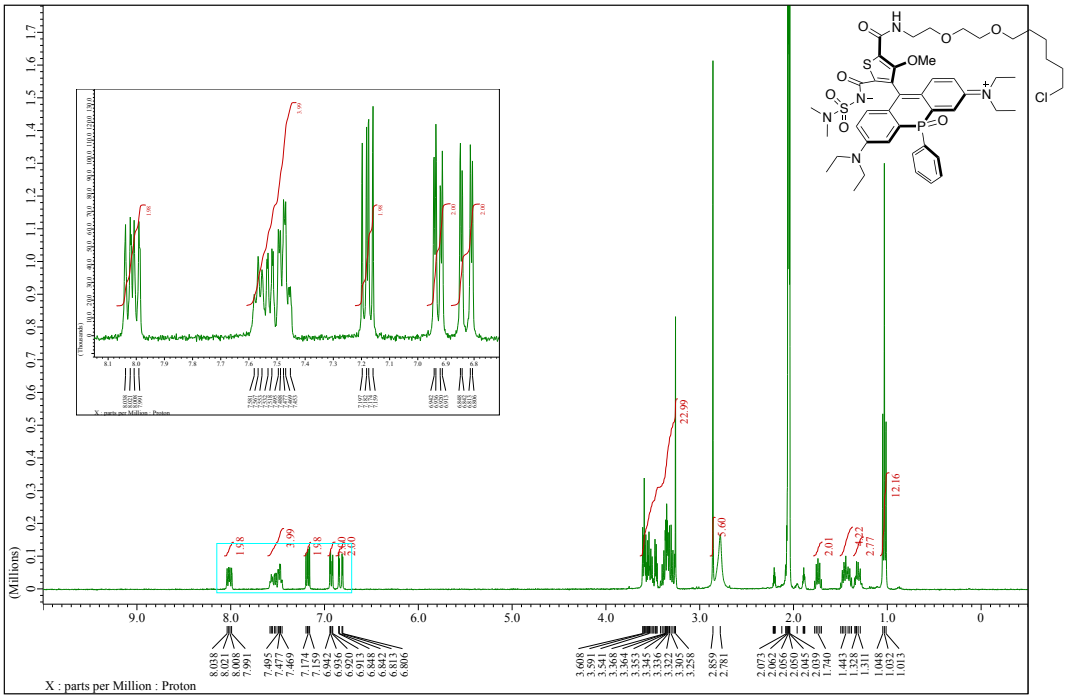

^{1}H NMR spectrum of ***trans*-PORSA715-Halo** (400 MHz, Acetone-d6)

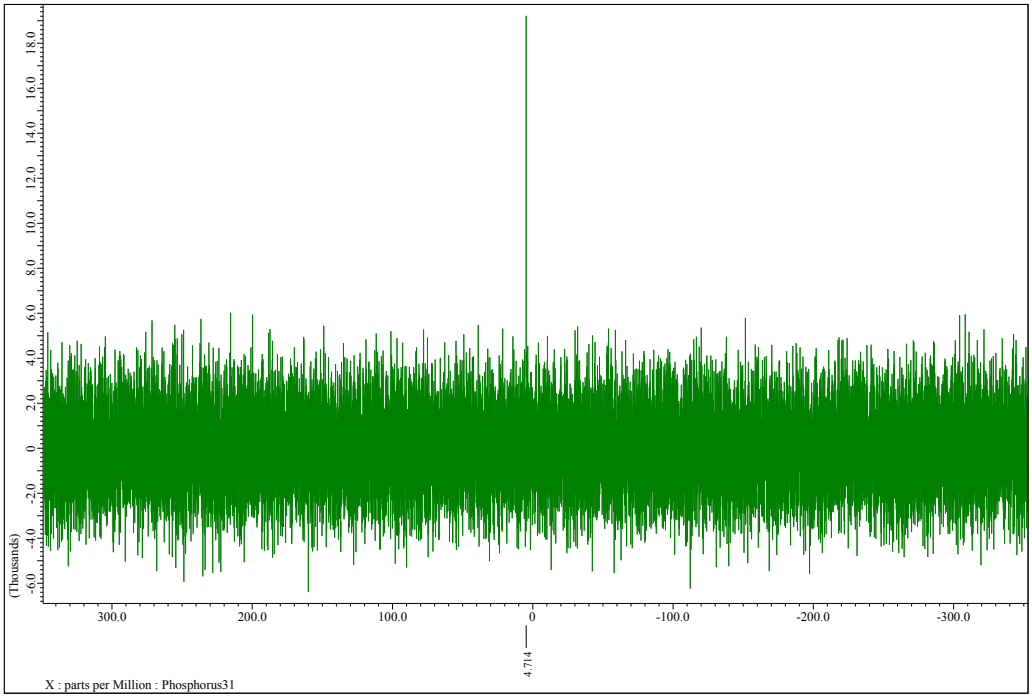

^{31}P NMR spectrum of ***trans*-PORSA715-Halo** (162 MHz, Acetone-d6)